DATABASE FOR STREAMFLOW AND SEDIMENT FLUX OF CALIFORNIA RIVERS

Douglas L. Inman, Scott A. Jenkins and Joseph Wasyl

Center for Coastal Studies
Scripps Institution of Oceanography
University of California, San Diego
La Jolla, CA 92093-0209

August 1998

SIO Reference Series No. 98-9

Contents

List of Tables

List of Figures

List of Appendices

ABSTRACT

The database for a study of the effects of climate change on the sediment flux of 20 of the larger streams entering the sea from the coasts of central and southern California is presented here. The database includes selected rainfall records, streamflow, hydrographs, sediment flux, and a 92-year record of Southern Oscillation Index (SOI) which serves as an indication of climate change. Procedures for determining sediment flux from streamflow and for delineating climate trends in the data are also presented.

Procedure

The database contains the streamflow and sediment flux records for the coastal watersheds bordering the Pacific Ocean along the central and southern California coast. The watersheds drain an area of 60,300 km^2 and extend for 750 km from Monterey Bay (Lat. 37^0N) to just south of the U. S./Mexico border (Lat. 32^0N) (Figure 1). The river drainage basins ranged in area from 120 to 10,800 km^2 with headwater elevations ranging from 460 to 3,770 m above MSL (Table 1). The coastal climate is Mediterranean with dry summers and winter rainfall along the coast of about 25 to 65 cm/yr with accumulation of snow at the higher elevations.

Streamflow and sediment flux near the river mouth are driven by rainfall received over the entire drainage basin, while rainfall records apply to the point of measurement, usually in cities or at airports. As a general indication of latitudinal variation, rainfall records were selected for four coastal cities that had the longest uninterrupted records and were representative of the latitudinal variation over the 750 km length of coast (Figures 2-5; Appendix A). The records are for the cities of Santa Cruz, San Luis Obispo, Ventura and San

Diego and their locations are shown in Figure 1. The figures show that there is a progressive decrease in rainfall from north to south.

One or more dams or other water retention structures are found on almost all streams in this study, and sand and gravel mining occurs on many. Several in the Los Angeles area have been altered by diversion facilities and contain extensive sections channelized with cement and/or rock, particularly in their lower reaches near the sea. We follow a drainage basin classification, modified from Brownlie and Taylor (1981), where the basins are designated as natural, moderately developed and extensively developed. Moderately developed (M) basins are those with one or more water retention structures, mostly on secondary streams. Extensively developed (E) basins have either major water retention/diversion structures with extensive channelized sections, or alternatively have dams that intercept more than 50% of the drainage area. The only natural (N) basin is Calleguas Creek, and it has extensive agricultural development that modifies its overland flow. Sweetwater River drainage area is natural above the gage station at an elevation of 1030 m, but the downstream 85% of the area is extensively developed with two dams. The basins are designated as M, E, N in Table 1. Drainage basins were also grouped into provinces according to their common geology and degree of urbanization. These provinces and the rivers that drain them are shown in Figure 1.

Available U. S. Geological Survey (USGS) gage stations on the coastal rivers between the Pajaro and the Tijuana were first identified and their corresponding hydrologic unit codes obtained from the INTERNET. The gage stations were located on USGS Hydrologic Unit Map-1978, State of California, and the gage station closest to the coast was identified and the area above the

gage station entered in Table 1. Total basin and province areas were obtained by digital integration from the hydrologic unit map. The hydrologic unit code of those stations was inserted into the USGS "web site", and the daily mean discharge data was downloaded for the period of record for each river (USGS, 1997). When gaps were found, the data search proceeded to the next upstream gage station until the gaps were filled. The upstream data used to fill gaps were normalized to the most seaward gage station using two approaches. If data were simultaneously available at both stations, an upstream flow rating curve was developed using statistical best-fit power laws. In the case of one minor stream, Ballona Creek, the upstream flow rating curve was based on the proportion of the drainage area located upstream of the two stations. An example of a power law flow rating curve derived from overlapping, simultaneously available data sets for two gage stations on the Santa Clara River is shown in Figure 6a. Daily mean flow rates were converted to daily flow volumes and summed over water years to produce annual mean flow rates (Appendix B & C). A water year extends from 1 October of the preceding calendar year to 30 September of the water year.

Estimates for the flux of suspended sediment for the gaps between measured values was derived by applying sediment rating curves to the annual mean streamflow. The rating curves were derived in a two step procedure modified from Brownlie and Taylor (1981) and Inman and Masters (1991). Varying amounts of monthly suspended-sediment flux measurements were available from the USGS (1998) monitoring programs for 15 of the 20 rivers. For 13 of these rivers, it was found that monthly rating curves based on monthly suspended sediment flux, when evaluated and summed over the year, gave better

correlations to measured annual sediment flux than the annual rating curves in the Brownlie and Taylor procedure. Accordingly, the cumulative monthly flow volume (Q_i, m^3/month) and the cumulative monthly suspended-sediment flux (J_i, ton/month) were correlated with a best-fit power function

$$J_i = aQ_i^b \quad (1)$$

where a and b are derived constants (Figure 6b). Data gaps in sediment flux were filled by applying monthly streamflow data to the rating curve. The monthly values of Q_i and J_i were then summed over the water year to provide the annual values of streamflow (Q, m^3/yr) and suspended-sediment flux (J, ton/yr) entered in Appendices B and C. For the San Luis Rey and Tijuana Rivers, the rating curves from Brownlie and Taylor (1981) were used to obtain annual sediment flux from annual streamflow as there has been no new measurements of sediment flux on these rivers since their 1981 analysis.

For five streams, sediment flux has not been measured. Instead, the monthly measurements of their streamflow were applied to the sediment rating curves of surrogate streams with similar basin and flow characteristics, as indicated in Table 1, and the results were summed by water year. The annual suspended sediment flux for the 20 coastal rivers is listed in Appendix C, with the actual measured values shown in bold italics. The sediment fluxes recorded in Appendices B and C are the fluxes of suspended-load material measured or assumed to occur within the streamflow from about 10 cm above the bed to the surface of the flow. This suspended load includes the wash load of silt and clay sized material and some sand, usually fine sand. Estimates of the coarser bedload material are not included in these suspended load estimates.

Quality Control

There are two basic types of error in the data and calculations used in this study of sediment flux of California rivers: (1) measurement error in the field when the data is taken by the USGS and (2) statistical error made in filling the data gaps in the measured data series. The U. S. Geological Survey has published three papers treating measurement concepts and error (Guy, 1970; Guy and Norman, 1970; Porterfield, 1972).

Measurement Error

Measurement error is due to sampling error in the field and to natural variability in the stream velocity and in the concentration of the suspended load. Sampling suspended load is done by a suction device that yo-yo's up-and-down on a cable taking samples over the depth of the stream. It is claimed that sampling errors related to transit time, transit rate and the number of vertical sampling increments can be limited to about ± 5% (Guy and Norman, 1970).

However, an additional error is associated with non-uniformities in the sediment concentration profile which are strongly dependent upon the percentage of coarse-grained sediments in the suspended load. For a suspended load consisting of 90% fines and 10% sands, the sediment flux error associated with natural variability is estimated to be about 5%. If the suspended sediment load is 50% sand-sized (greater than 62μ), these errors are estimated to be as high as 20%.

Therefore, sediment flux measurements in the dry period or for minor to average size floods probably have a measurement error of ± 10% (5% due to sampling and 5% due to natural variability). Measurements by Williams (1979) show that the sand-sized fraction of the suspended load varied between 9% and

22% in the Santa Clara River during the peak flow of the 1969 flood. For this flood the measurement error is likely to be ± 15% (5% due to sampling and 10% due to natural variability). The error would be higher in subsequent floods when the percentage of sand size material was higher (e.g., Alexander et al., 1996). However, no accounting is given for the particular sampling method used in relation to particular flood events. Suspended-sediment flux measured by the USGS is shown by bold italics in Appendix C.

Statistical Error

Whereas, the bold values of sediment flux in Appendix C contain the above mentioned measurement errors, the values shown in normal font have a statistical error resulting from the accuracy of the calculation method used in the sediment rating curve procedure. This statistical error has been studied in successive iterations for the best fit values of the parameters ***a*** and ***b*** of the rating curves (e.g., Figure 6); and in several numerical experiments to assess round-off errors in tabulations of long period averages. Based upon these iterations and numerical experiments the statistical error of sediment flux estimates from rating curve calculations is believed to be ± 20%. If the measurement errors and the statistical errors that are based upon them are independent of each other, then the two types of error are additive. Thus, assuming that the measurement errors are ± 15% and that the statistical errors are ± 20%, an overall error of about ± 35% could occur for the worst case scenario in data that is calculated from rating curves.

Suspended-sediment measurements began in the Santa Clara and Santa Ana Rivers in water year 1968. During the 27 years from 1969 to 1995 there were 146 year-long measurements of suspended-sediment flux in the 15 rivers (A and

C in Table 1). Thus, 36% of the data tabulated for these rivers in Appendix C is from USGS measurements and 64% is based on sediment rating curves. Streams with the most suspended-sediment measurements were Santa Ana (18 yr), Santa Clara (16 yr), San Juan Creek (16 yr) and Ventura River (14 yr). The sediment rating curves (e.g., Figure 6b) generated from these data had regression coefficients that ranged $0.82 < r^2 < 0.94$ with a modal cluster of nine points at about 0.89 (Table 2).

Determining Climate Trends

The occurrence of climate change is not easily detected from graphic representation of rainfall and streamflow over time, because these representations invariably produce confused, noisy time histories. However, trends become more apparent when the data are expressed in terms of cumulative residuals Q_n, taken as the continued cumulative sum of departures of annual values of a time series Q_i from their long-term mean values $\overline{Q}$, such that,

$$Q_n = \sum_{o}^{n} (Q_i - \overline{Q}) \qquad (2)$$

where n is the sequential value of a time series of N years. This method was first used by Hurst (1951, 1957) to determine the storage capacity of reservoirs on the Nile River, where the range between the maximum and minimum of the cumulative residual gives the needed deficit or credit storage capacity necessary for runs of excessively dry or wet years.

A comparison of the cumulative residuals for annual rainfall, streamflow and sediment flux for the Ventura River are shown in Figure 7. Note that in these diagrams, periods with low values of rainfall, streamflow and sediment flux represent dry climate and appear as intervals of decreasing residual (nega-

tive slope), while high values are wet periods and are represented by intervals of increasing residual (positive slope). All dates in the diagrams refer to the end of the water year except the initial point which indicates the start of the time series, and is the beginning of that water year. Thus, the date 1930 refers to the beginning of the water year, while 1995 refers to the end of the water year of this 66 year time series.

There is a systematic smoothing of the cumulative residual curves in Figure 7 progressing from rainfall to streamflow and sediment flux. The smoothing appears to result from the progressive integration of the many details of the driving force (rainfall) to its single summed resultant (streamflow). In turn, there is a carry-over to sediment flux which is a dependent series that smooths and lags streamflow through the power relation shown in Figure 6b (e.g., Soutar and Crill, 1977). A comparison of histograms and cumulative residual time series for rainfall is given in Figures 2-5.

The Hurst method is applied here to records of rainfall, streamflow, river sediment flux and the Southern Oscillation Index (SOI) to show trends and changes in climate. When the streamflow and sediment flux are plotted as cumulative residuals vs time for the 56-year period 1940 to 1995, all of the 20 rivers displayed a clear change from wet to dry climate in 1944 as shown in Figures 8 (1-20) for the streamflow and in Figures 9 (1-20) for sediment flux.
The cumulative residual plots for these figures begin in 1940 and end in 1995, but are based on the 52-year mean spanning the period from the beginning of the dry cycle in 1944 to the end of the database in 1995. The wet period beginning in 1969 is still continuing through water year 1998.

The multidecadal changes in streamflow (Figures 8) and sediment flux

(Figures 9) for the central and southern California rivers was compared with the global scale climate modification known as the southern oscillation. The intensity of the oscillation is often measured in terms of the Southern Oscillation Index (SOI), defined as the monthly mean sea level pressure anomaly in mb normalized by the standard deviation of the monthly means for the period 1951-1980 at Tahiti minus that at Darwin, Australia (NOAA, 1997; CAC version). A cumulative residual time series of SOI over the 92 year period 1904-1995 is shown in Figure 10 based on data in Appendix D.

The decades of dry climate along the coast of central and southern California in general coincide with periods when the La Niña portion of the southern oscillation predominate. Conversely, wet climate occurs when the El Niño portion of the southern oscillation predominates (e.g., Inman and Jenkins, 1997). La Niña events give rise to positive values of SOI while El Niño events are associated with negative values of SOI. The cumulative residual values for SOI in Figure 10 are plotted with positive values increasing downward so that the trends visually coincide with those for dry (downward sloping) and wet (upward sloping) periods plotted in Figures 2 through 9. Figure 10 shows a positive residual trend in SOI over most of the early and mid-20th Century particularly from 1942 to 1976, indicating that La Niña events predominated over El Niño events. The SOI record changed abruptly in calendar years 1976/77. The steep decline in the SOI cumulative residual beginning in 1977/78 was the result of a succession of very strong El Niño events, characterized by large negative values of SOI, particularly in 1978, 1983, and 1993 and 1995.

Along the central and southern coast of California, the change from dry to wet climate occurred with the flood of 1969. This flood was associated with a

relatively mild El Niño beginning in the 3rd quarter of calendar year 1968 (Appendix D), that was embedded in the La Niña trend that continued through calendar year 1976 (Figure 10). The 1969 flood was an important event along the central and southern coast of California, as it was a first flush event that broke the preceding 25-year drought. Because of the importance of this flood, the hydrographs for various streams for the water years 1969 and 1970 are shown in Figures 11 through 19.

The dry climate in central and southern California is reflected in years with no measurable streamflow on some southern California rivers. During the 1944-1968 dry period there were 2.3 years of no-flow per river draining the Transverse Ranges (6 rivers), and 5.8 years per river draining the Peninsular Ranges (8 rivers) (Table 3). During the wet period the number of no-flow years per river decreased to about 1 year per river draining these ranges.

Acknowledgments

This study was initiated under support from the Office of Naval Research, Ocean Modeling and Prediction, Contract N00014-95-1-0005, as part of a model study of the sediment budget for a mine scour study in the nearshore waters of the Oceanside Littoral Cell. The study was expanded to include central California and other rivers in the California Bight under support by Montrose Chemical Corporation of California, Zeneca Holdings, Inc., Stauffer Management Company, Rhone-Poulenc, Inc., Atkemix Thirty-Seven, Inc., and Chris-Craft Industries, Inc.

We thank John Dingler, Hideki Miyashita-Henry and Julia Huff of USGS for assistance in obtaining sediment flux and streamflow data; and Larry Riddle of the Scripps Institution of Oceanography for assistance in obtaining precipitation data. We thank Professor Malcolm Spaulding of the University of Rhode Island and John List of the California Institute of Technology for their reviews and thoughtful comments on preliminary drafts of this manuscript.

References Cited

Alexander R. B., Ludtke, A. S., Fitzgerald, K. K. and Schertz, T. L., 1996, Data from selected U. S. Geological Survey National Stream Water-Quality Monitoring Networks (WQN) on CD-ROM, U. S. Geological Survey, Open-File Report 96-337.

Brownlie, W. R. and Taylor, B. D., 1981, Coastal sediment delivery by major rivers in southern California, Sediment Management of Southern California Mountains, Coastal Plains, and Shorelines, Part C, California Institute of Technology, Pasadena, CA, Environmental Quality Laboratory Report No. 17-C, 314 pp.

Guy, H. P., 1970, Fluvial sediment concepts, Book 3, Ch. C1 in Techniques of Water-Resources Investigations of the U. S. Geological Survey, U. S. Government Printing Office, Washington, DC, 55 pp.

Guy, H. P. and Norman, V. W., 1970, Field methods for measurement of fluvial sediment, Book 3, Ch. C2 in Techniques of Water-Resources Investigations of the U. S. Geological Survey, U. S. Government Printing Office, Washington, DC, 55 pp.

Hurst, H. E., 1951, Long-term storage capacity of reservoirs, American Soc. Civil Engineers, Trans. v. 116, p. 770-799.

Hurst, H. E., 1957, A suggested statistical model of some time series which occur in nature, Nature, v. 180, n. 4584, p. 494.

Inman, D. L. and Jenkins, S. A., 1997, Changing wave climate and littoral drift along the California coast, p. 538-549 in O. T. Magoon et al., eds, California and the World Ocean '97, Amer. Soc. Civil Engin., Reston, VA, 1756 pp. San Diego, CA, 12 pp.

Inman, D. L. and Masters, P. M., 1991, Coastal sediment transport concepts and mechanisms, Chapter 5 (43 pp.) in State of the Coast Report, San Diego Region, Coast of California Storm and Tidal waves Study, U. S. Army Corps of Engineers, Los Angeles District, Chapters 1-10, Appen. A-Q.

NCDC, 1998, National Climatic Data Center at URL Address:

http://www.ncdc.noaa.gov/ol/climate/climatedata.html

NOAA, 1997, Climatological Archives @ INTERNET URL http://www.nwsla.noaa.gov/zones

Porterfield, G., 1972, Computation of fluvial-sediment discharge, Book 3, Ch. 3 in Techniques of Water-Resources Investigations of the U. S. Geological Survey, U. S. Government Printing Office, Washington, DC, 55 pp.

Soutar, A. and Crill, P. A., 1977, Sedimentation and climatic patterns in Santa Barbara Basin during the 19th and 20th Centuries, Geological Soc. Amer. Bull., v. 88,. p. 1161-72.

USGS, 1997, California Hydrologic Database, at INTERNET URL http://water.usgs.gov/swr/CA/dta.m

USGS, 1998, USGS Digital Data Series DDS-37 at INTERNET URL http://wwwrvares.er.usgs.gov/wqn96cd/wqn/wq/region18/hydrologic unit code.

Williams, R. P., 1979, Sediment discharge in the Santa Clara River basin, Ventura and Los Angeles Counties, California, U. S. Geological Survey, Water-Resources Investigations, 79-78, 51 pp.

Table 1. River and basin statistics.

River	Basin Class [a]	Gage Station	Station #	Drainage Area, [b] km^2	Headwater Elevation, m	Period of Record	Rating Procedure/ Surrogate [c]	Inter-Decadal Break [d]
1. Pajaro (36.8^{0}N)	M	Chittenden	11159000	2,550[e]	1720	1949-95	A/none	1968/69
2. Salinas (36.7^{0}N)	M	Spreckels	11152500	10,760	1920	1929-95	A/none	1968/69
3. Arroyo Grande (35.1^{0}N)	E	Arroyo Grande	11141500	264	930	1939-95	B/Lopez Cr.	X
4. Santa Maria (35.0^{0}N)	E	Guadalupe	11141000	4,510	2460	1940-95	A/none	X
5. Santa Ynez (34.7^{0}N)	M	Lompoc	11133500	2,050	2240	1906-95	B/S.Antonio	1968/69
6. Ventura (34.2^{0}N)	M	Ventura	11118500	487	1970	1929-95	A/none	1968/69
7. Santa Clara (34.2^{0}N)	M	Montalvo	11114000	4,130	2900	1927-95	A/none	1968/69
8. Calleguas Cr. (34.1^{0}N)	N	Camarillo	11106550	642	1230	1968-95	A/none	1968/69
9. Malibu Cr. (34.1^{0}N)	M	Crater Camp	11105500	272	930	1931-95	A/none	1968/69
10. Ballona Cr. (34.0^{0}N)	E	Culver City	11103500	232	460	1928-95	B/Topanga Cr.	1968/69
11. Los Angeles (33.8^{0}N)	E	Long Beach	11103000	2,140	2340	1929-95	A/none	1968/69
12. San Gabriel (33.7^{0}N)	E	Spring St.	11088000	1,610	3300	1936-95	B/Los Angeles	1968/69
13. Santa Ana (33.6^{0}N)	E	Santa Ana	11078000	4,400	3770	1923-95	A/none	1968/69
14. San Diego Cr. (33.6^{0}N)	E	Campus Dr.	11048555	306	580	1977-95	A/none	1968/69
15. San Juan Cr. (33.5^{0}N)	M	San Juan Cap.	11046550	303	1870	1969-95	A/none	1968/69

Table 1. Continued. [Page 2]

River	Basin Class [a]	Gage Station	Station #	Drainage Area,[b] km^2	Headwater Elevation, m	Period of Record	Rating Procedure/ Surrogate [c]	Inter-Decadal Break [d]
16. Santa Margarita (33.2^{0}N)	M	Ysidora	11046000	1,920	2230	1923-95	A/none	1968/69
17. San Luis Rey (33.2^{0}N)	M	Oceanside	11042000	1,440	2140	1912-95	C/none	1977/78
18. San Diego R. (32.8^{0}N)	E	Santee	11022500	976	2140	1912-95	A/none [g]	1977/78
19. Sweetwater (32.6^{0}N)	N/E[h]	Descanso	11015000	118	1730	1905-95	B/San Diego	1977/78
20. Tijuana (32.5^{0}N)	E	Nestor	11013500	4,390	1060	1936-95	C/none	1977/78

a M, E, N are moderately developed, extensively developed, natural; see text.
b Area above gage station.
c Sediment Rating Procedure: A) monthly values summed by water year; B) monthly values using surrogates summed by water year; C) annual values per Brownlie & Taylor (1981).
d Indicates water year of the dry to wet climate break; X indicate undeterminant break.
e Sediment Rating Curve developed from 1952-92 monitoring data at Chittenden with streamflow and drainage area from the sum of Gilroy (Pajaro River) and Hollister (San Benito River).
f Sediment Rating Curve developed from 1972-85 monitoring data at Culver Dr. (#11048500) with streamflow from Campus Drive.
g Sediment Rating Curve developed from 1984 monitoring data at Fashion Valley (#11023000).
h Natural to gage station at elevation 1030 m; downstream 85% of basin extensively developed.

Table 2. Regression statistics for rating curves.

River	Rating Curve Parameters[a]		Number of Data Points[b]	Regression Sum of Squares	Residual Sum of Squares	Mean Square Error	Coefficient of Determination, r^2
	a	b					
1. Pajaro	4.47×10^{-11}	1.865	56	112.127	13.79148	0.2554	0.89047
2. Salinas	5.83×10^{-11}	1.878	120	173.221	19.6032	0.1661	0.89833
4. Santa Maria	5.23×10^{-3}	1.078	10	44.0813	5.67273	0.7091	0.88598
6. Ventura	3.20×10^{-7}	1.539	131	104.187	22.5269	0.1746	0.8222
7. Santa Clara	7.48×10^{-7}	1.502	110	460.456	66.7526	0.6181	0.87338
8. Calleguas Cr.	4.13×10^{-9}	1.892	126	47.0649	10.3696	0.0836	0.81945
9. Malibu Cr.	5.04×10^{-9}	1.872	56	142.877	17.5325	0.3246	0.89070
11. Los Angeles	5.07×10^{-9}	1.614	56	158.41	16.4131	0.3039	0.90611
13. Santa Ana	1.84×10^{-4}	1.175	123	265.968	39.1752	0.3238	0.87162
14. San Diego Cr.	2.03×10^{-4}	1.163	142	74.227	6.2487	0.0446	0.9223
15. San Juan Cr.	2.12×10^{-8}	1.649	181	197.106	27.8323	0.1555	0.87626
16. Santa Margarita	9.14×10^{-8}	1.546	36	139.29	16.1846	0.4760	0.89590
18. San Diego River	4.21×10^{-7}	1.413	9	15.241	1.04437	0.1492	0.9358

a Parameters a & b refer to $J_i = aQ_i^b$ per text page 4.

b Number of non-zero monthly suspended-sediment flux measurements.

Table 3. Years with no measurable streamflow.

River	Number of No-Flow Years		Comments:
	Dry Climate 1944-68	Wet Climate 1969-95	
Coast Ranges			All streams have measurable flow during the year.
1. Pajaro	0	0	
2. Salinas	0	0	
3. Arroyo Grande	0	0	
Transverse Ranges			dry climate = 14 yr no-flow on 6 rivers wet climate = 8 yr no-flow on 6 rivers
4. Santa Maria	11	7	
5. Santa Ynez	0	1	
6. Ventura	1	0	
7. Santa Clara	1	0	
8. Calleguas Cr.	1	0	
9. Malibu Cr.	0	0	
Los Angeles Urban Area			Most streams have measurable flow during the year.
10. Ballona Cr.	1	0	
11. Los Angeles	0	0	
12. San Gabriel	0	0	

Table 3. Continued. [page 2]

Peninsular Ranges			
13. Santa Ana	2	0	dry climate = 46 yr no-flow on 8 rivers
14. San Diego Cr.	0	0	
15. San Juan Cr.	2	0	wet climate = 6 yr no-flow on 8 rivers
16. Santa Margarita	13	5	
17. San Luis Rey	18	0	
18. San Diego R.	1	0	
19. Sweetwater	1	0	
20. Tijuana	9	1	

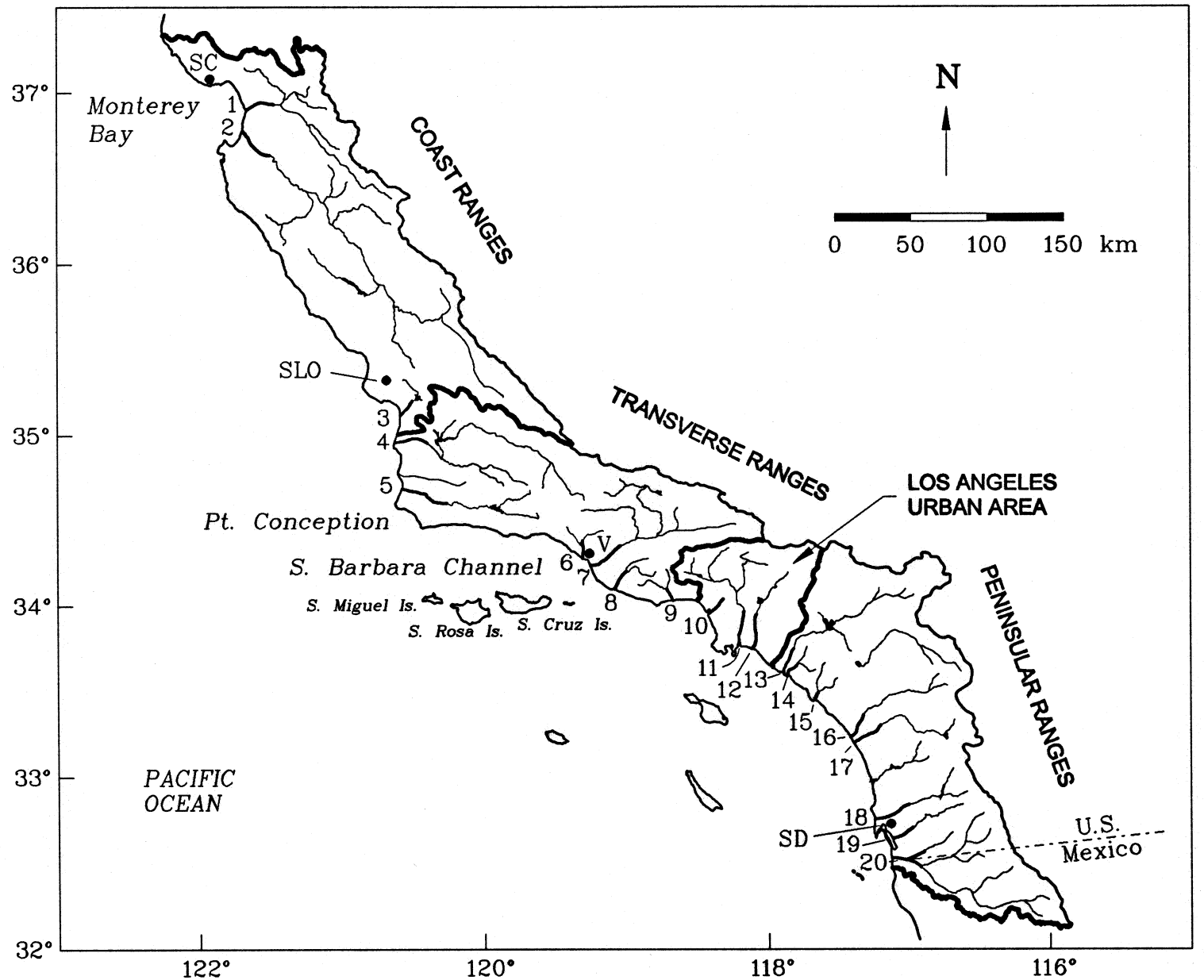

Figure 1. Location map for the rivers, basins and provinces analyzed in this study. The rivers are designated 1 through 20 and their names listed in Table 1. Location of cities with rainfall records are shown as Santa Cruz (SC), San Luis Obispo (SLO), Ventura (V) and San Diego (SD).

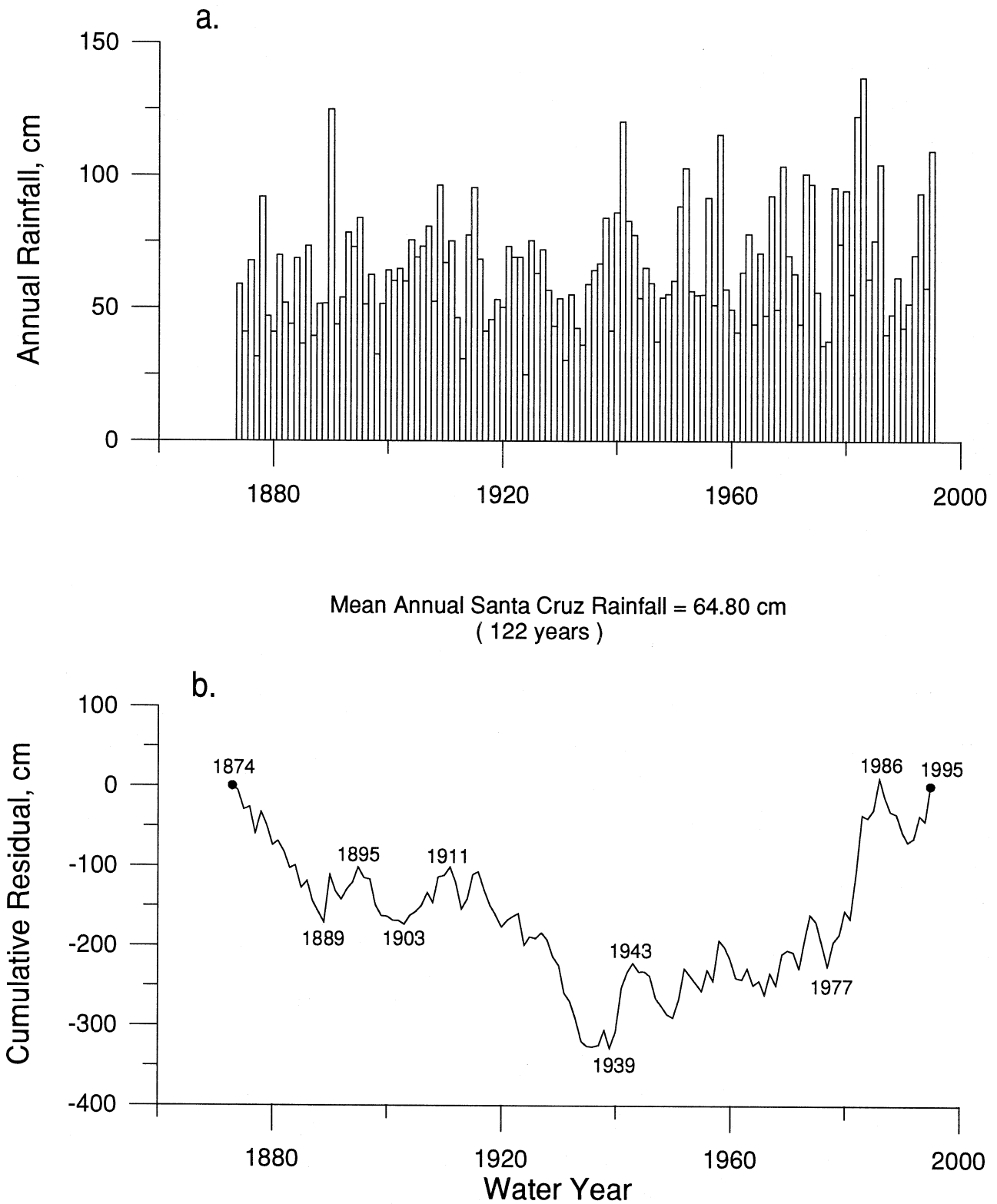

Figure 2. Annual rainfall histogram (a) and cumulative residual time series (b) for the city of Santa Cruz, California (data from Appendix A).

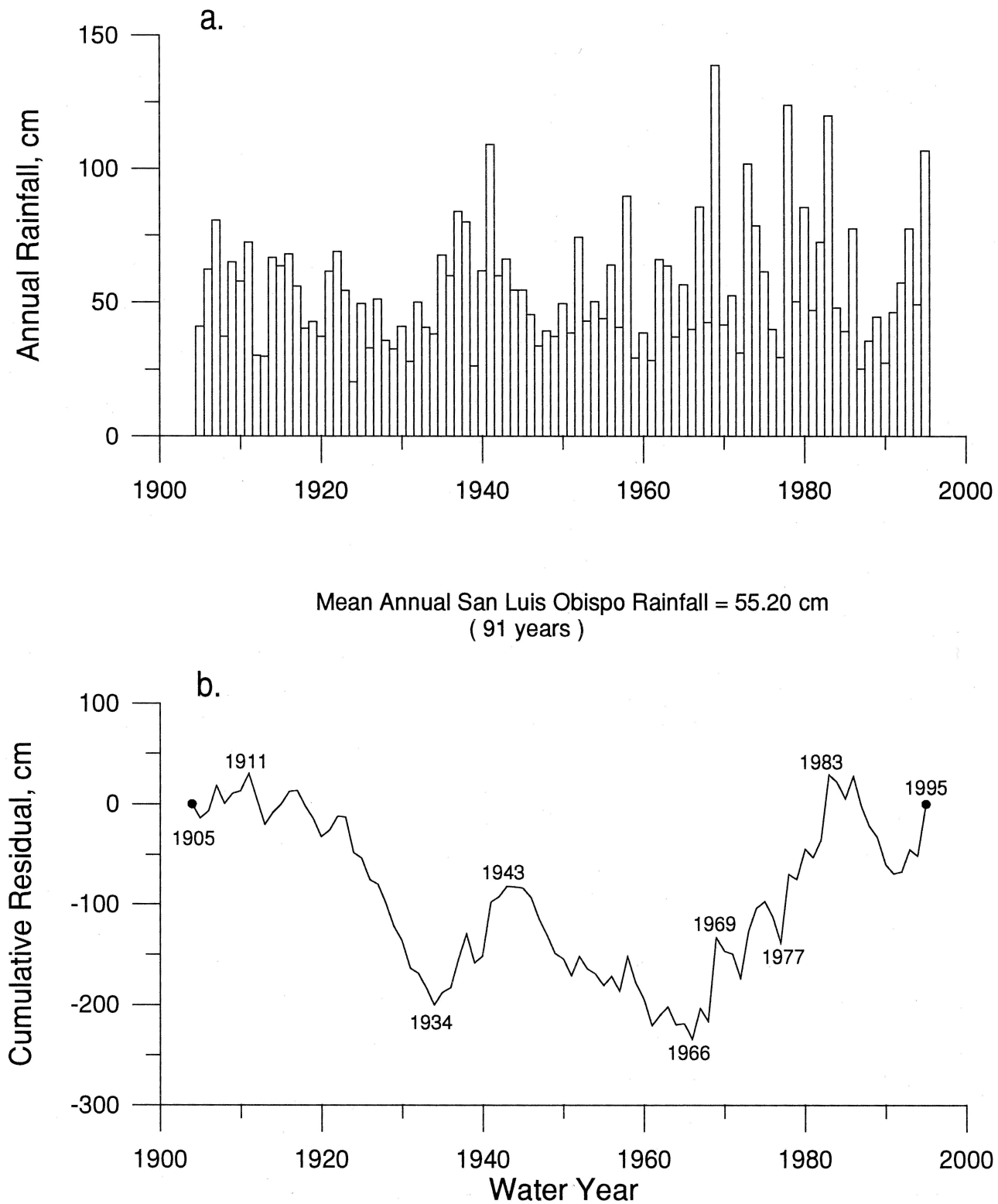

Figure 3. Annual rainfall histogram (a) and cumulative residual time series (b) for the city of San Luis Obispo, California (data from Appendix A).

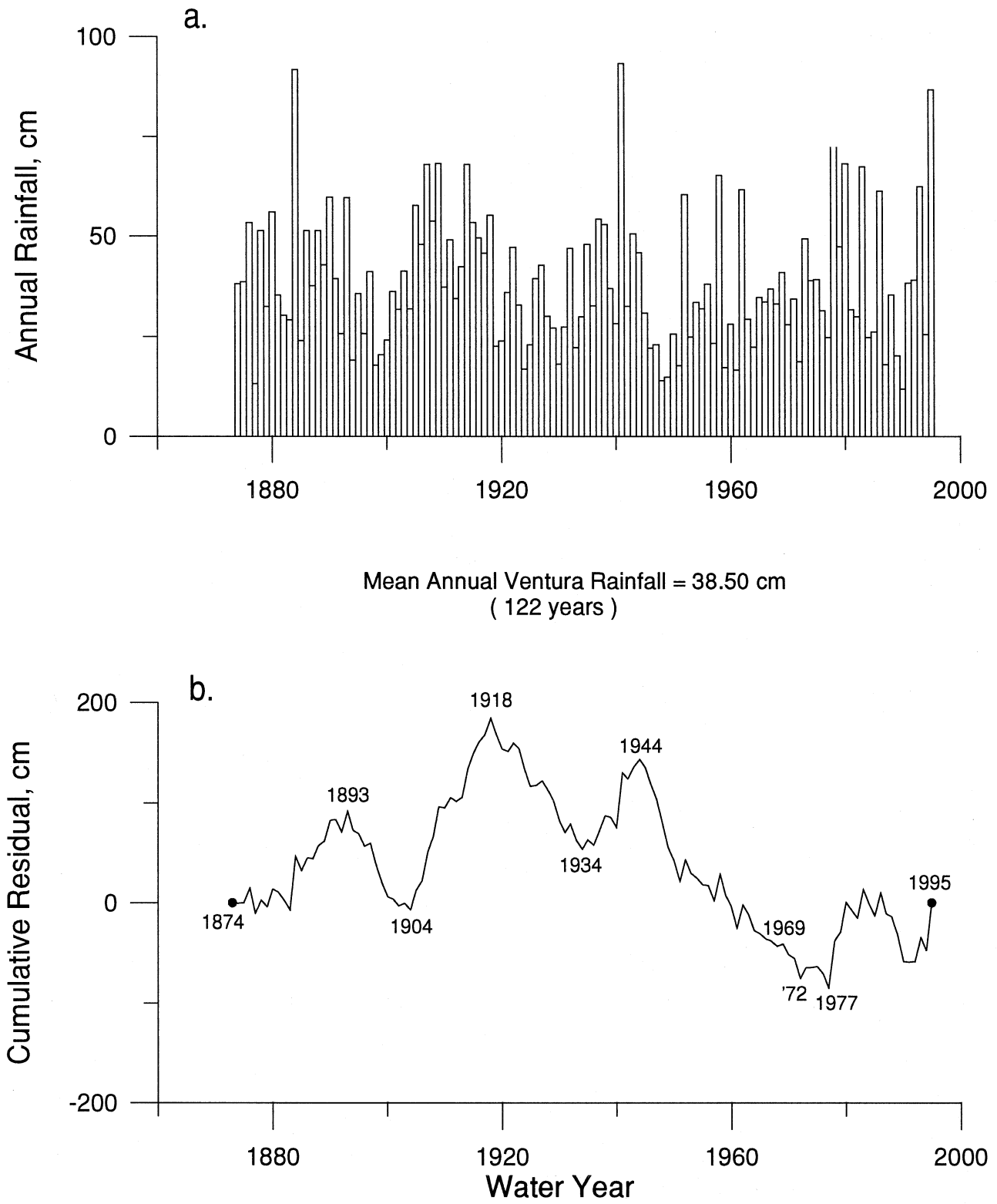

Figure 4. Annual rainfall histogram (a) and cumulative residual time series (b) for the city of Ventura, California (data from Appendix A).

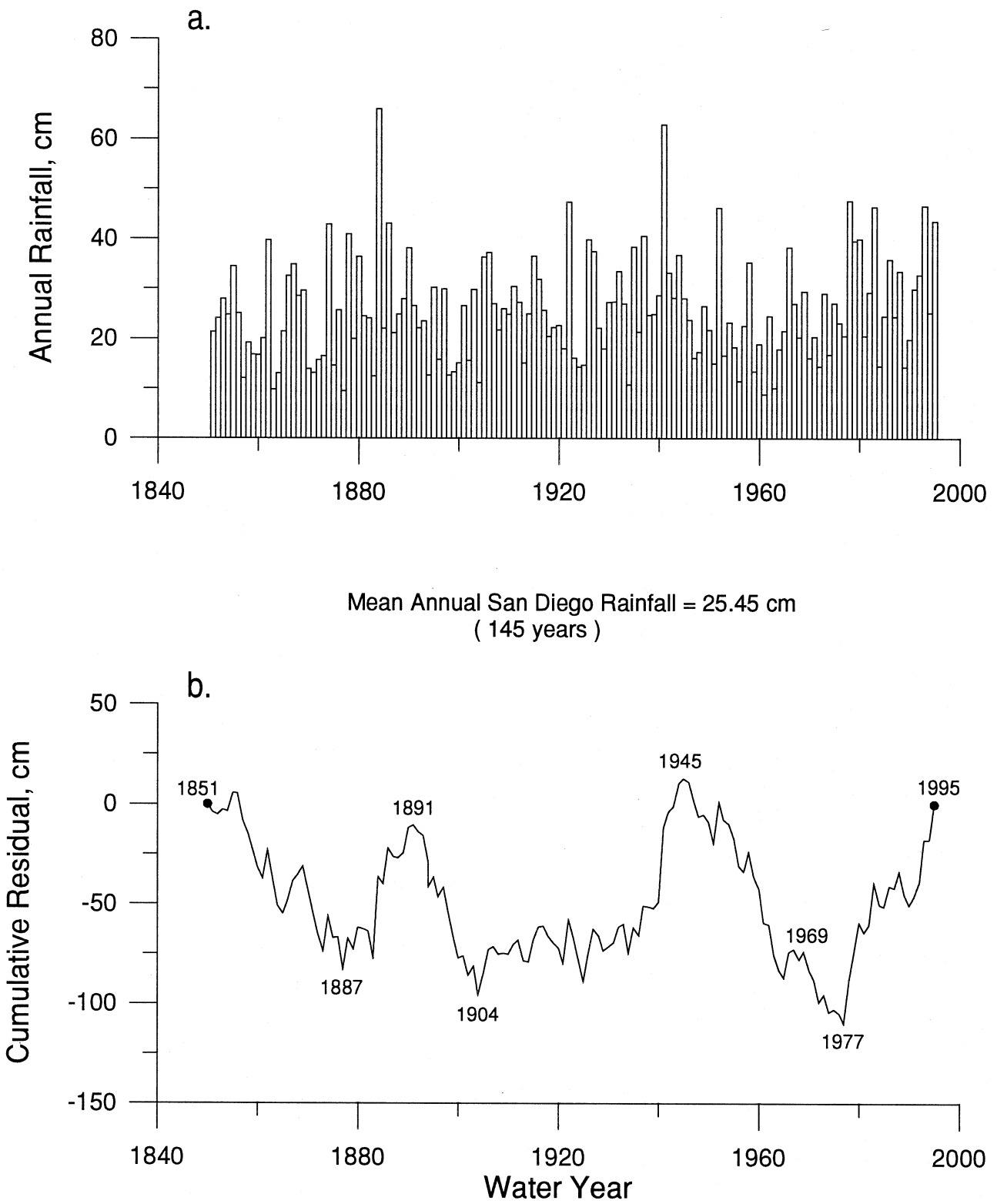

Figure 5. Annual rainfall histogram (a) and cumulative residual time series (b) for the city of San Diego, California (data from Appendix A).

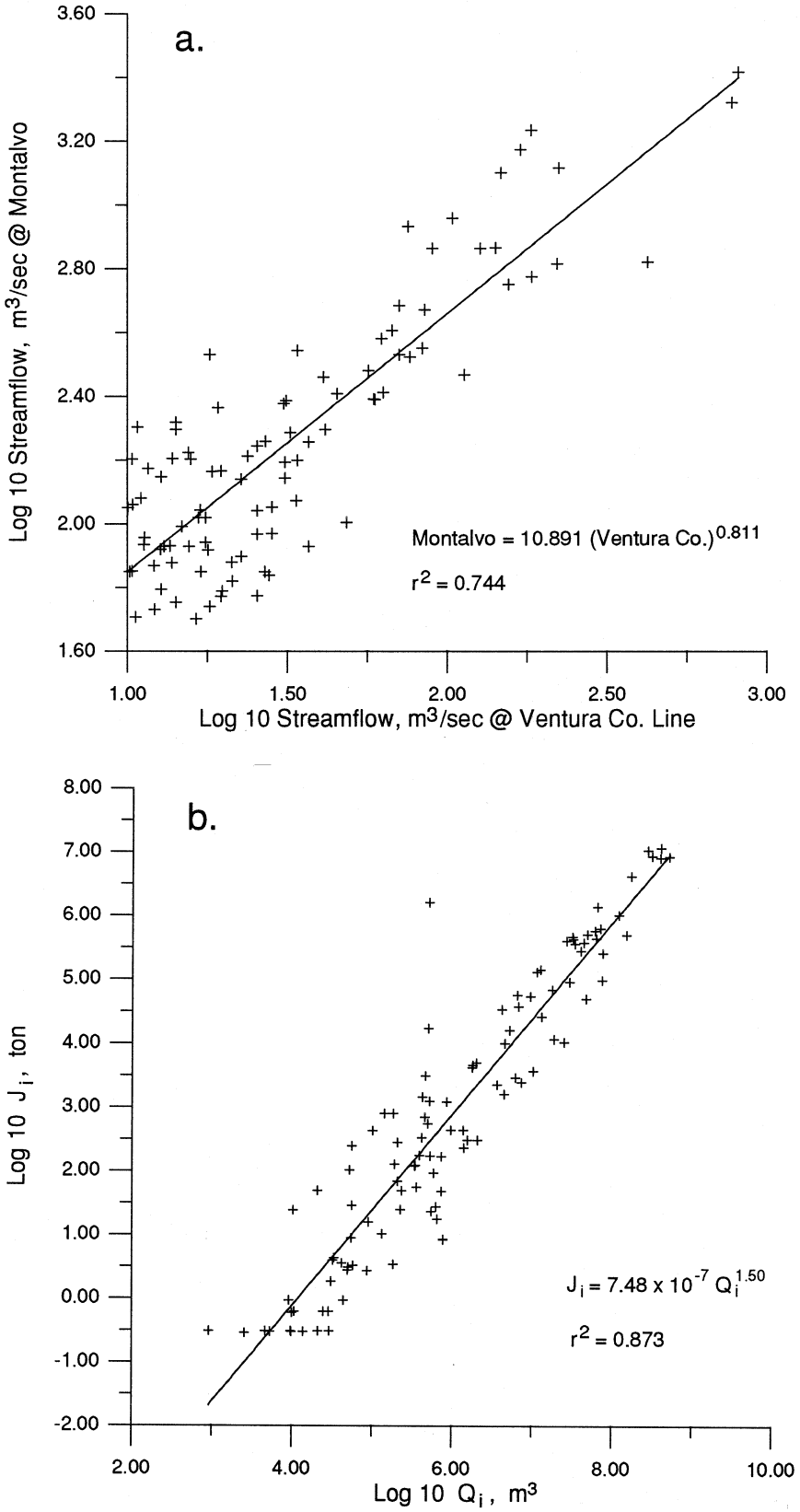

Figure 6. Examples of rating curves for the Santa Clara River: a) streamflow of coastal gaging station (Montalvo, #11114000) vs upstream gage (Ventura Co. Line, #11108500) used to fill gaps in the coastal station; b) rating curve for monthly flux of suspended-sediment (J_i) vs monthly streamflow (Q_i) at the coastal gaging station (Montalvo).

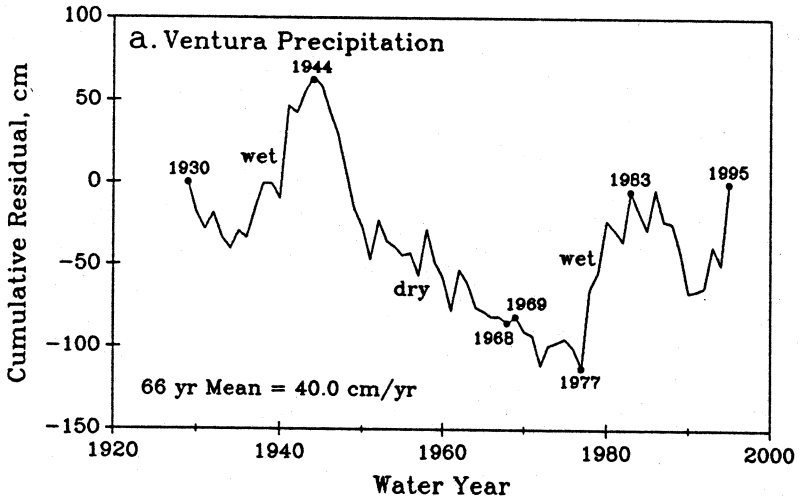

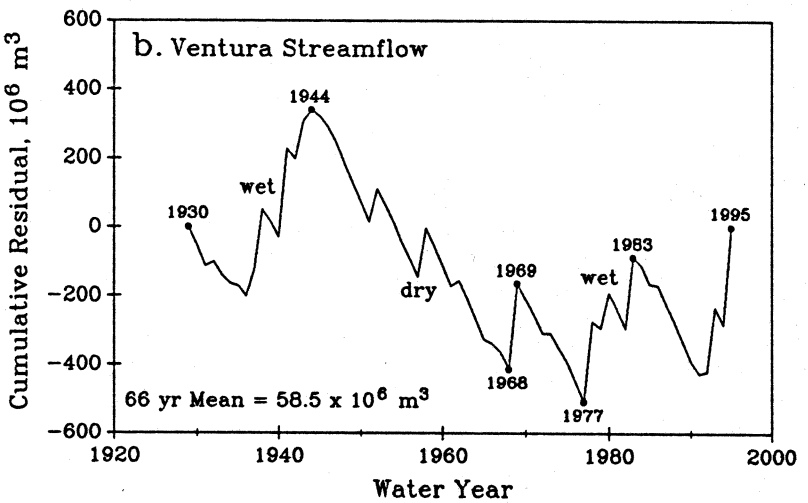

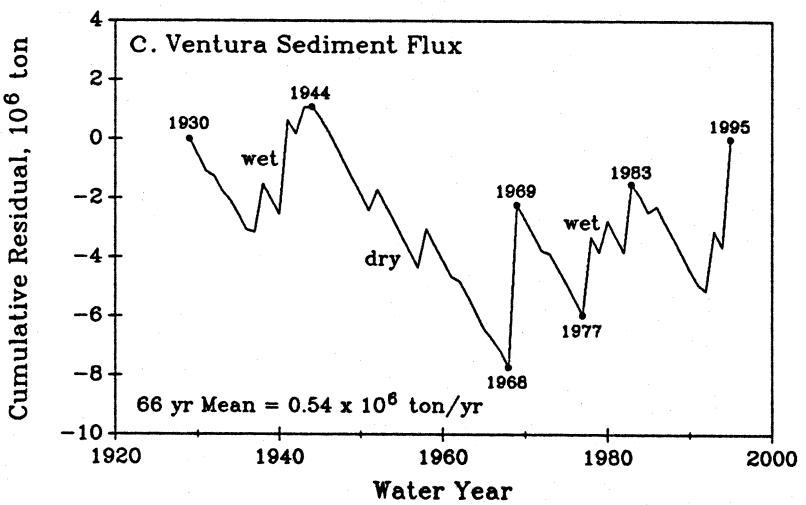

Figure 7. Cumulative residual plots of (a) annual rainfall; (b) annual streamflow; and, (c) annual suspended-sediment flux for Ventura River at Ventura for the period averaged over 1930-1995. All dates refer to the end of the water year except the initial point which refers to the start of the period of record which is the beginning of that water year (data from Appendices A, B and C).

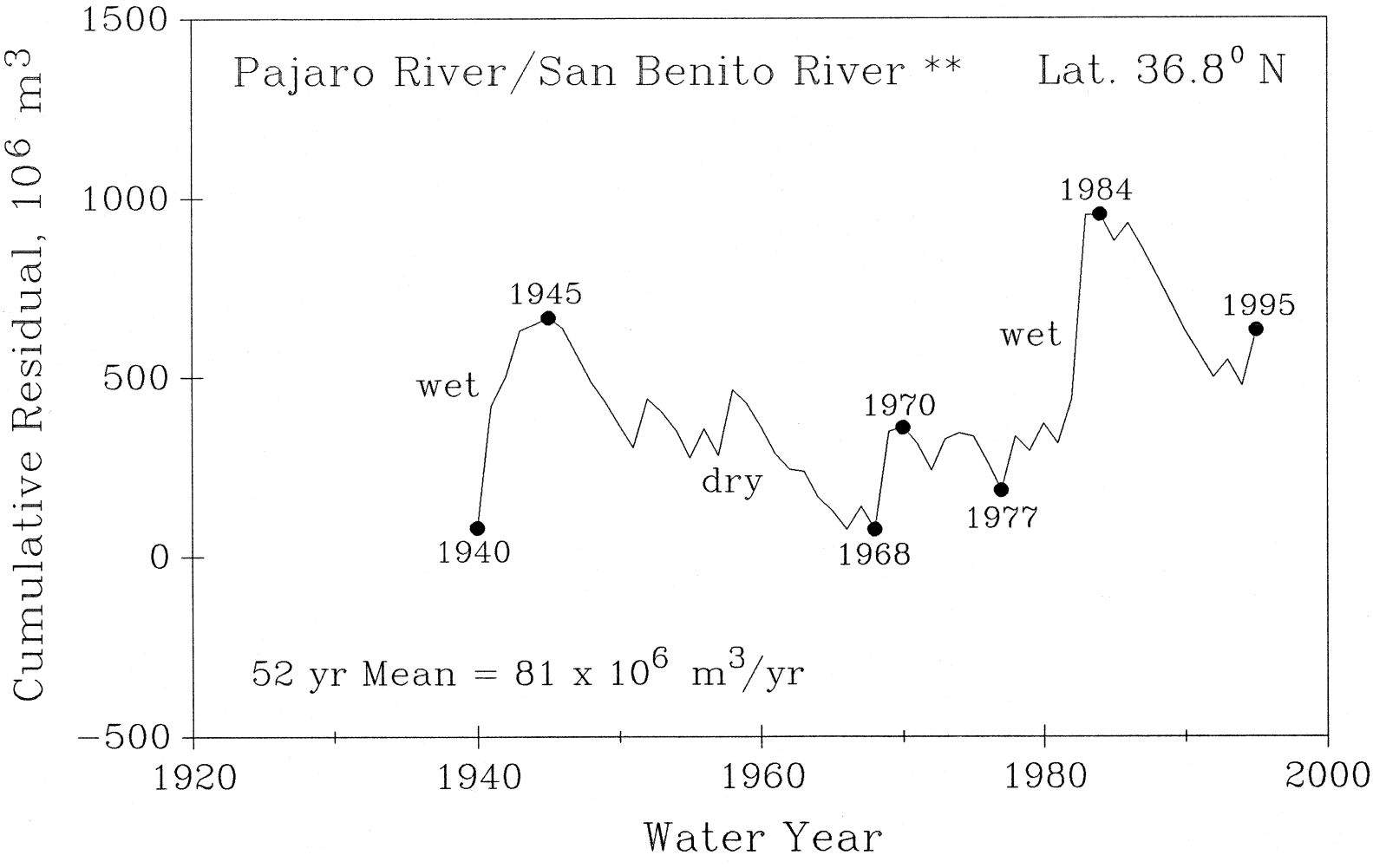

Figure 8 (1). Cumulative residual time series of streamflow for Pajaro River calculated using a 52-year mean (1944-1995) over the period of record of 1940-1995 (data from Appendix C).

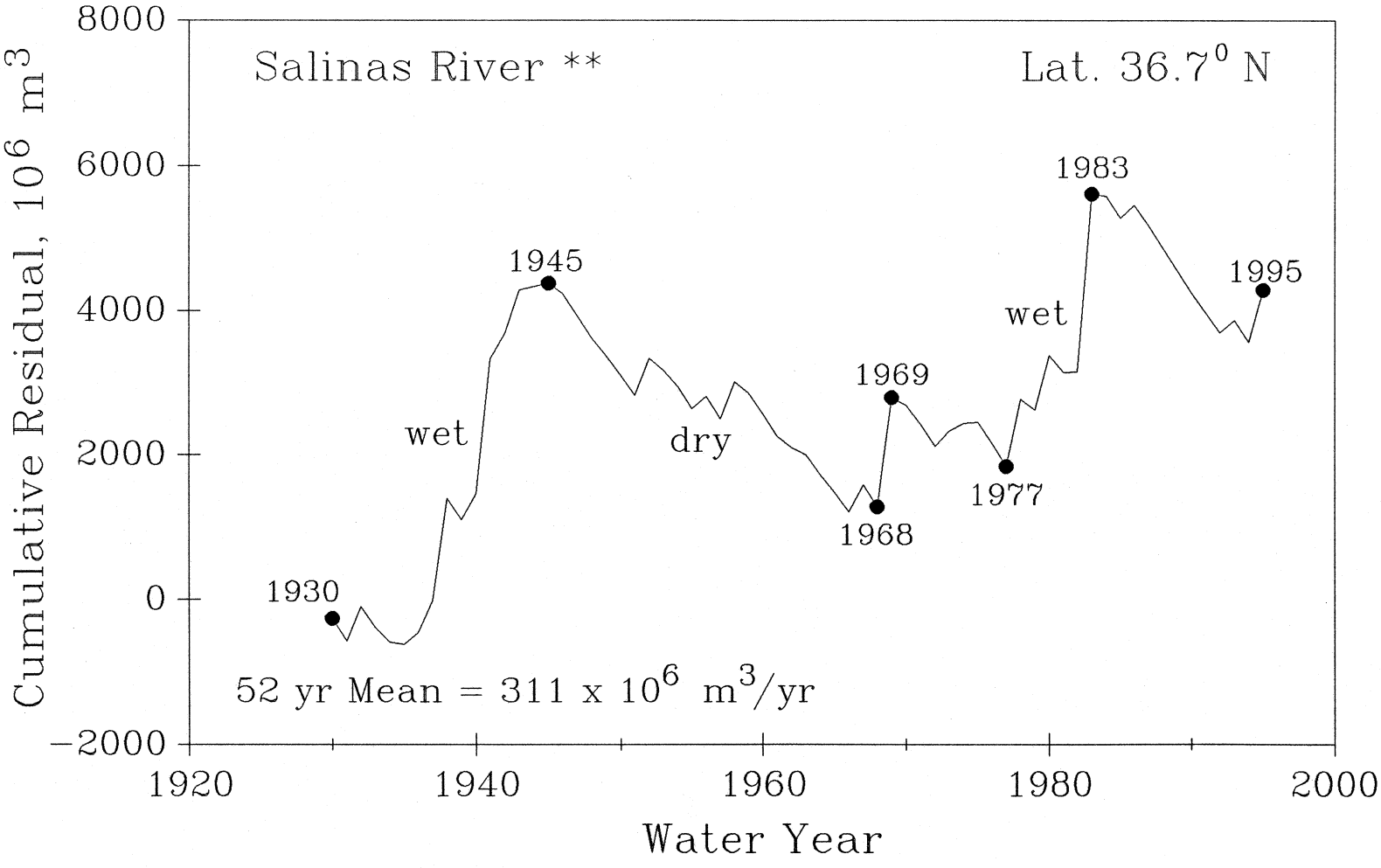

Figure 8 (2). Cumulative residual time series of streamflow for Salinas River calculated using a 52-year mean (1944-1995) over the period of record of 1940-1995 (data from Appendix C).

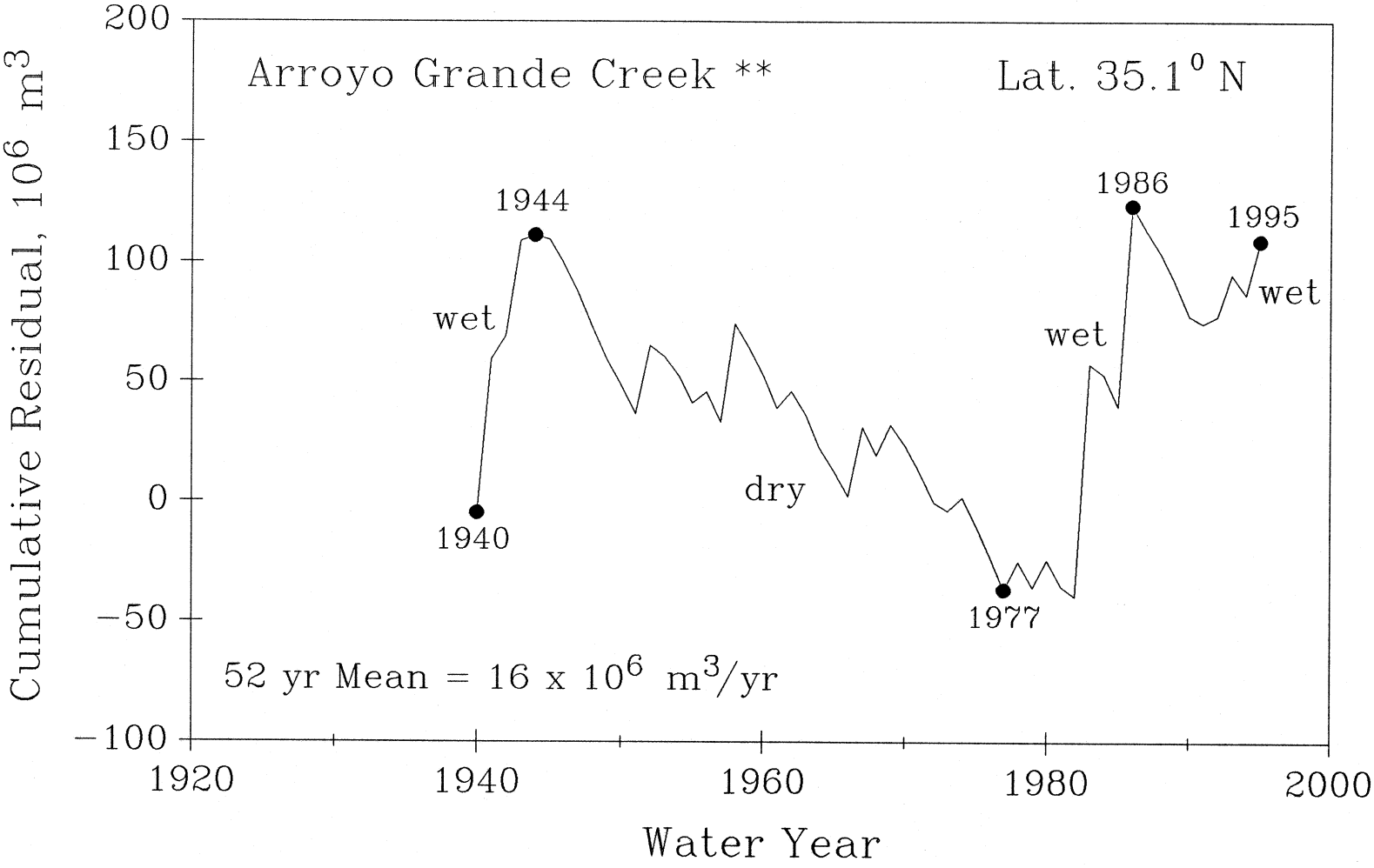

Figure 8 (3). Cumulative residual time series of streamflow for Arroyo Grande Creek calculated using a 52-year mean (1944-1995) over the period of record of 1940-1995 (data from Appendix C).

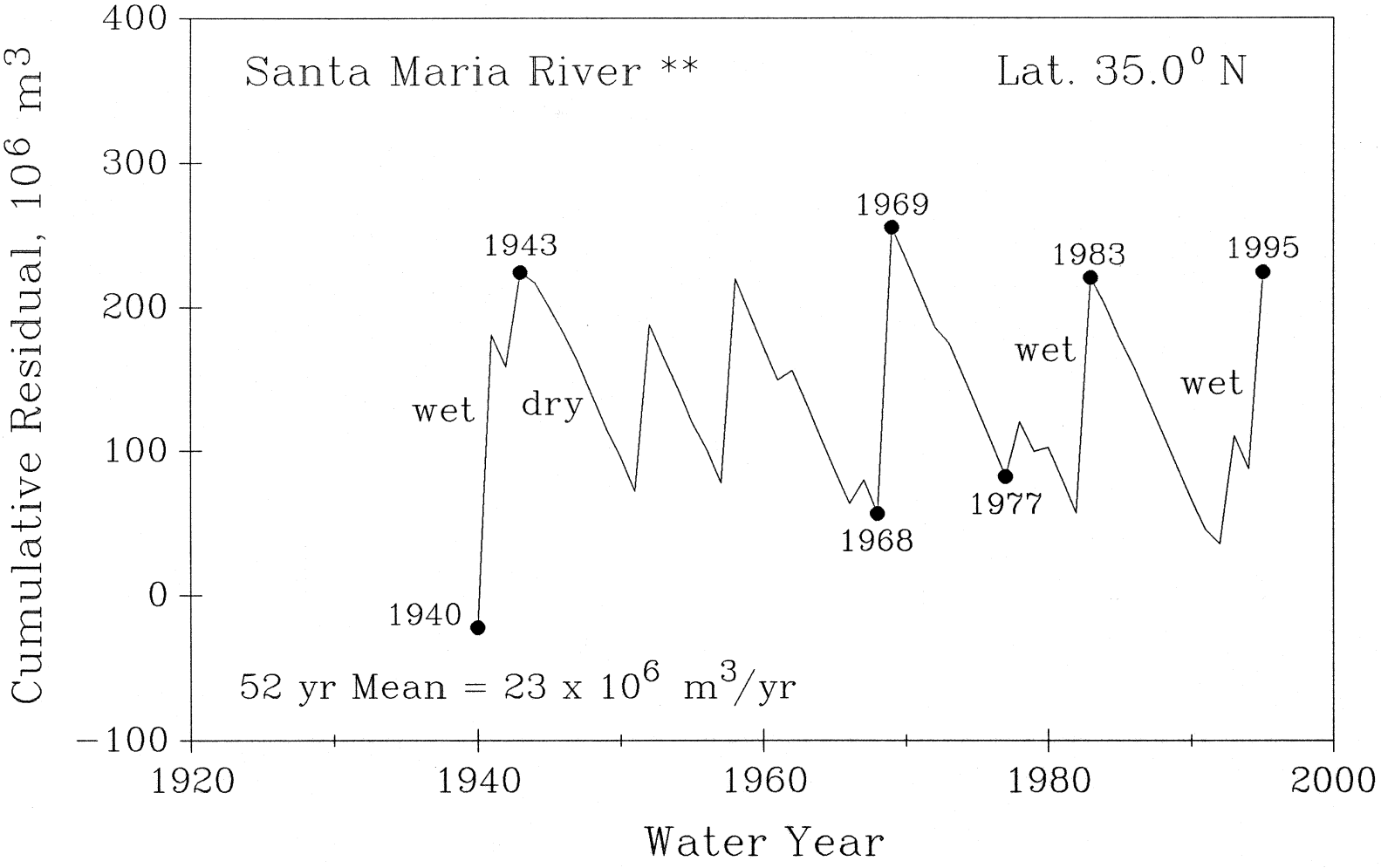

Figure 8 (4). Cumulative residual time series of streamflow for Santa Maria River calculated using a 52-year mean (1944-1995) over the period of record of 1940-1995 (data from Appendix C).

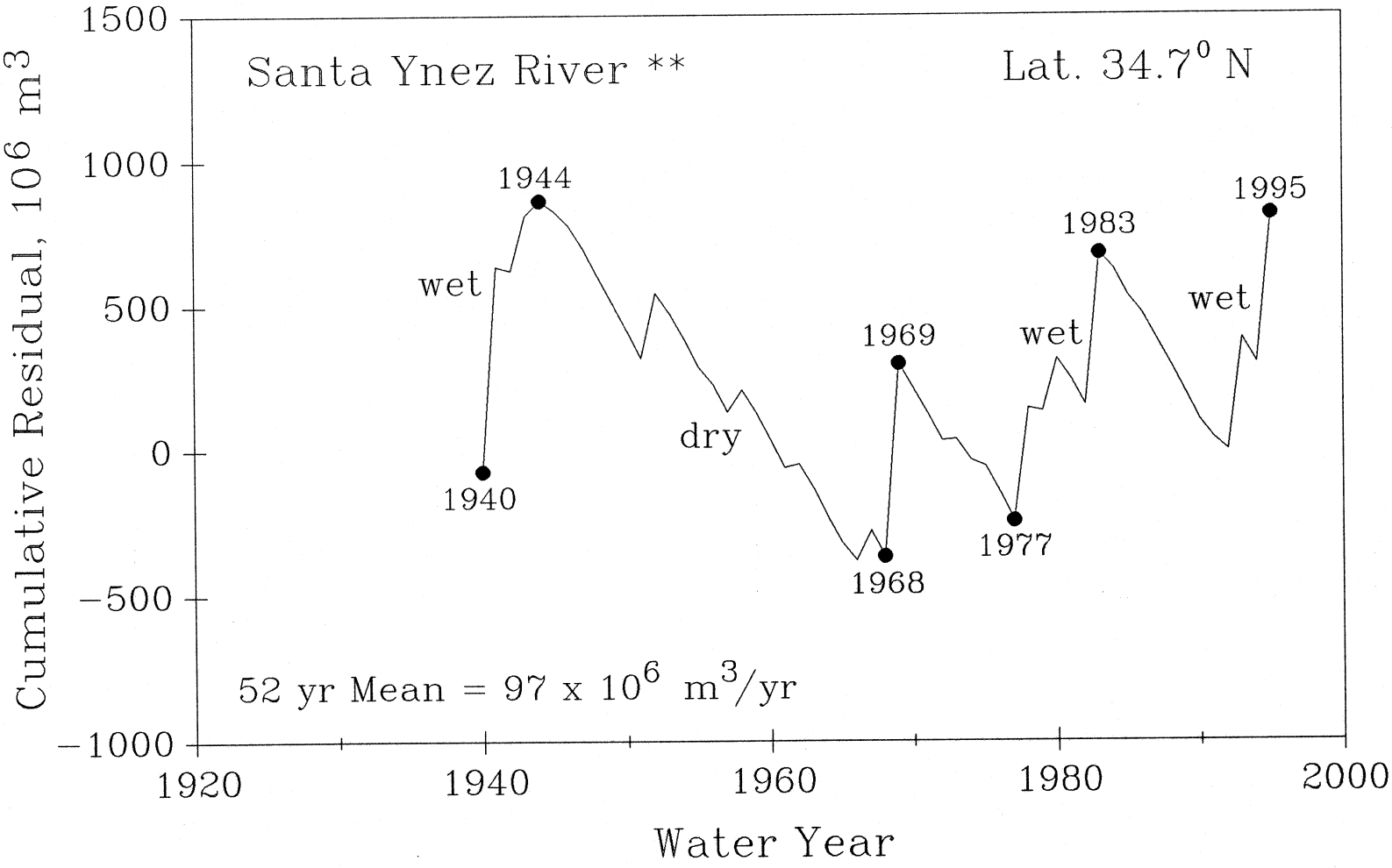

Figure 8 (5). Cumulative residual time series of streamflow for Santa Ynez River calculated using a 52-year mean (1944-1995) over the period of record of 1940-1995 (data from Appendix C).

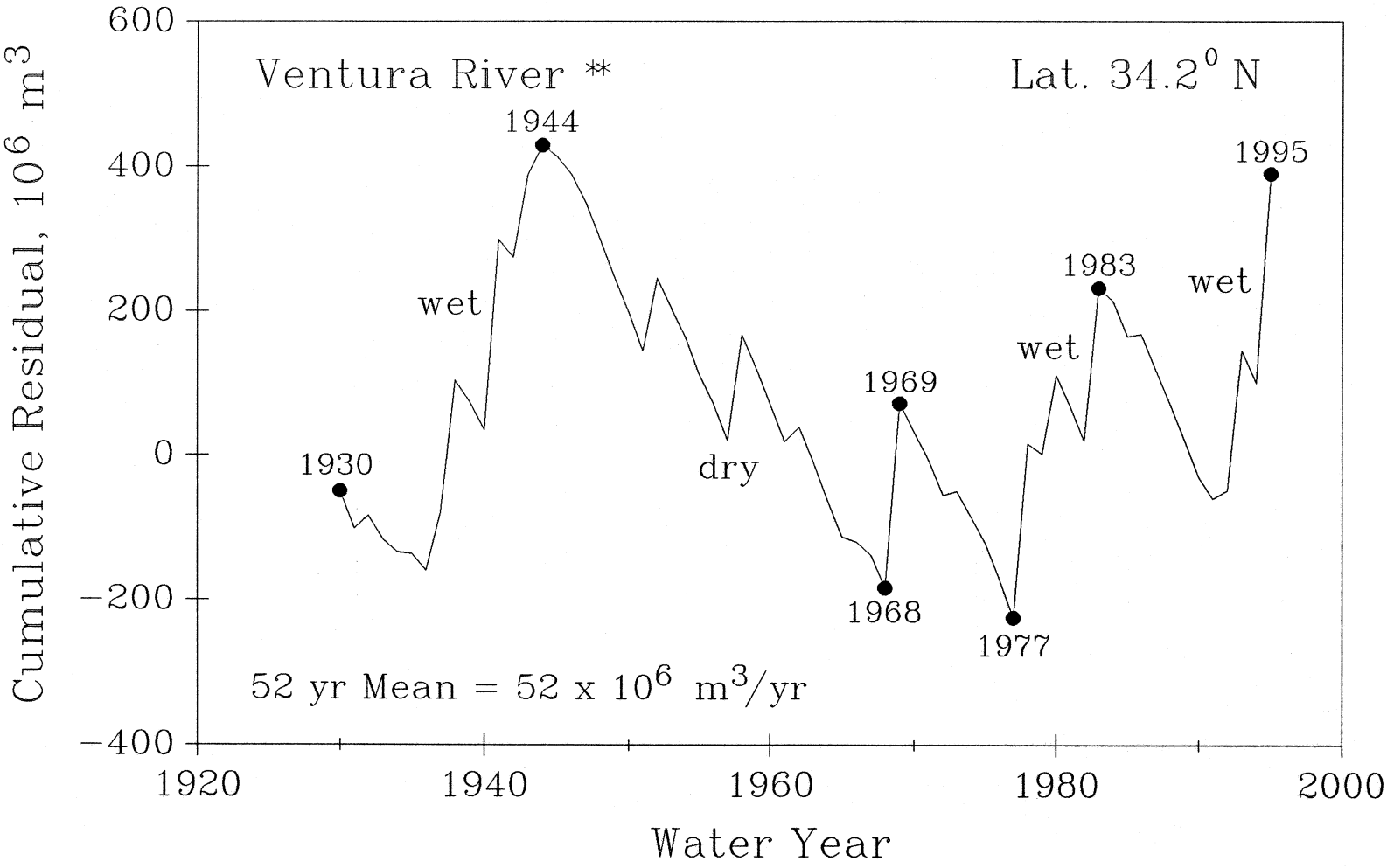

Figure 8 (6). Cumulative residual time series of streamflow for Ventura River calculated using a 52-year mean (1944-1995) over the period of record of 1940-1995 (data from Appendix C).

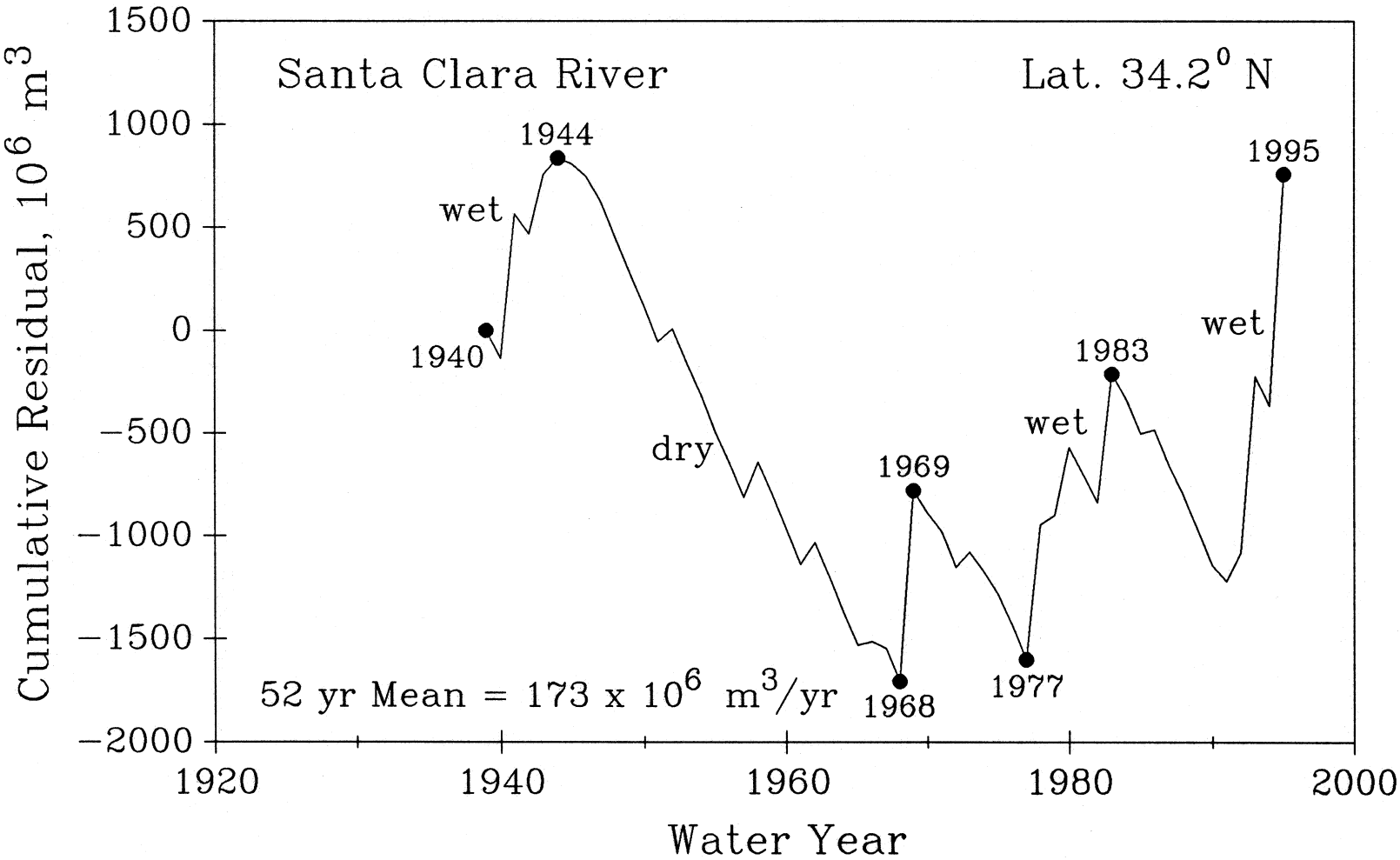

Figure 8 (7). Cumulative residual time series of streamflow for Santa Clara River calculated using a 52-year mean (1944-1995) over the period of record of 1940-1995 (data from Appendix C).

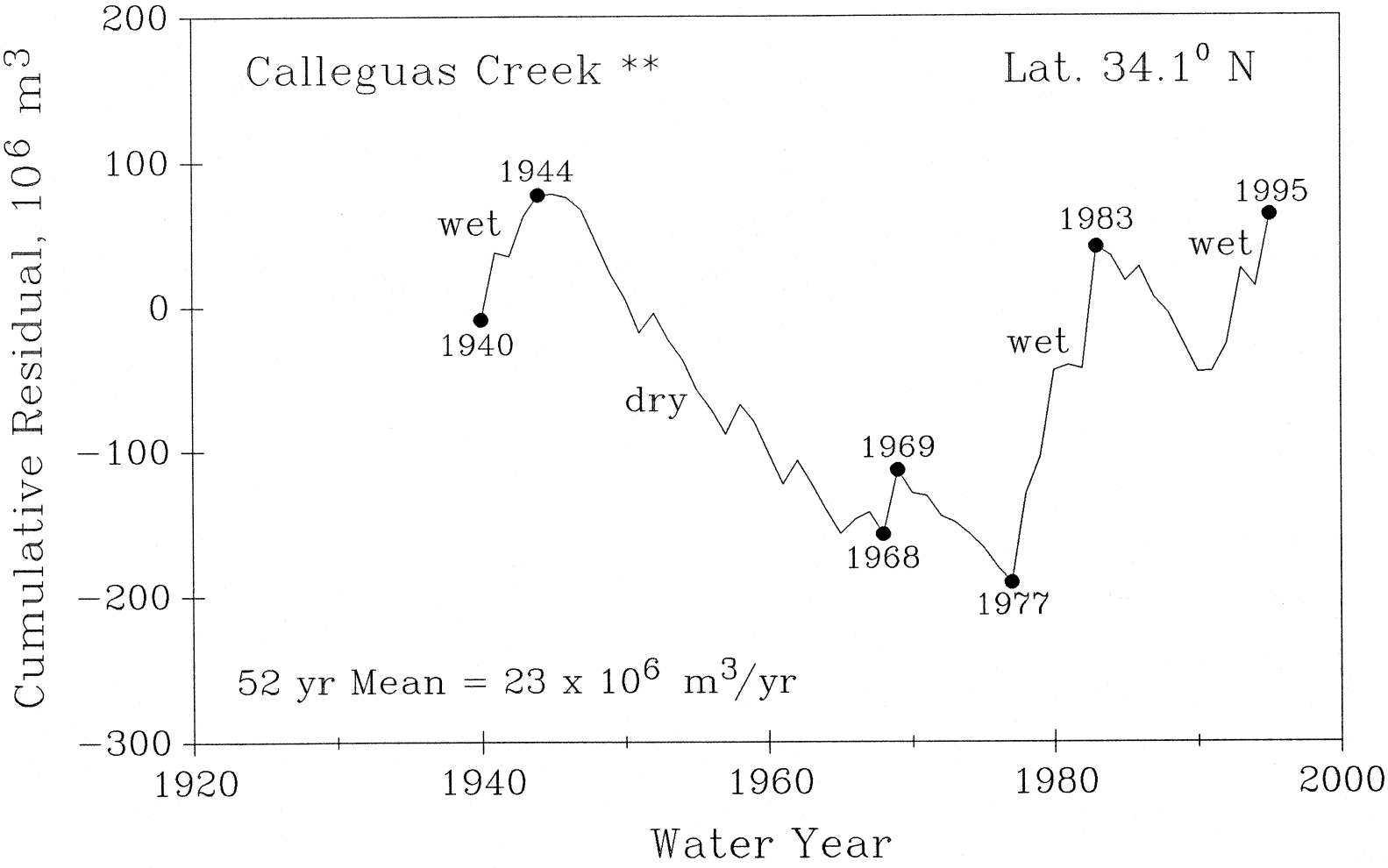

Figure 8 (8). Cumulative residual time series of streamflow for Calleguas Creek calculated using a 52-year mean (1944-1995) over the period of record of 1940-1995 (data from Appendix C).

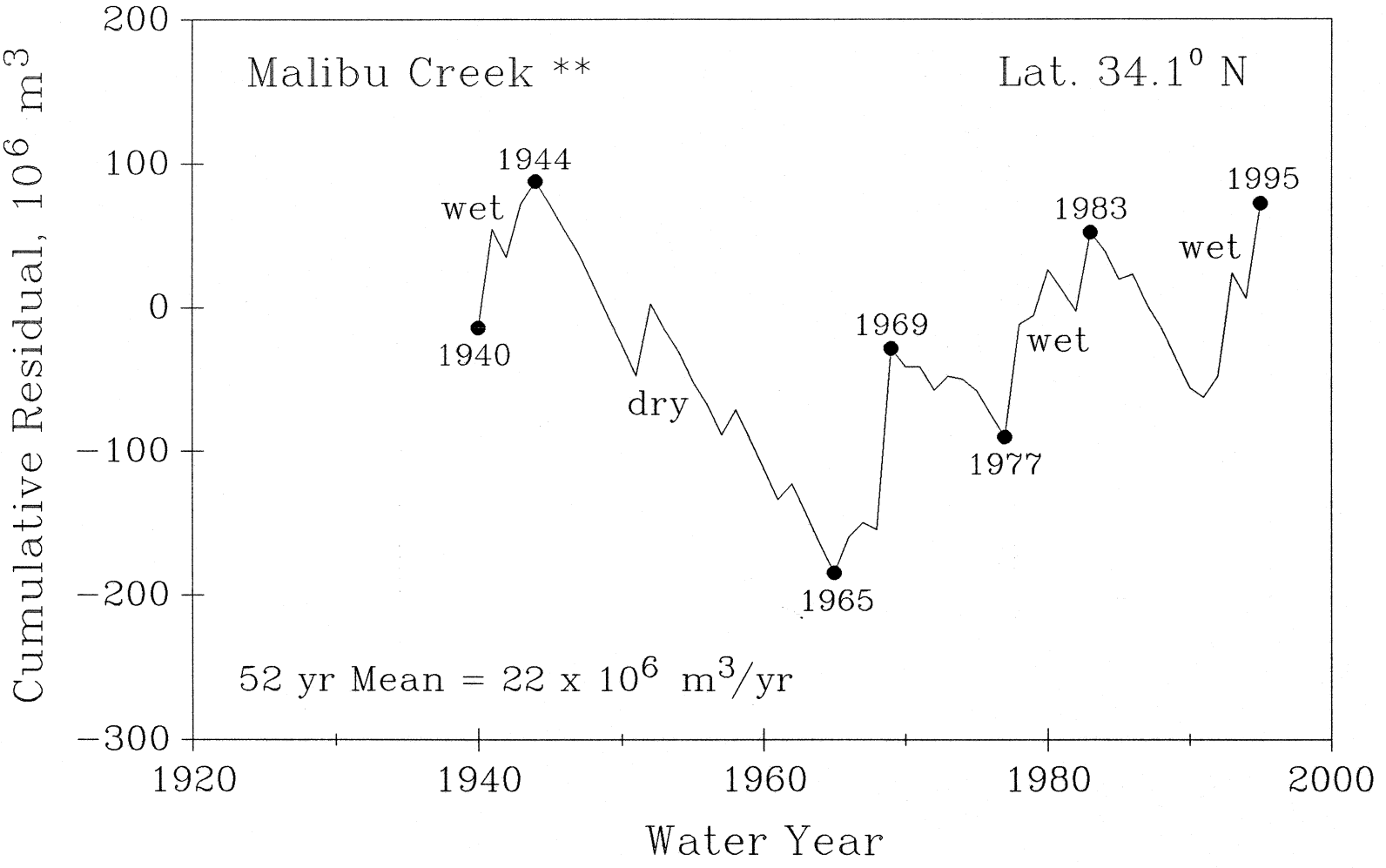

Figure 8 (9). Cumulative residual time series of streamflow for Malibu Creek calculated using a 52-year mean (1944-1995) over the period of record of 1940-1995 (data from Appendix C).

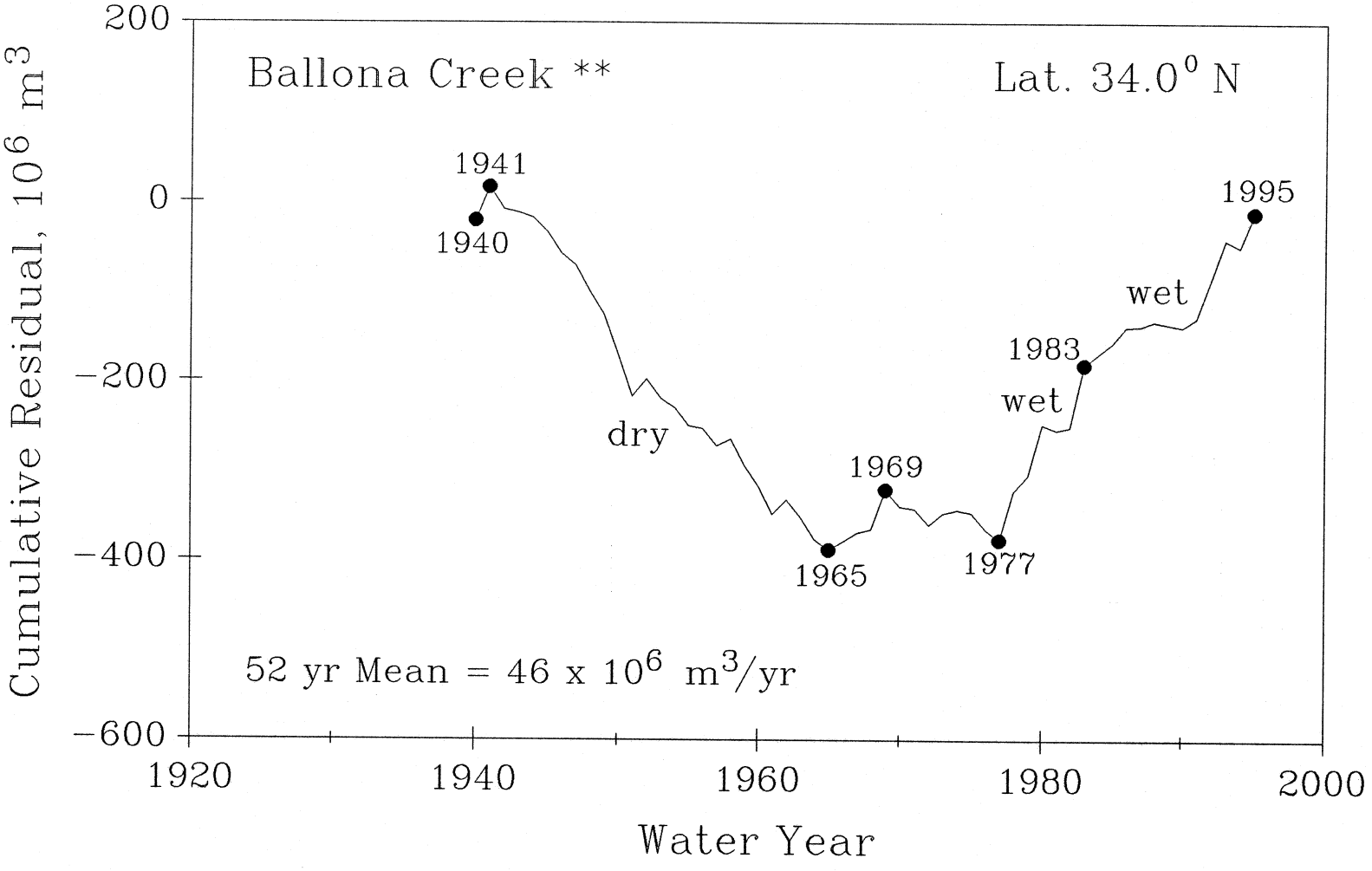

Figure 8 (10). Cumulative residual time series of streamflow for Ballona Creek calculated using a 52-year mean (1944-1995) over the period of record of 1940-1995 (data from Appendix C).

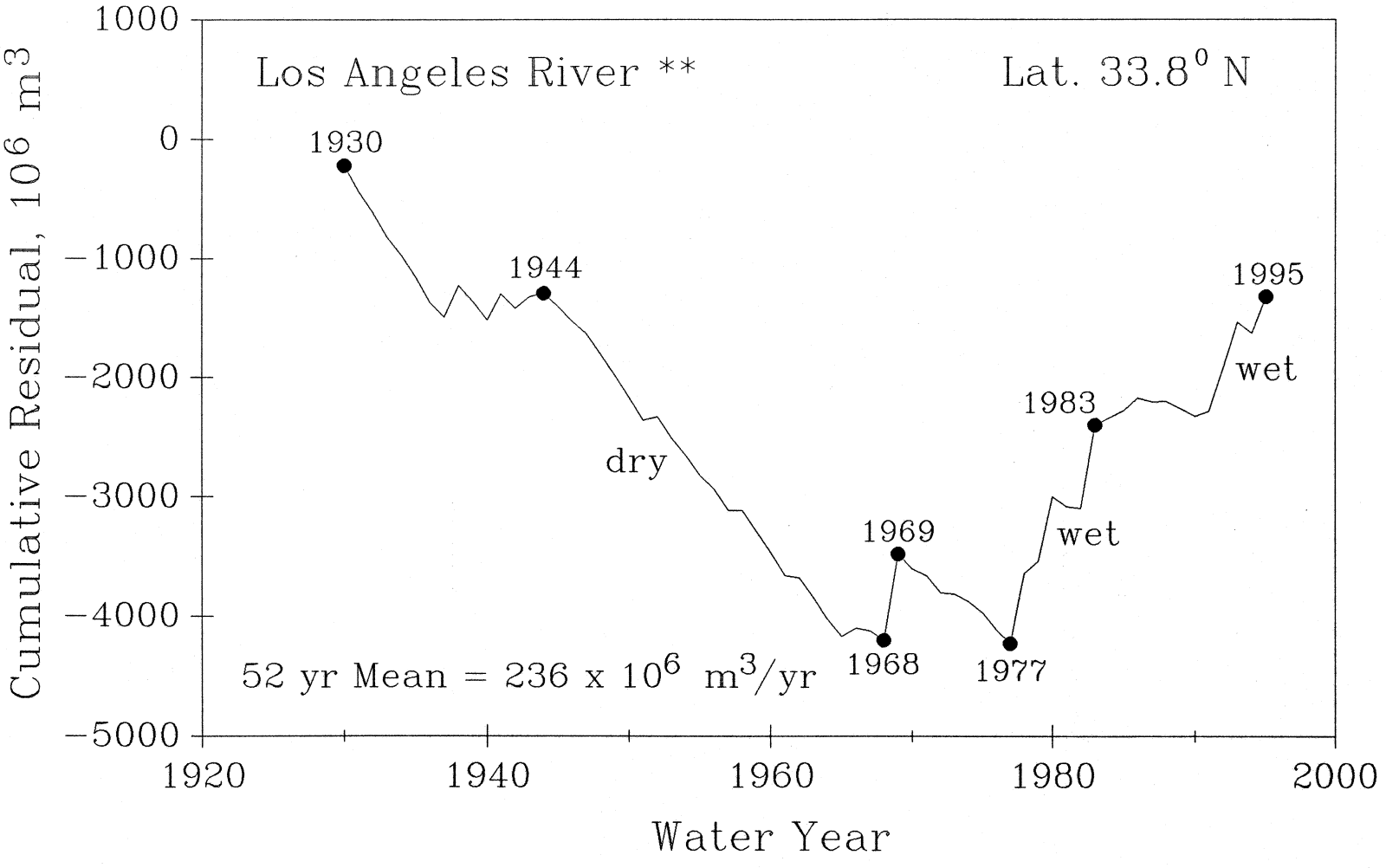

Figure 8 (11). Cumulative residual time series of streamflow for Los Angeles River calculated using a 52-year mean (1944-1995) over the period of record of 1940-1995 (data from Appendix C).

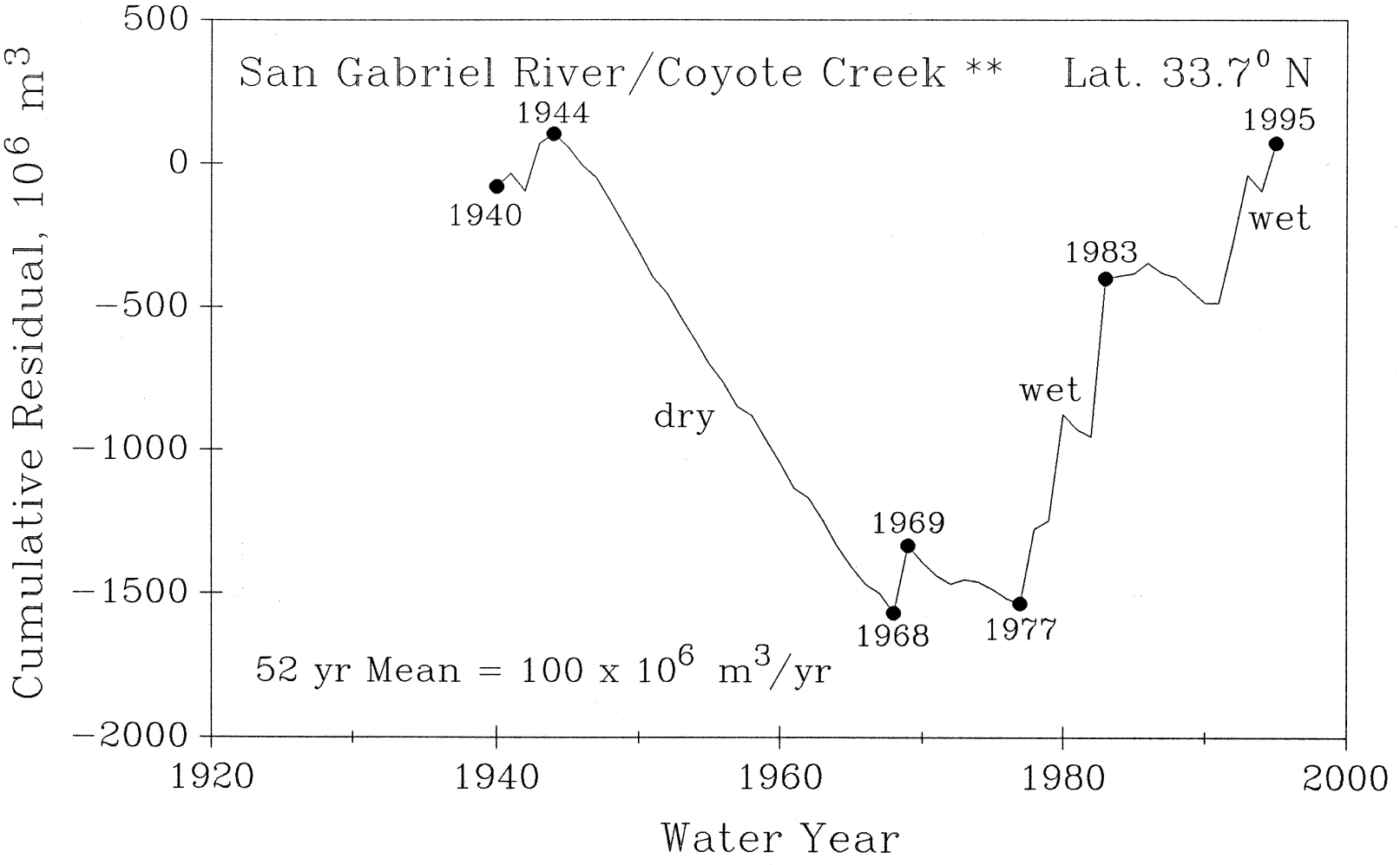

Figure 8 (12). Cumulative residual time series of streamflow for San Gabriel River/Coyote Creek calculated using a 52-year mean (1944-1995) over the period of record of 1940-1995 (data from Appendix C).

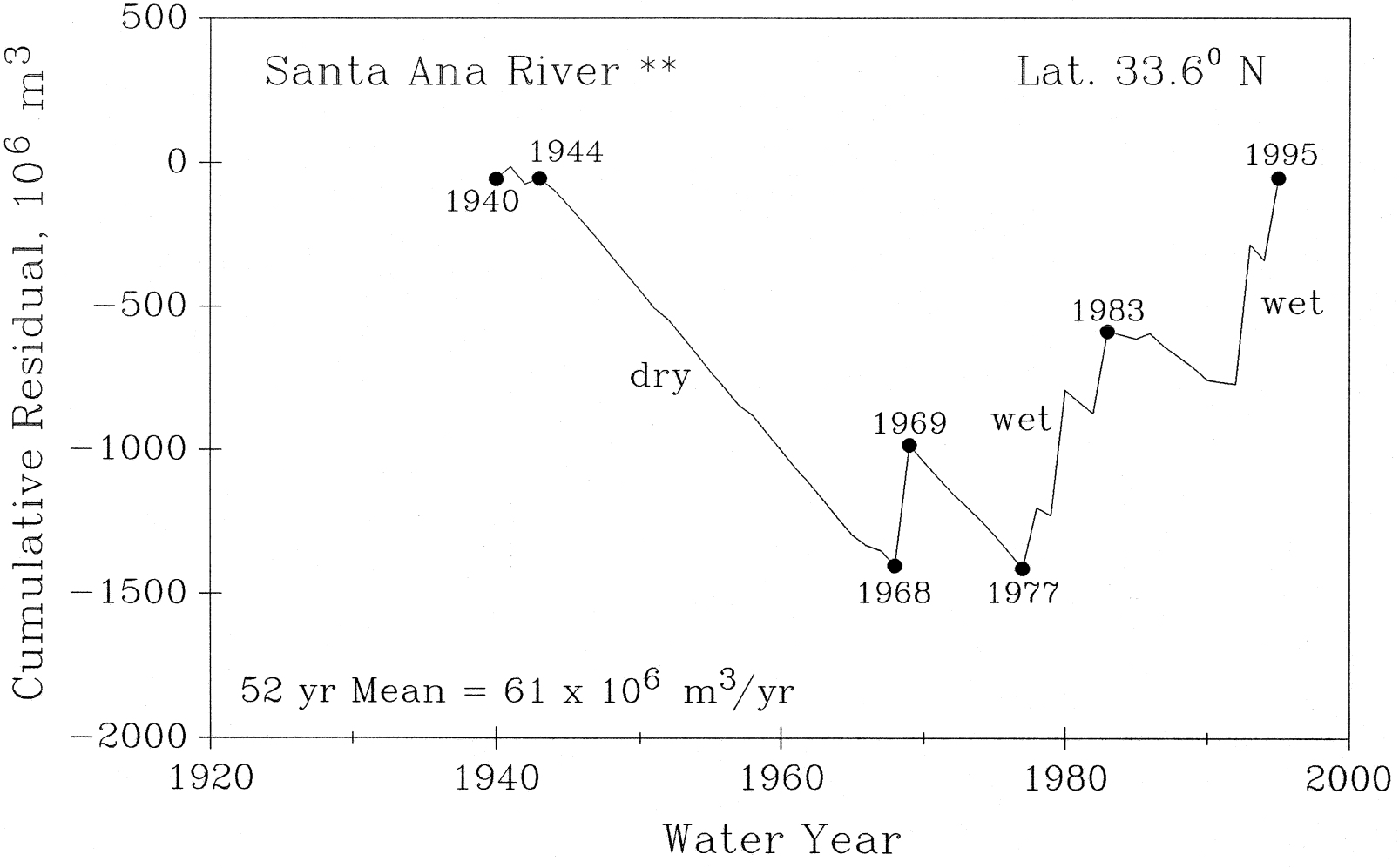

Figure 8 (13). Cumulative residual time series of streamflow for Santa Ana River calculated using a 52-year mean (1944-1995) over the period of record of 1940-1995 (data from Appendix C).

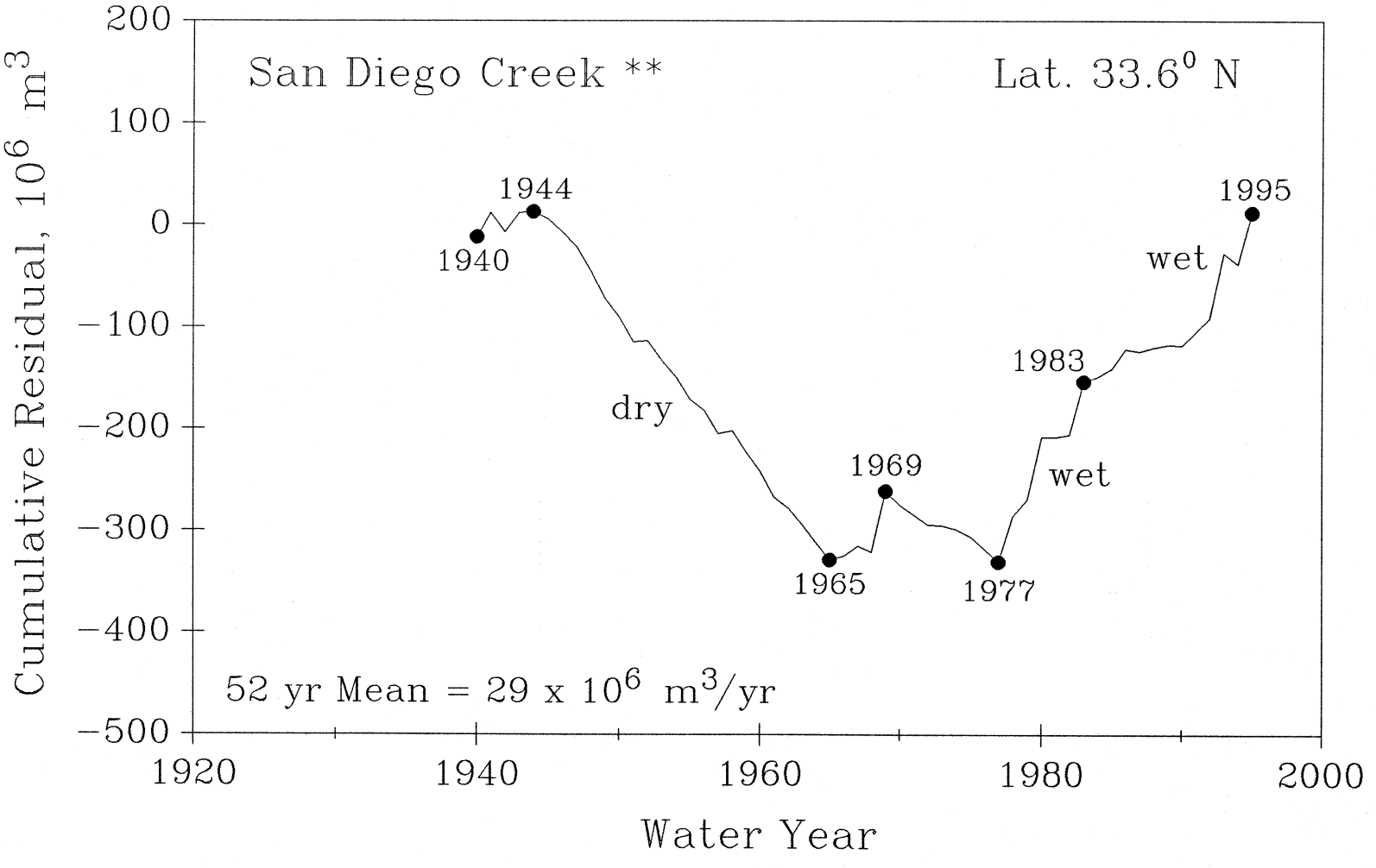

Figure 8 (14). Cumulative residual time series of streamflow for San Diego Creek calculated using a 52-year mean (1944-1995) over the period of record of 1940-1995 (data from Appendix C).

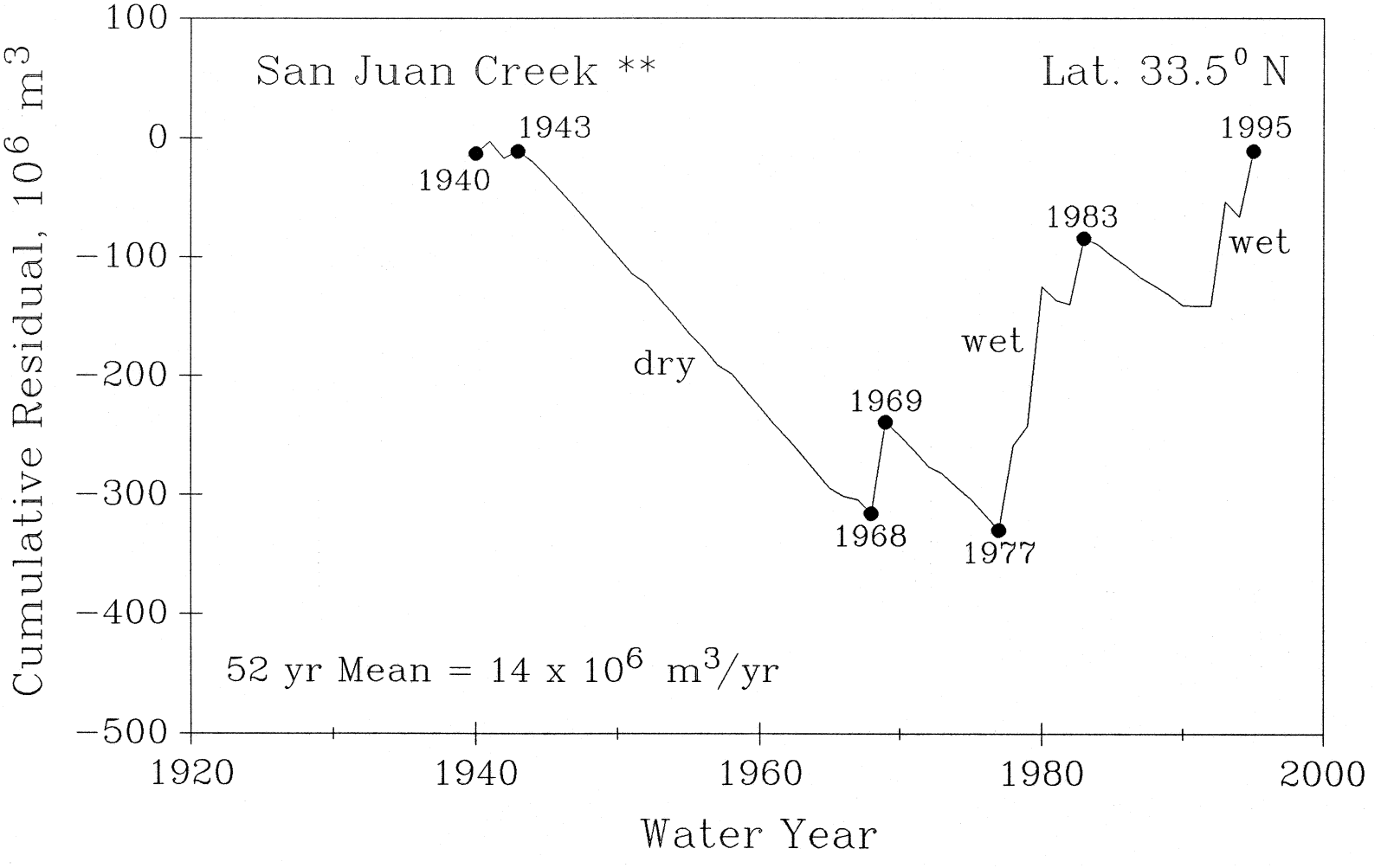

Figure 8 (15). Cumulative residual time series of streamflow for San Juan Creek calculated using a 52-year mean (1944-1995) over the period of record of 1940-1995 (data from Appendix C).

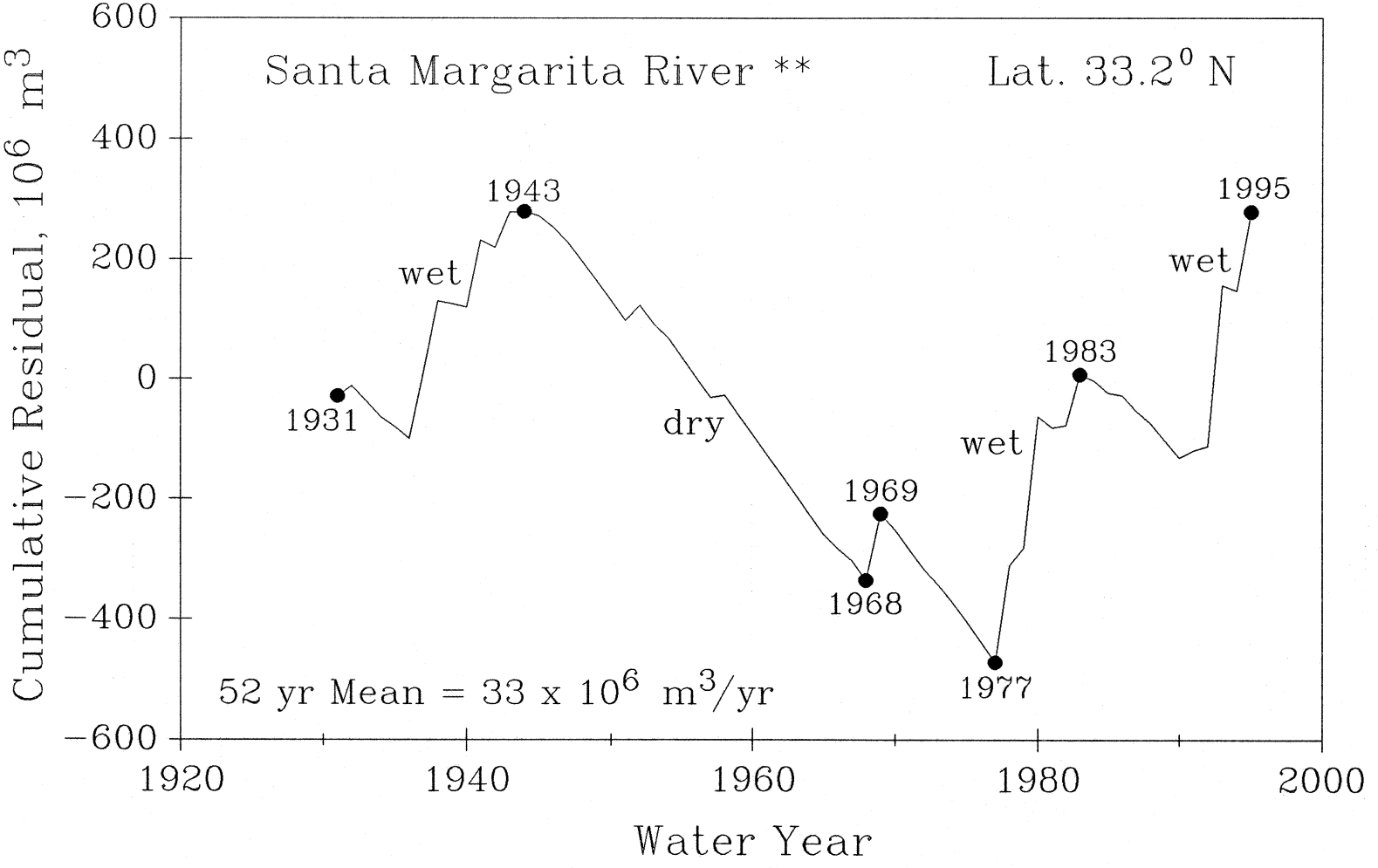

Figure 8 (16). Cumulative residual time series of streamflow for Santa Margarita River calculated using a 52-year mean (1944-1995) over the period of record of 1940-1995 (data from Appendix C).

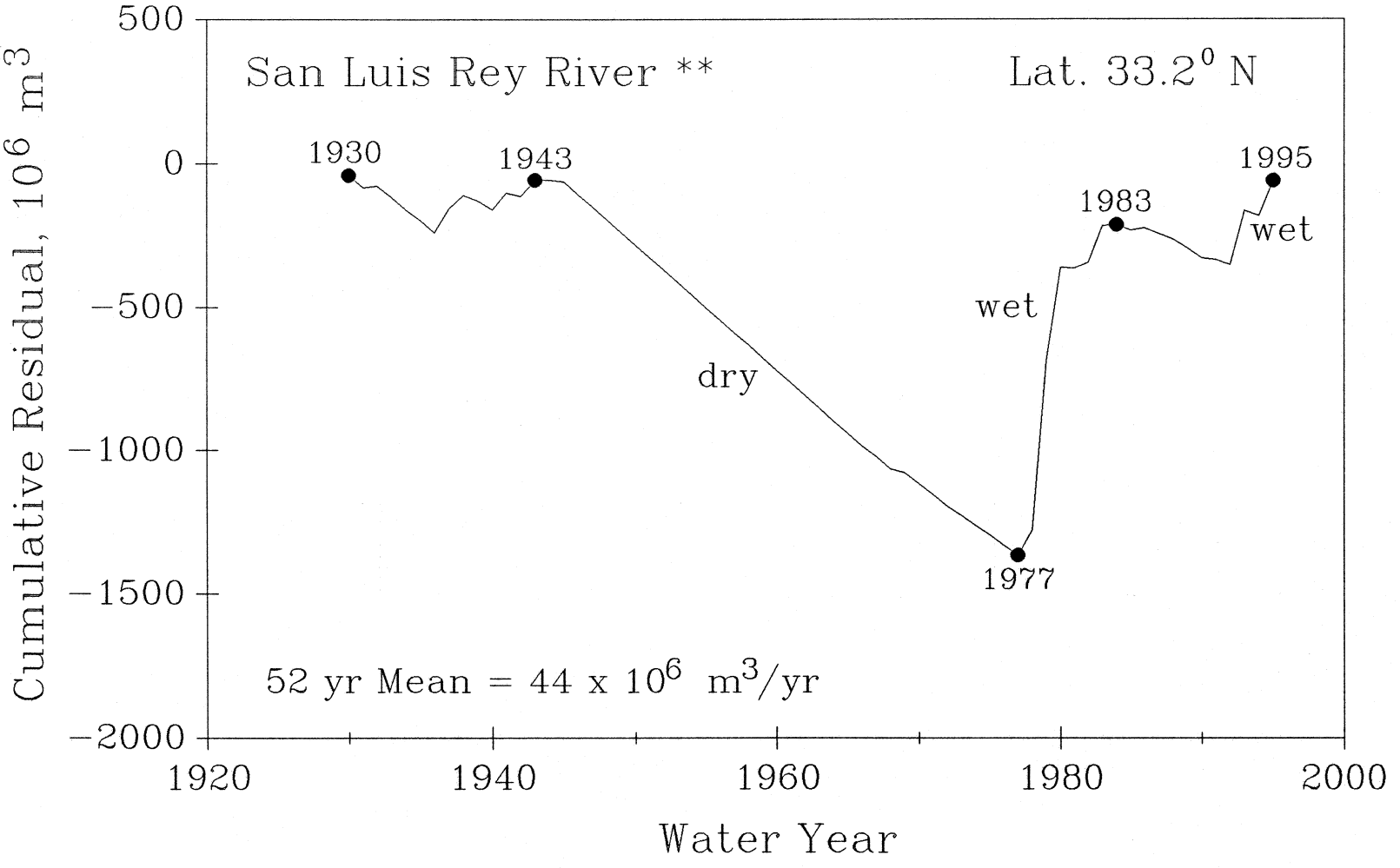

Figure 8 (17). Cumulative residual time series of streamflow for San Luis Rey River calculated using a 52-year mean (1944-1995) over the period of record of 1940-1995 (data from Appendix C).

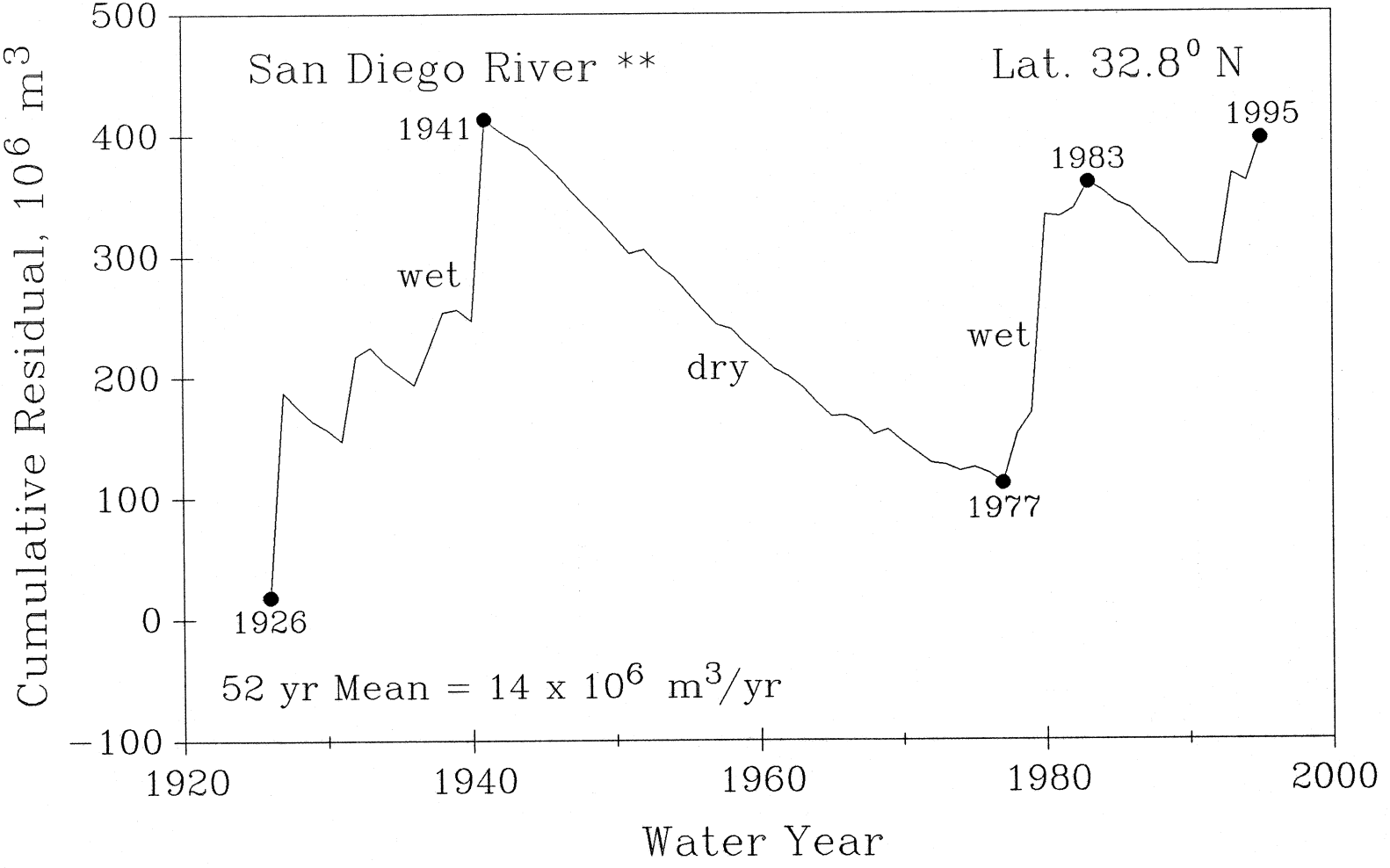

Figure 8 (18). Cumulative residual time series of streamflow for San Diego River calculated using a 52-year mean (1944-1995) over the period of record of 1940-1995 (data from Appendix C).

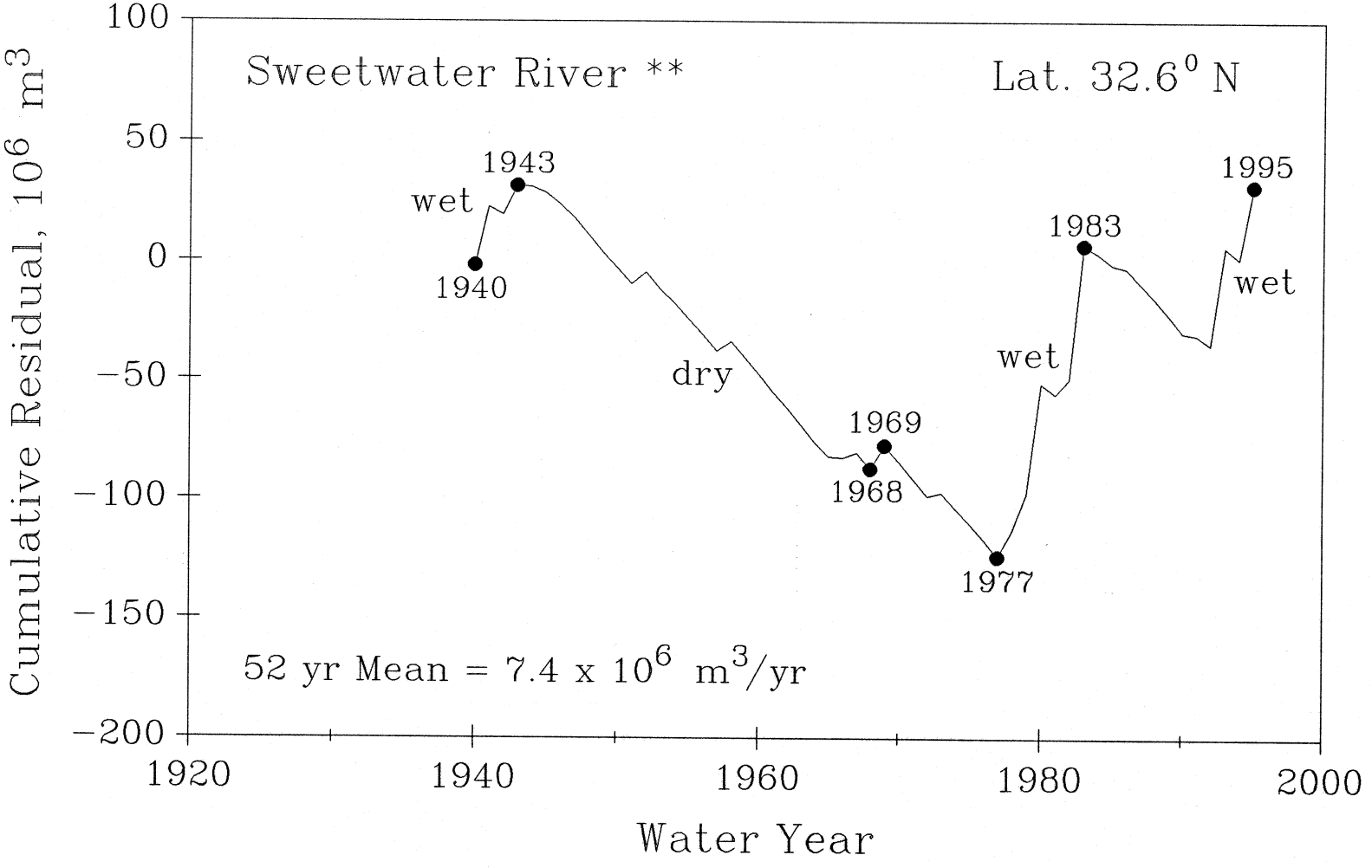

Figure 8 (19). Cumulative residual time series of streamflow for Sweetwater River calculated using a 52-year mean (1944-1995) over the period of record of 1940-1995 (data from Appendix C).

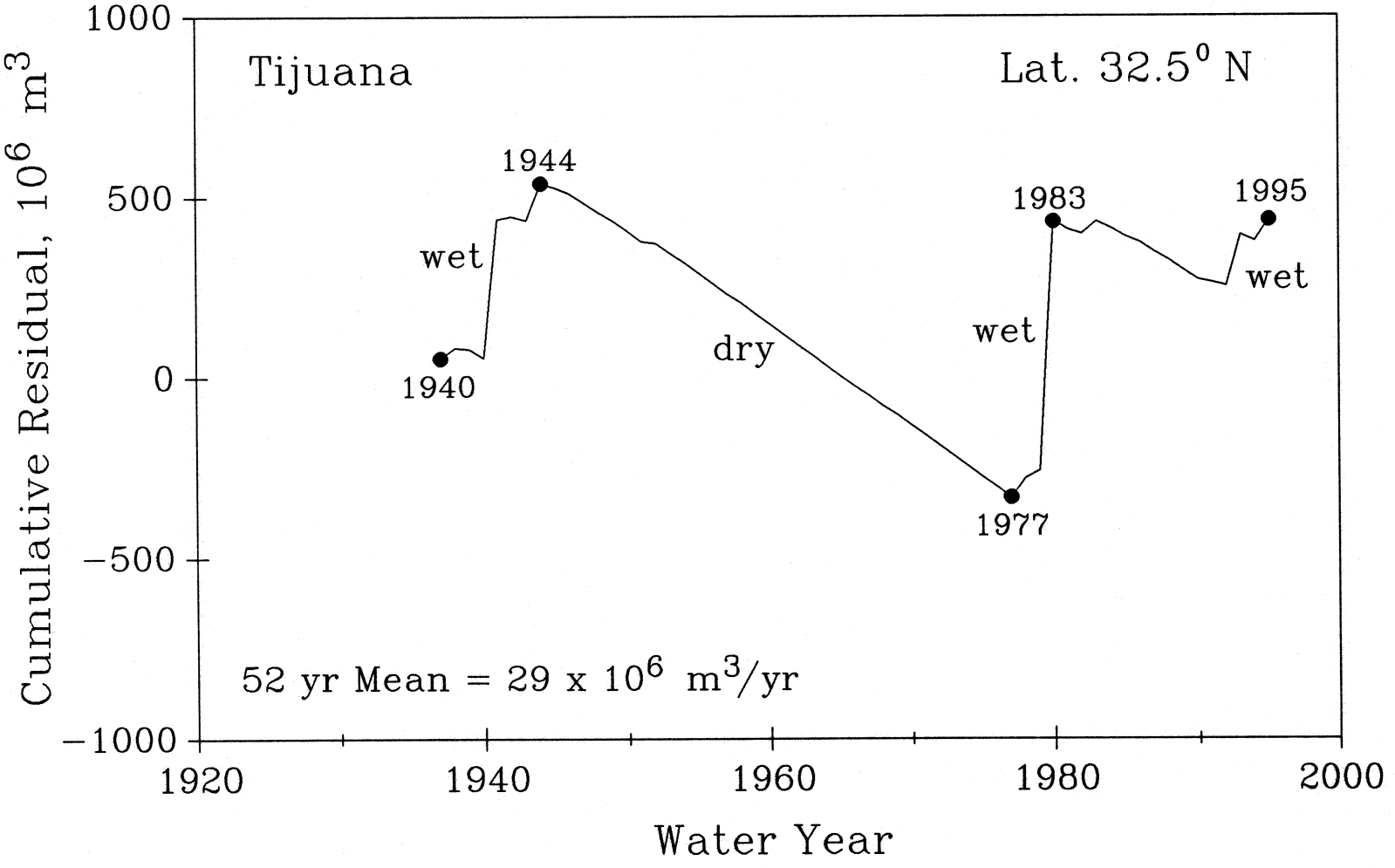

Figure 8 (20). Cumulative residual time series of streamflow for Tijuana River calculated using a 52-year mean (1944-1995) over the period of record of 1940-1995 (data from Appendix C).

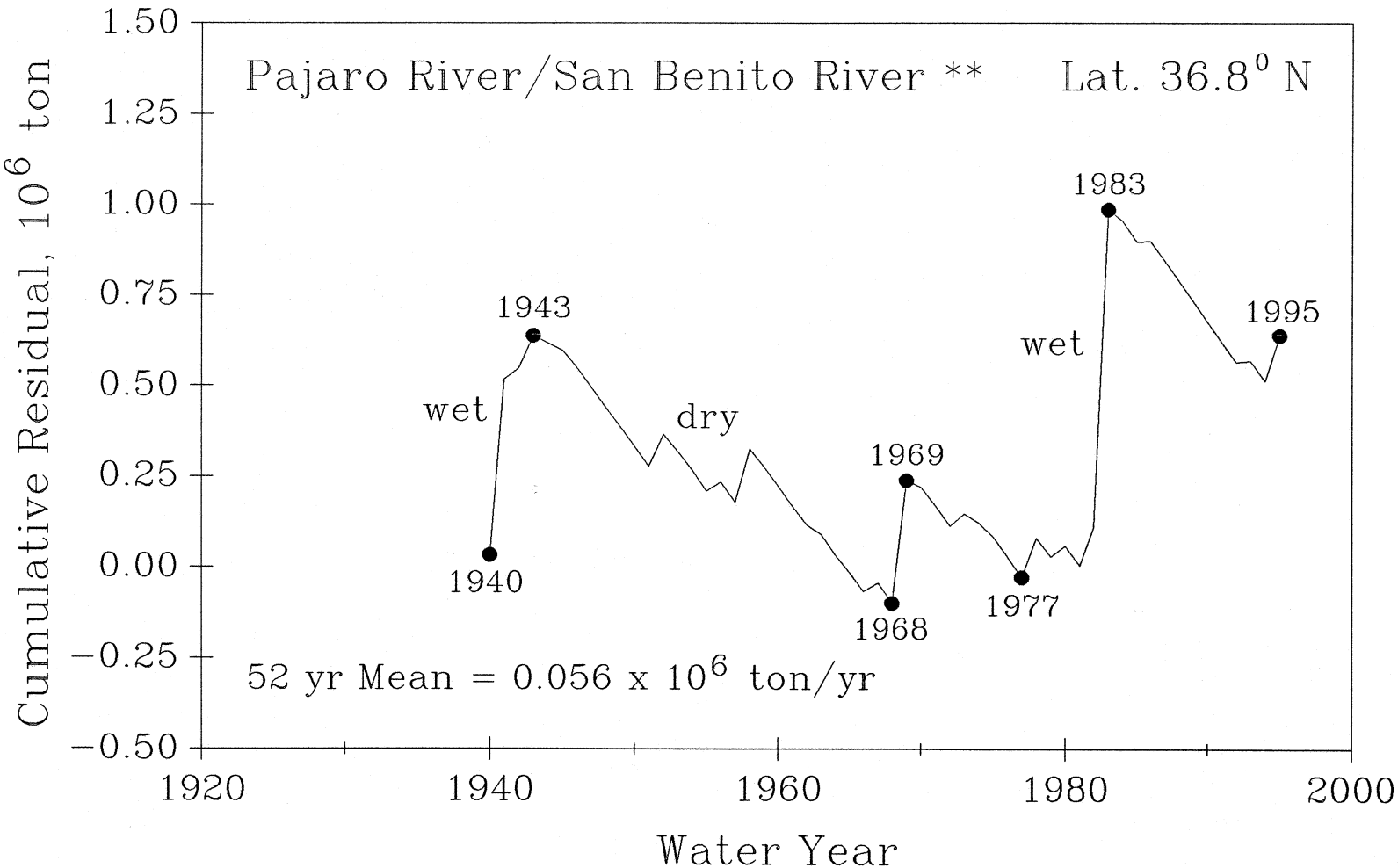

Figure 9 (1). Cumulative residual time series of sediment flux for Pajaro River calculated using a 52-year mean (1944-1995) over the period of record of 1940-1995 (data from Appendix C).

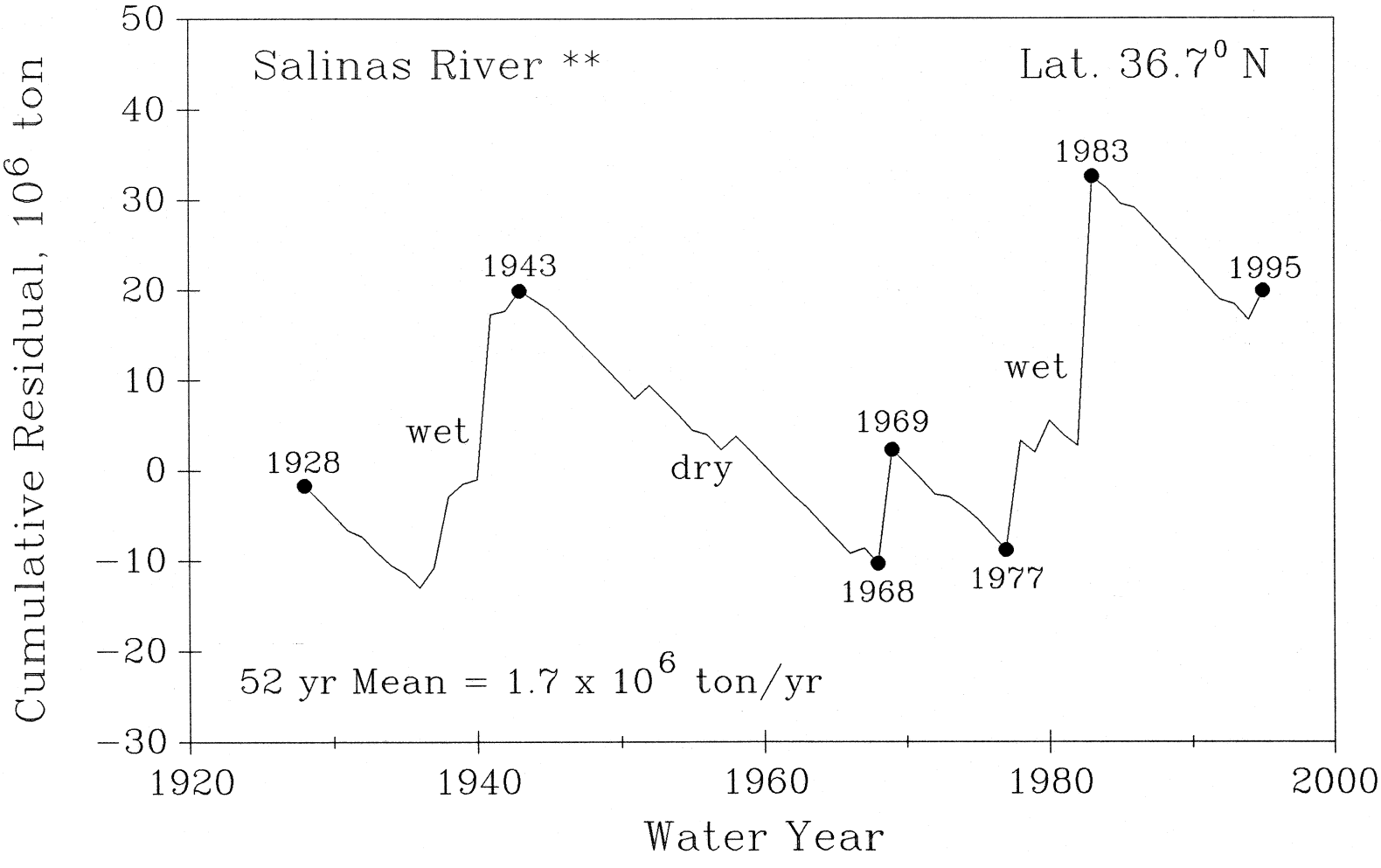

Figure 9 (2). Cumulative residual time series of sediment flux for Salinas River calculated using a 52-year mean (1944-1995) over the period of record of 1940-1995 (data from Appendix C).

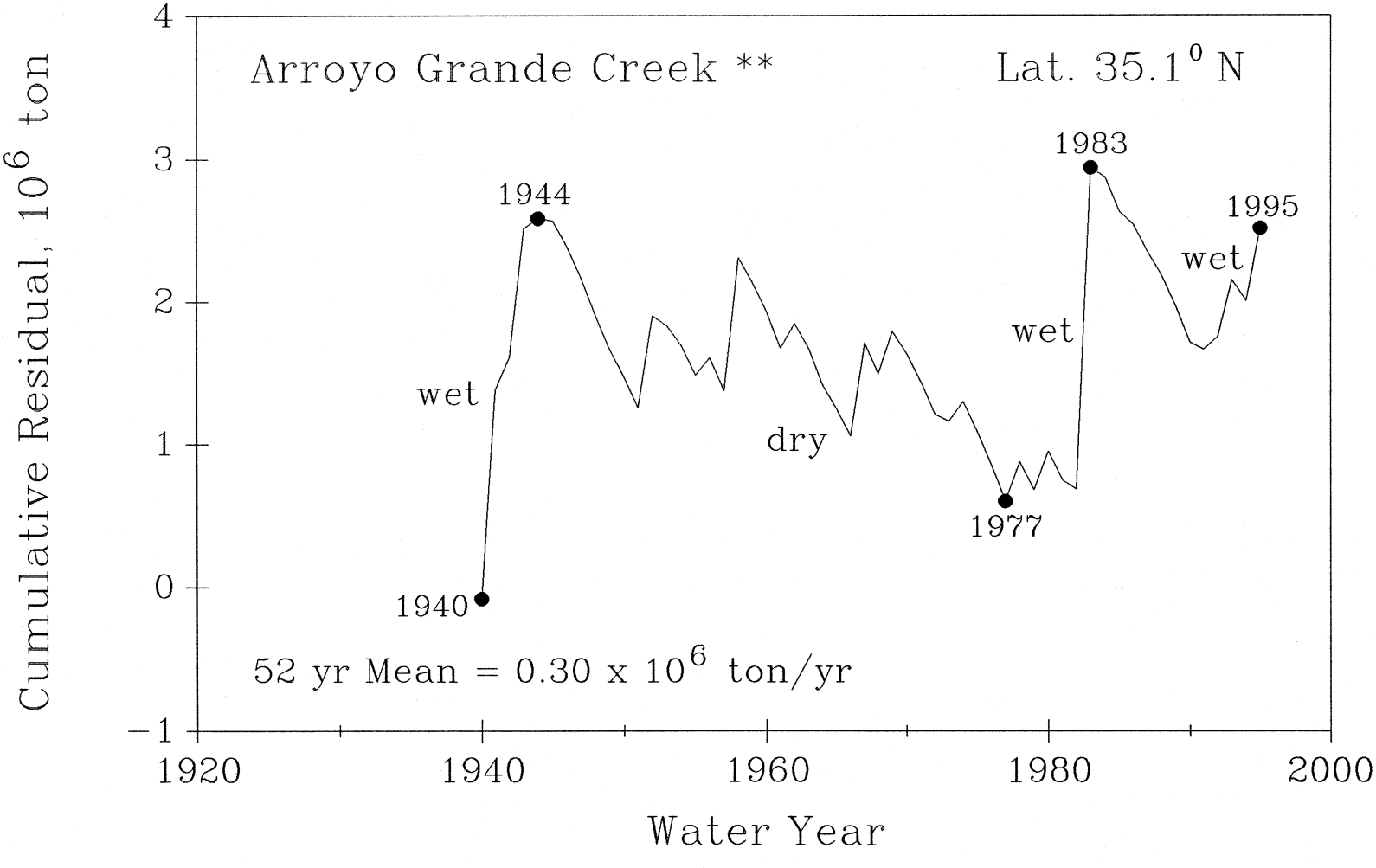

Figure 9 (3). Cumulative residual time series of sediment flux for Arroyo Grande Creek calculated using a 52-year mean (1944-1995) over the period of record of 1940-1995 (data from Appendix C).

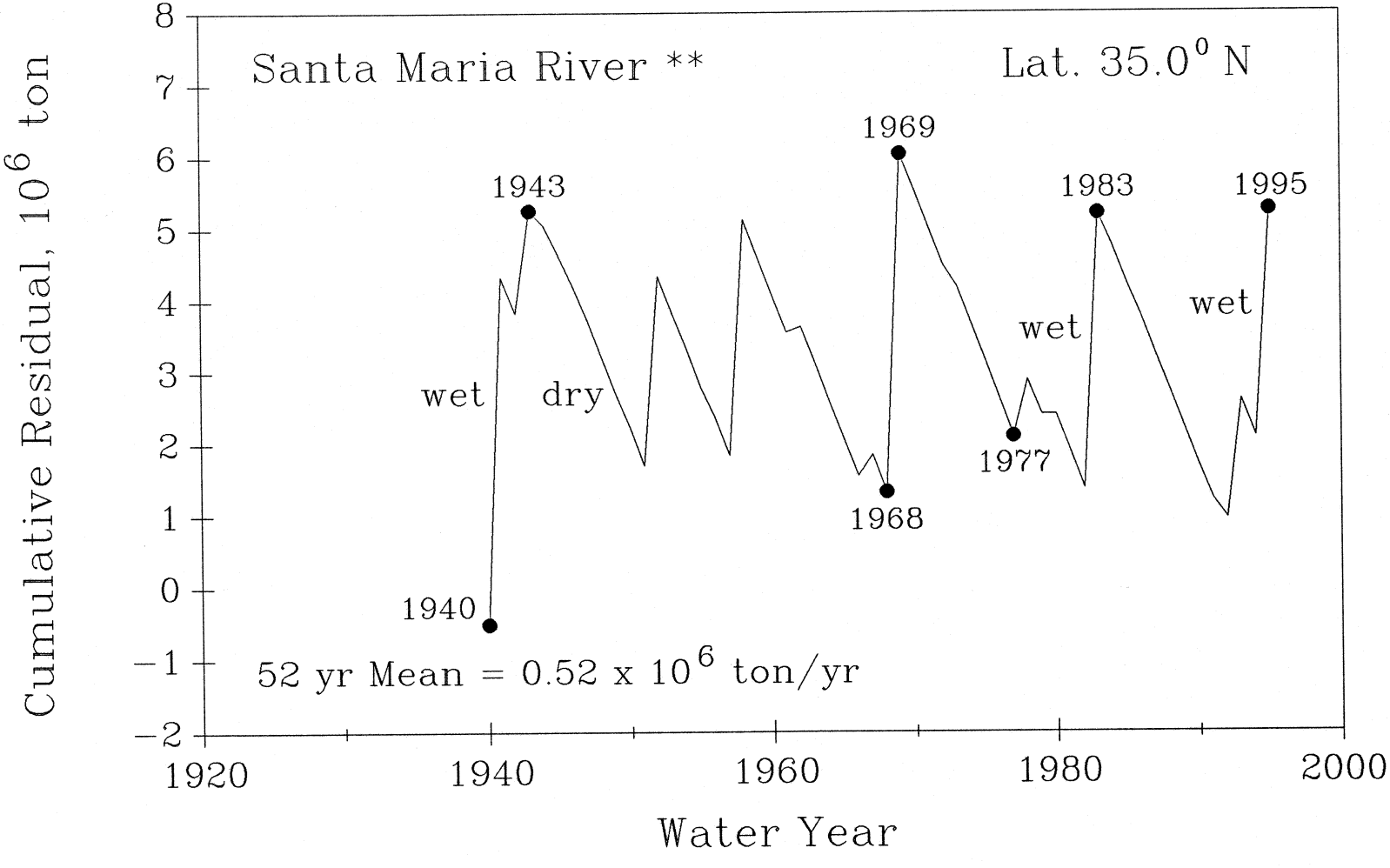

Figure 9 (4). Cumulative residual time series of sediment flux for Santa Maria River calculated using a 52-year mean (1944-1995) over the period of record of 1940-1995 (data from Appendix C).

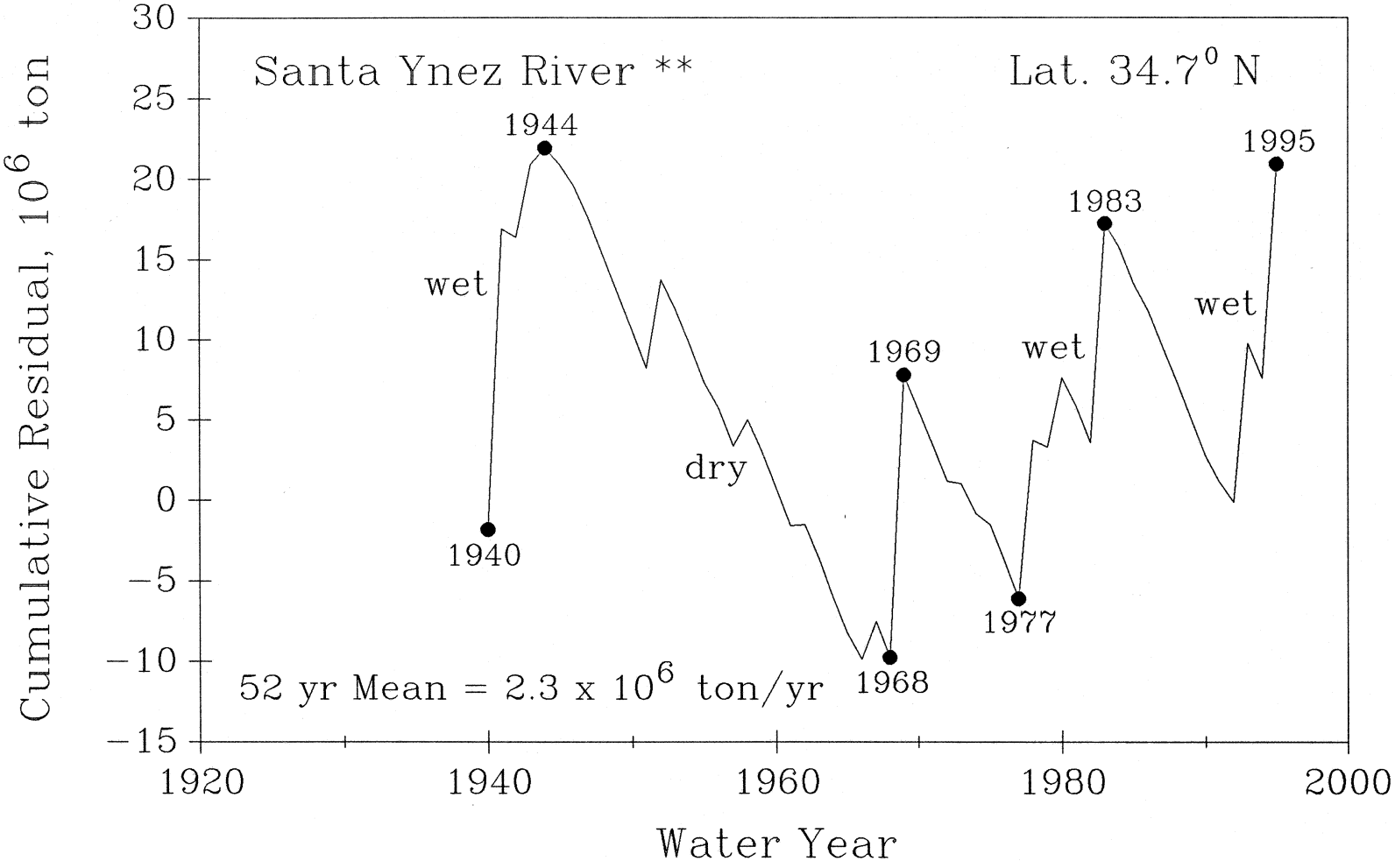

Figure 9 (5). Cumulative residual time series of sediment flux for Santa Ynez River calculated using a 52-year mean (1944-1995) over the period of record of 1940-1995 (data from Appendix C).

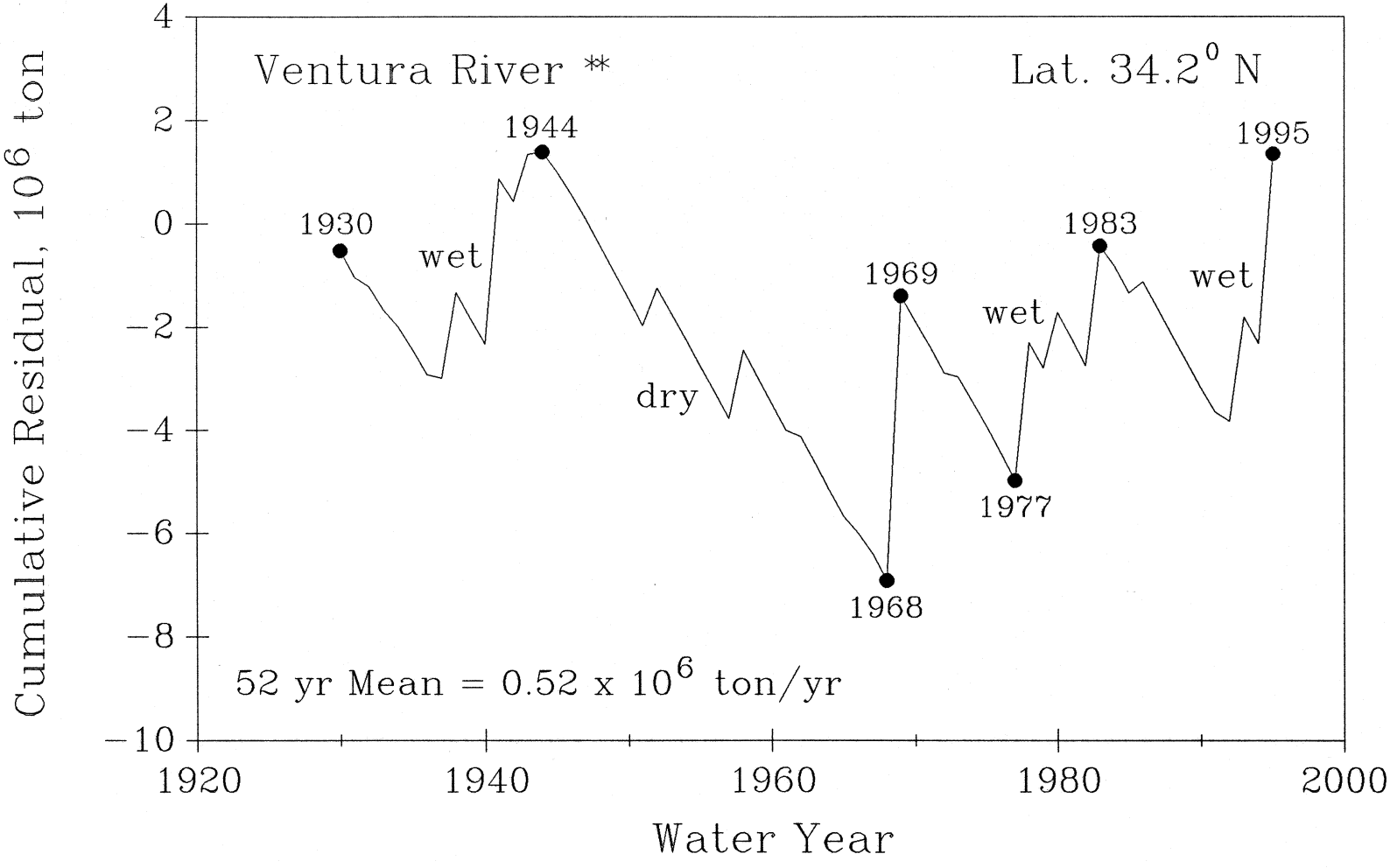

Figure 9 (6). Cumulative residual time series of sediment flux for Ventura River calculated using a 52-year mean (1944-1995) over the period of record of 1940-1995 (data from Appendix C).

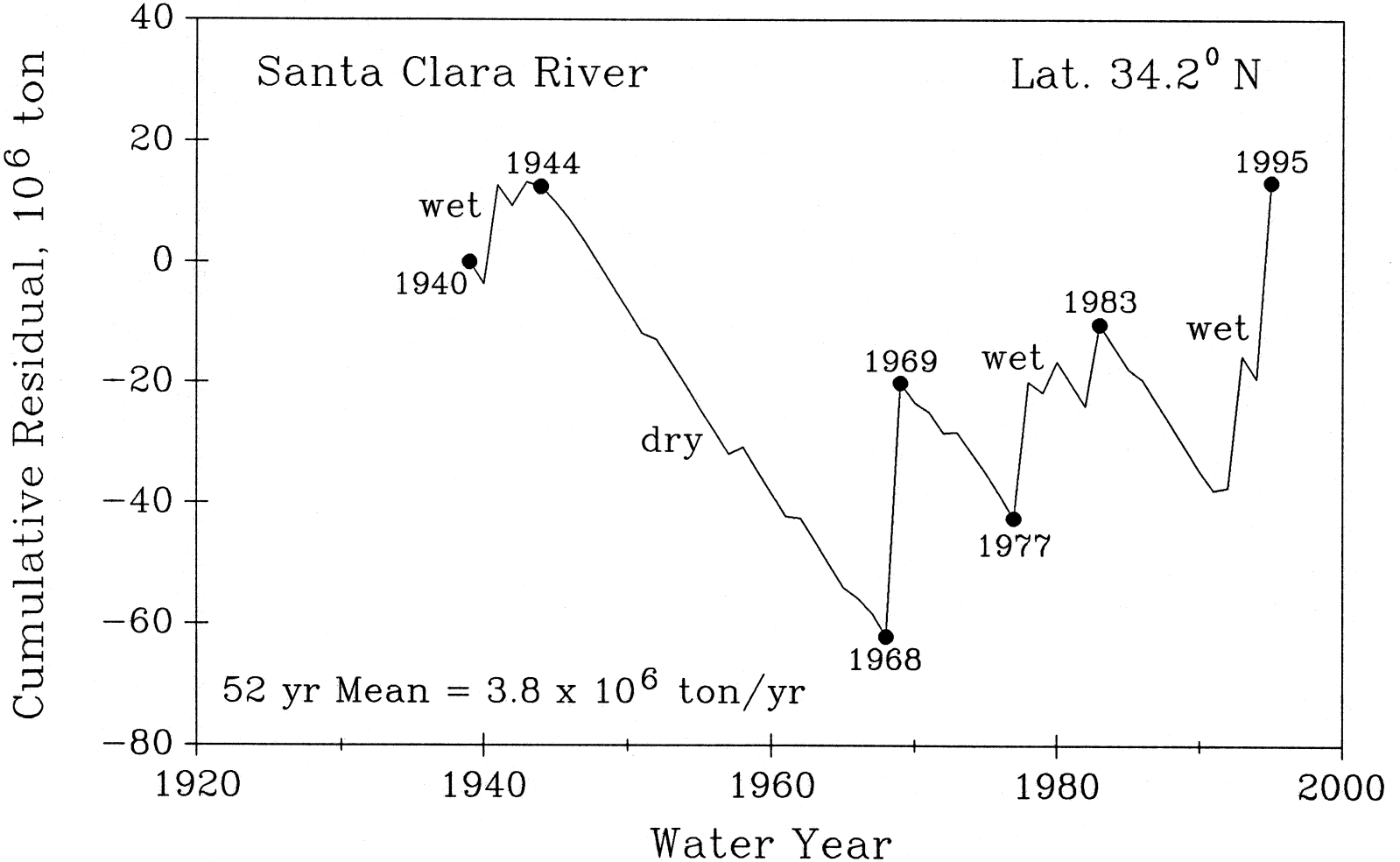

Figure 9 (7). Cumulative residual time series of sediment flux for Santa Clara River calculated using a 52-year mean (1944-1995) over the period of record of 1940-1995 (data from Appendix C).

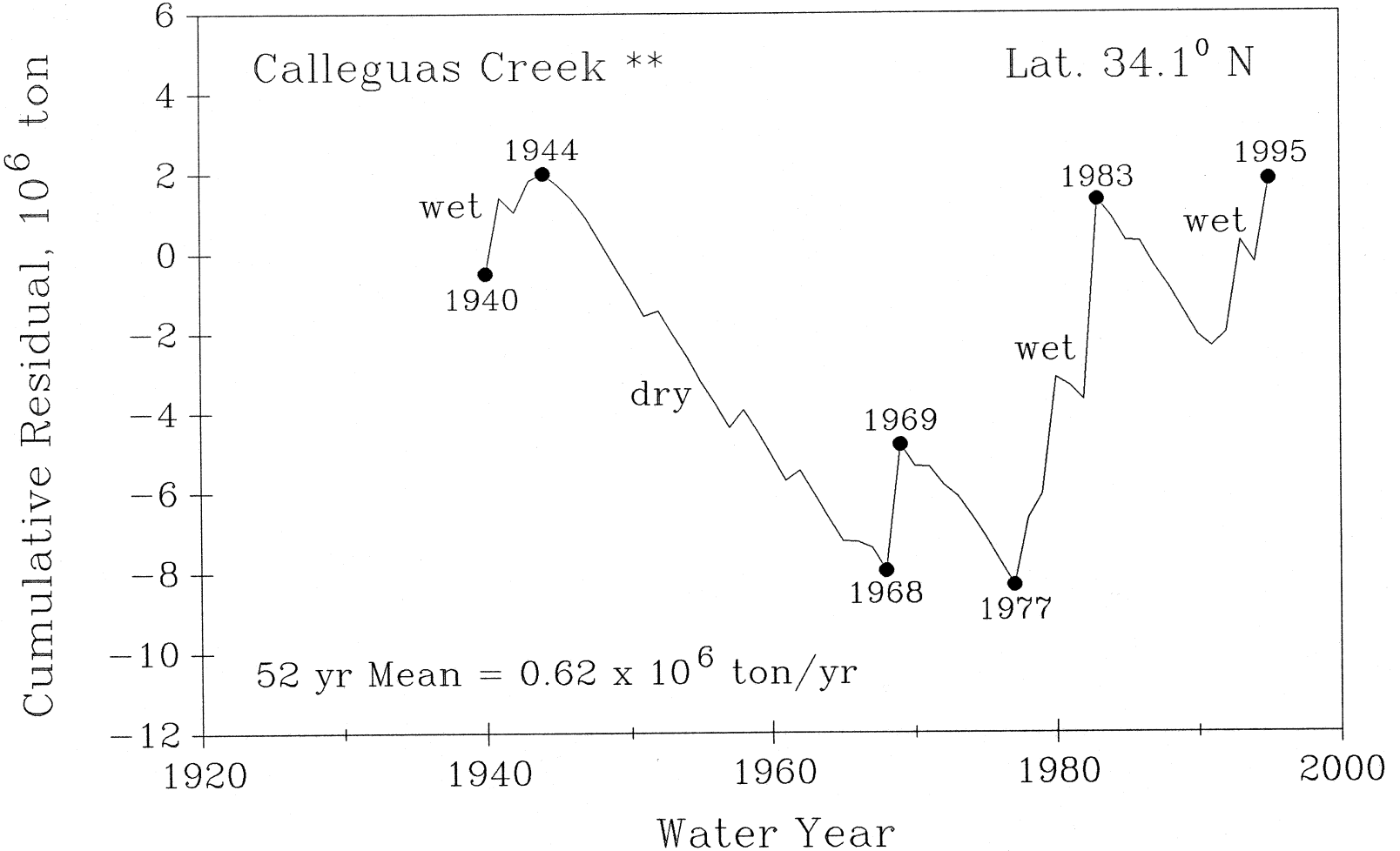

Figure 9 (8). Cumulative residual time series of sediment flux for Calleguas Creek calculated using a 52-year mean (1944-1995) over the period of record of 1940-1995 (data from Appendix C).

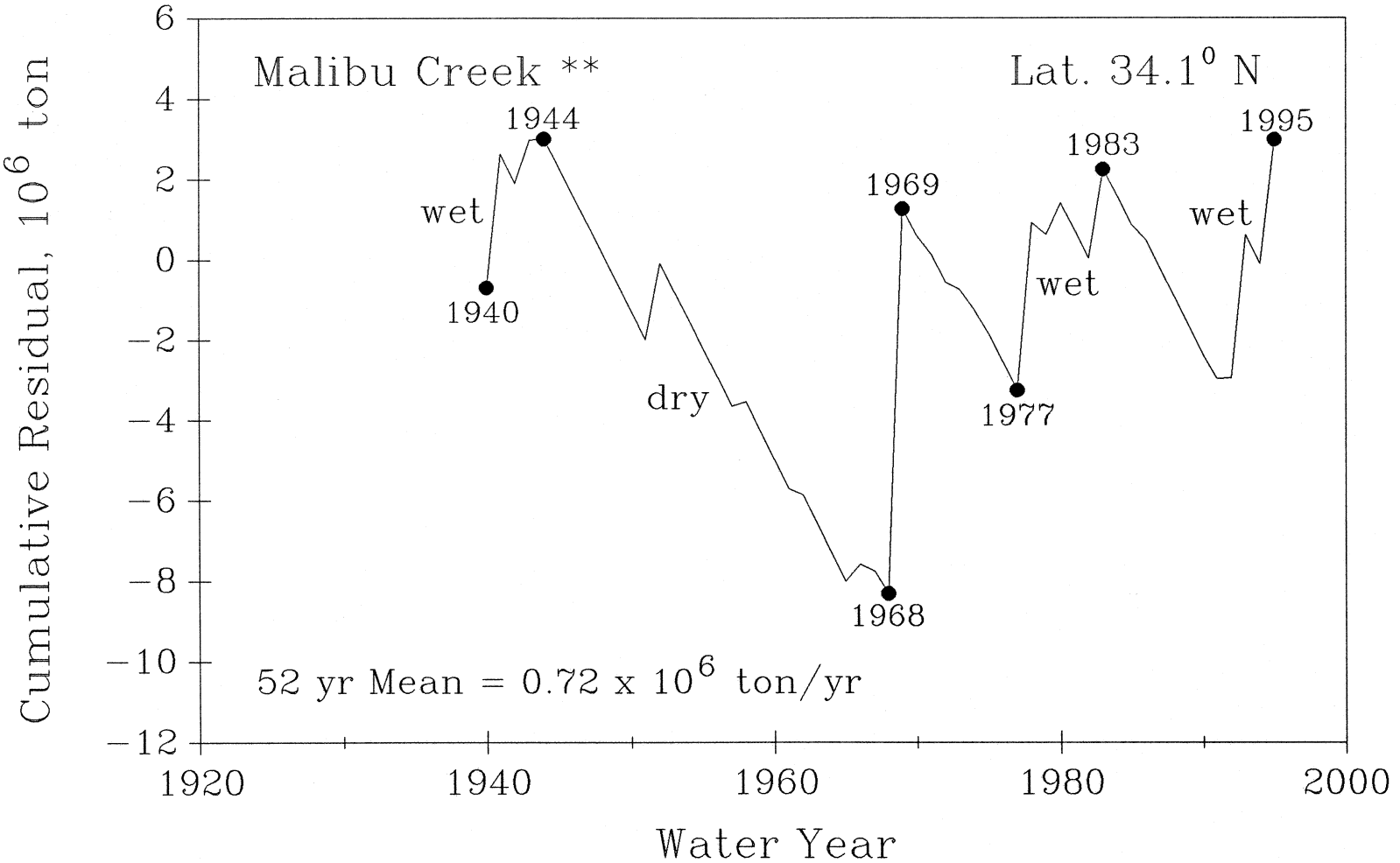

Figure 9 (9). Cumulative residual time series of sediment flux for Malibu Creek calculated using a 52-year mean (1944-1995) over the period of record of 1940-1995 (data from Appendix C).

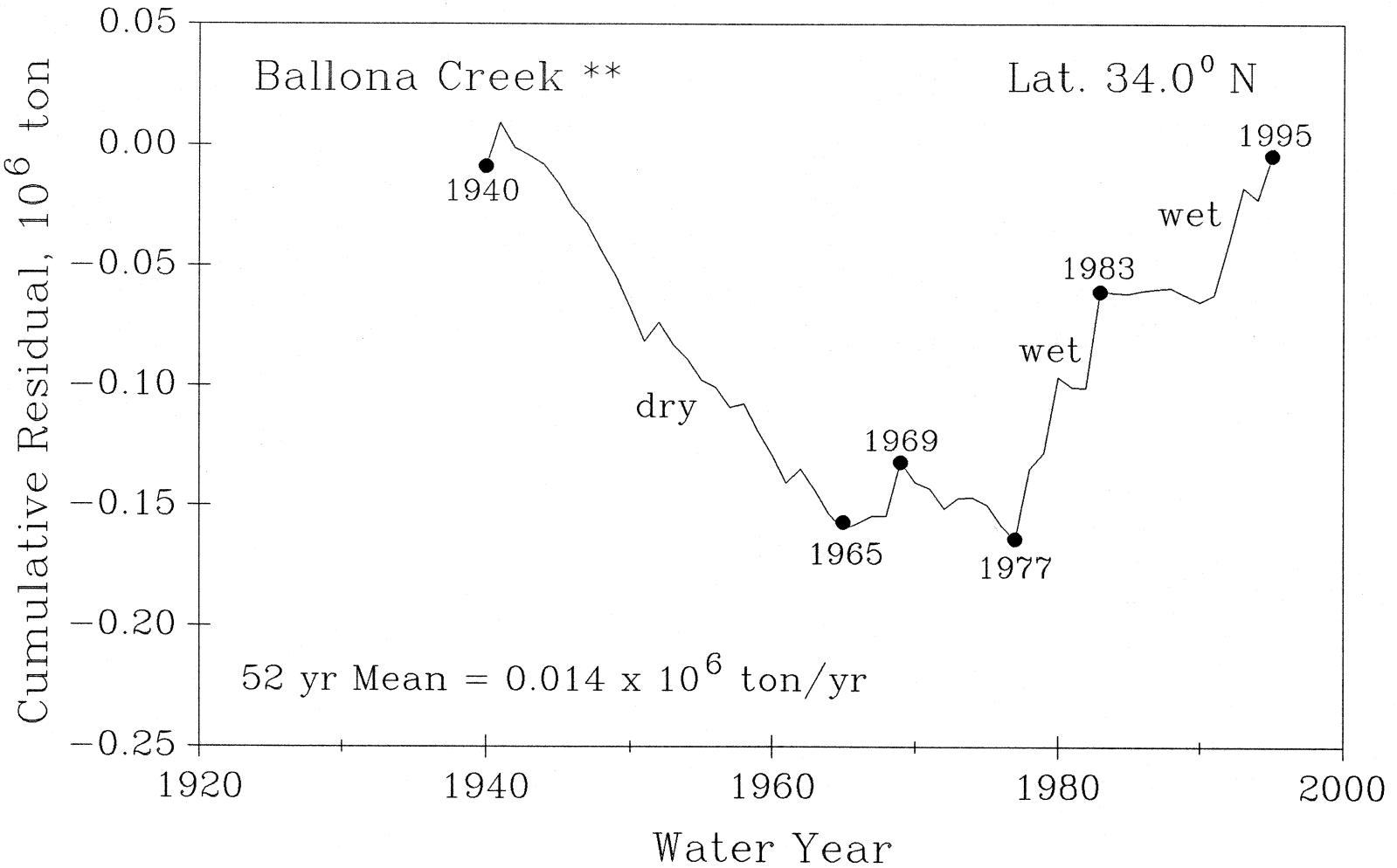

Figure 9 (10). Cumulative residual time series of sediment flux for Ballona Creek calculated using a 52-year mean (1944-1995) over the period of record of 1940-1995 (data from Appendix C).

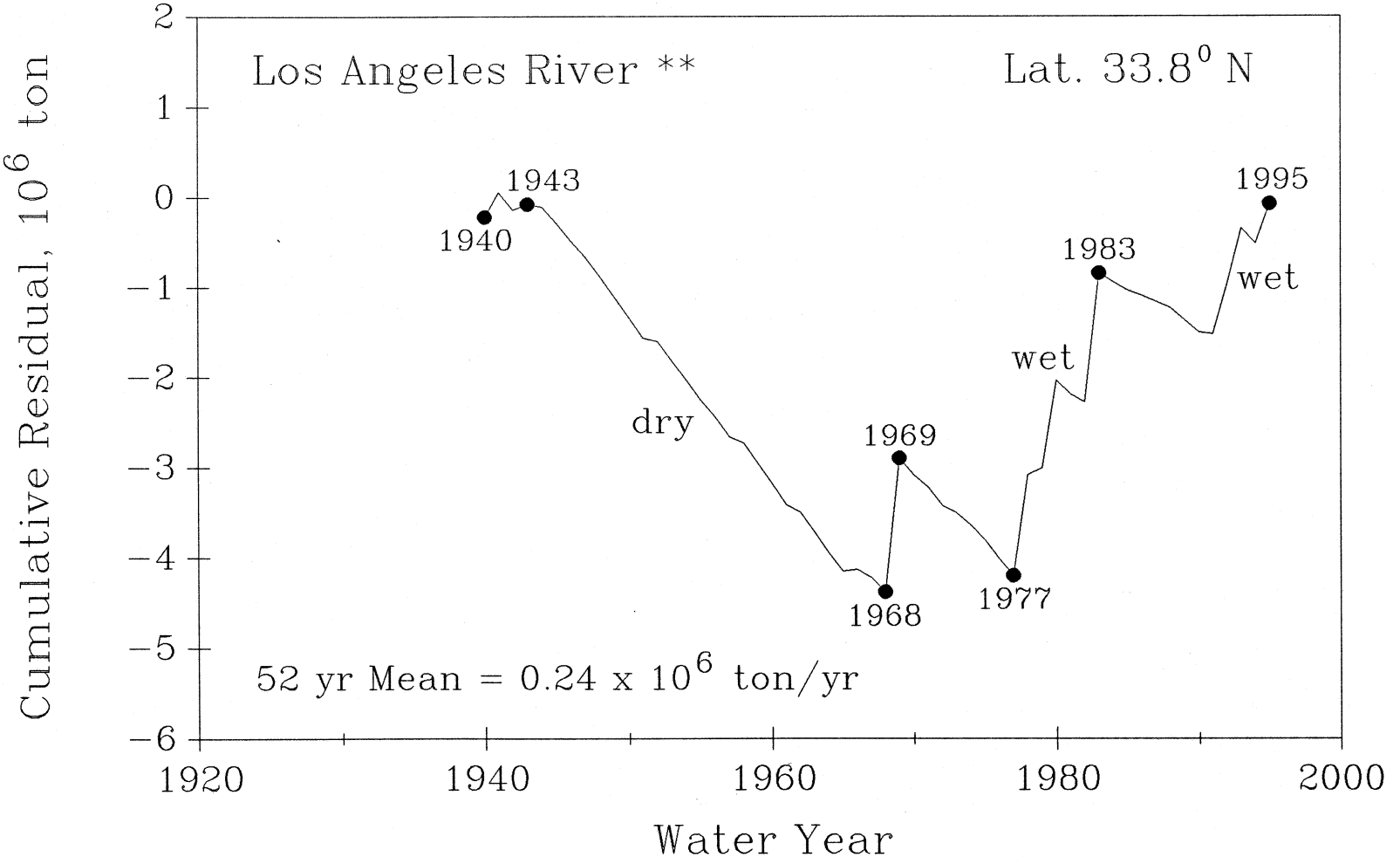

Figure 9 (11). Cumulative residual time series of sediment flux for Los Angeles River calculated using a 52-year mean (1944-1995) over the period of record of 1940-1995 (data from Appendix C).

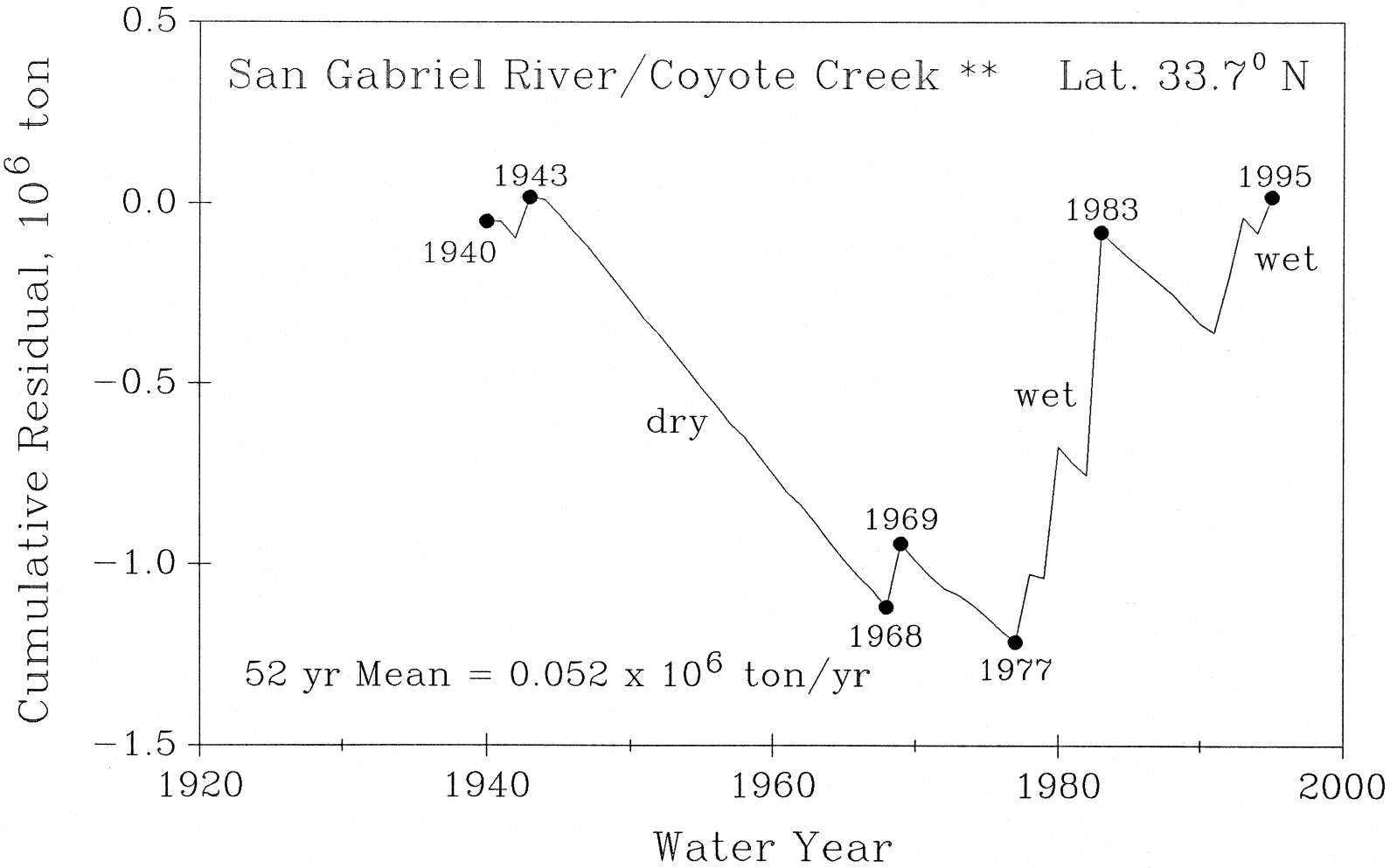

Figure 9 (12). Cumulative residual time series of sediment flux for San Gabriel River/Coyote Creek calculated using a 52-year mean (1944-1995) over the period of record of 1940-1995 (data from Appendix C).

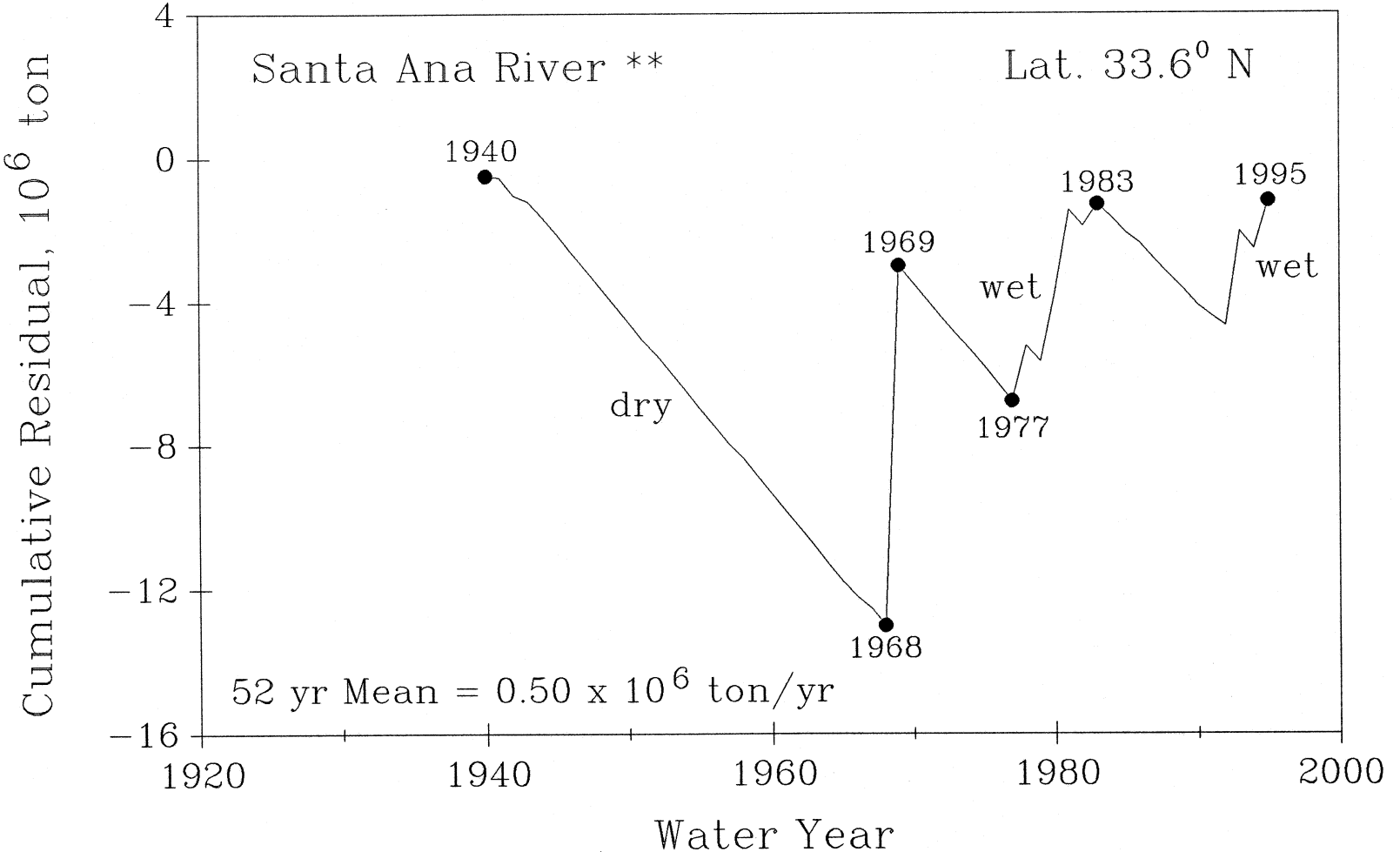

Figure 9 (13). Cumulative residual time series of sediment flux for Santa Ana River calculated using a 52-year mean (1944-1995) over the period of record of 1940-1995 (data from Appendix C).

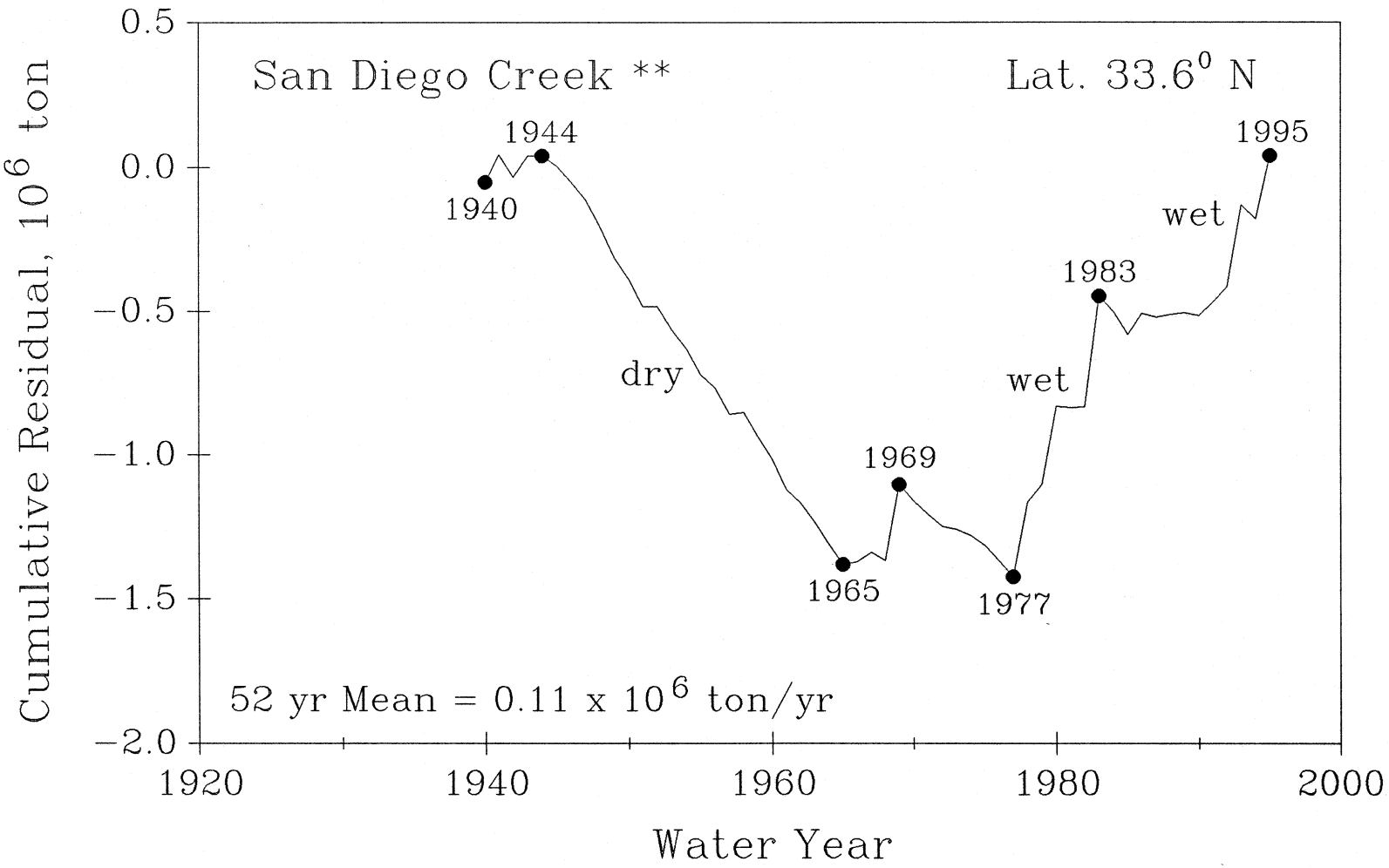

Figure 9 (14). Cumulative residual time series of sediment flux for San Diego Creek calculated using a 52-year mean (1944-1995) over the period of record of 1940-1995 (data from Appendix C).

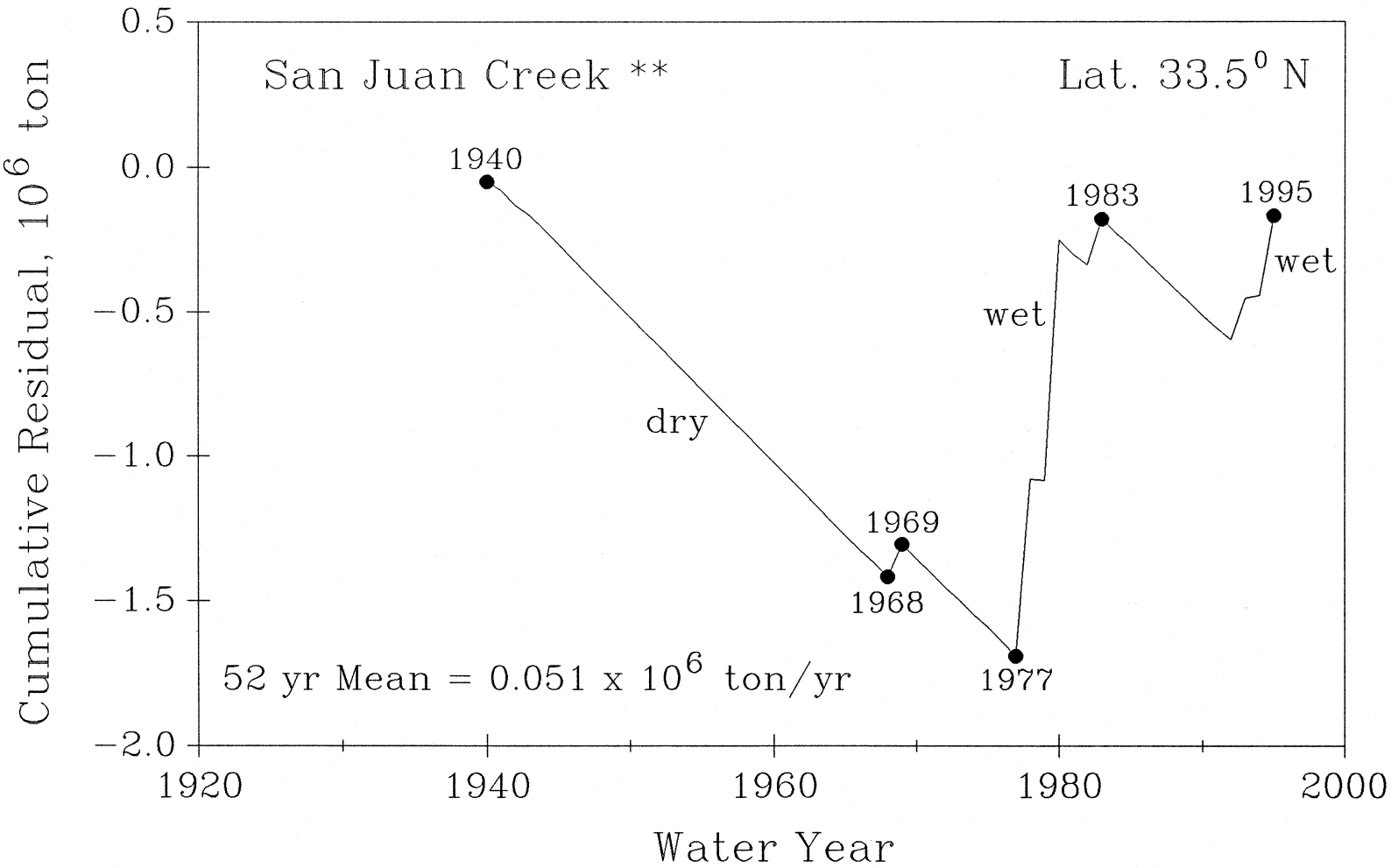

Figure 9 (15). Cumulative residual time series of sediment flux for San Juan Creek calculated using a 52-year mean (1944-1995) over the period of record of 1940-1995 (data from Appendix C).

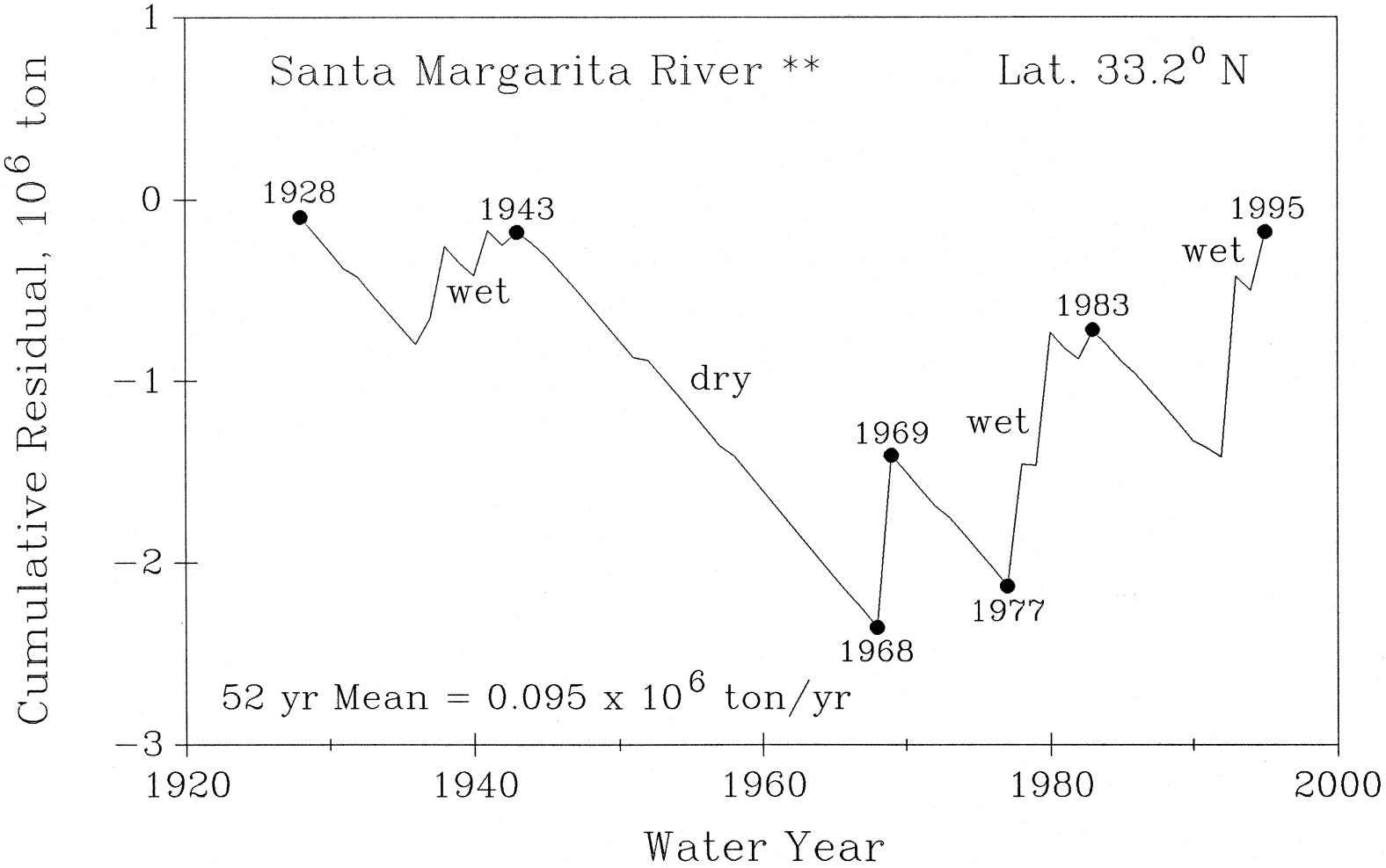

Figure 9 (16). Cumulative residual time series of sediment flux for Santa Margarita River calculated using a 52-year mean (1944-1995) over the period of record of 1940-1995 (data from Appendix C).

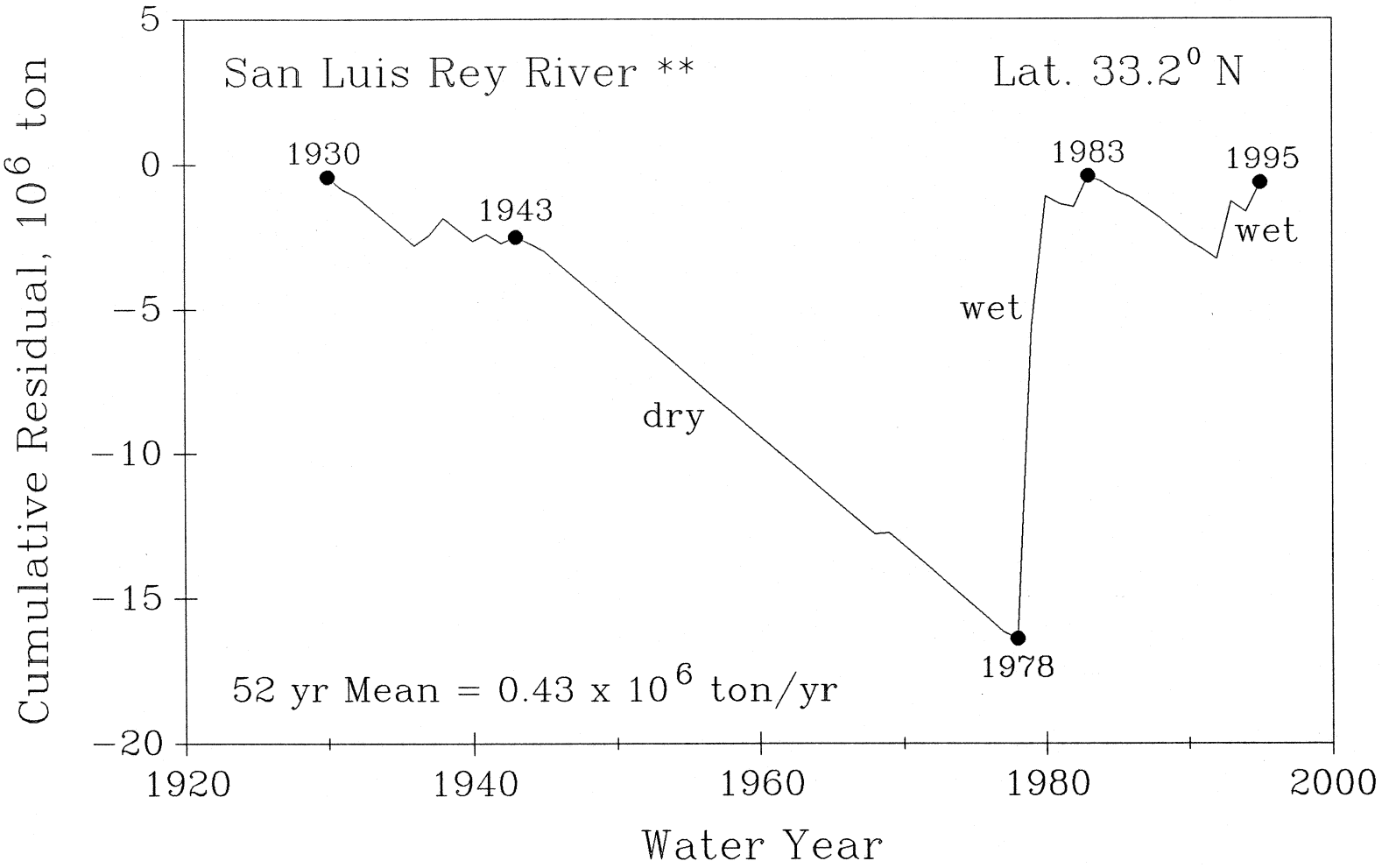

Figure 9 (17). Cumulative residual time series of sediment flux for San Luis Rey River calculated using a 52-year mean (1944-1995) over the period of record of 1940-1995 (data from Appendix C).

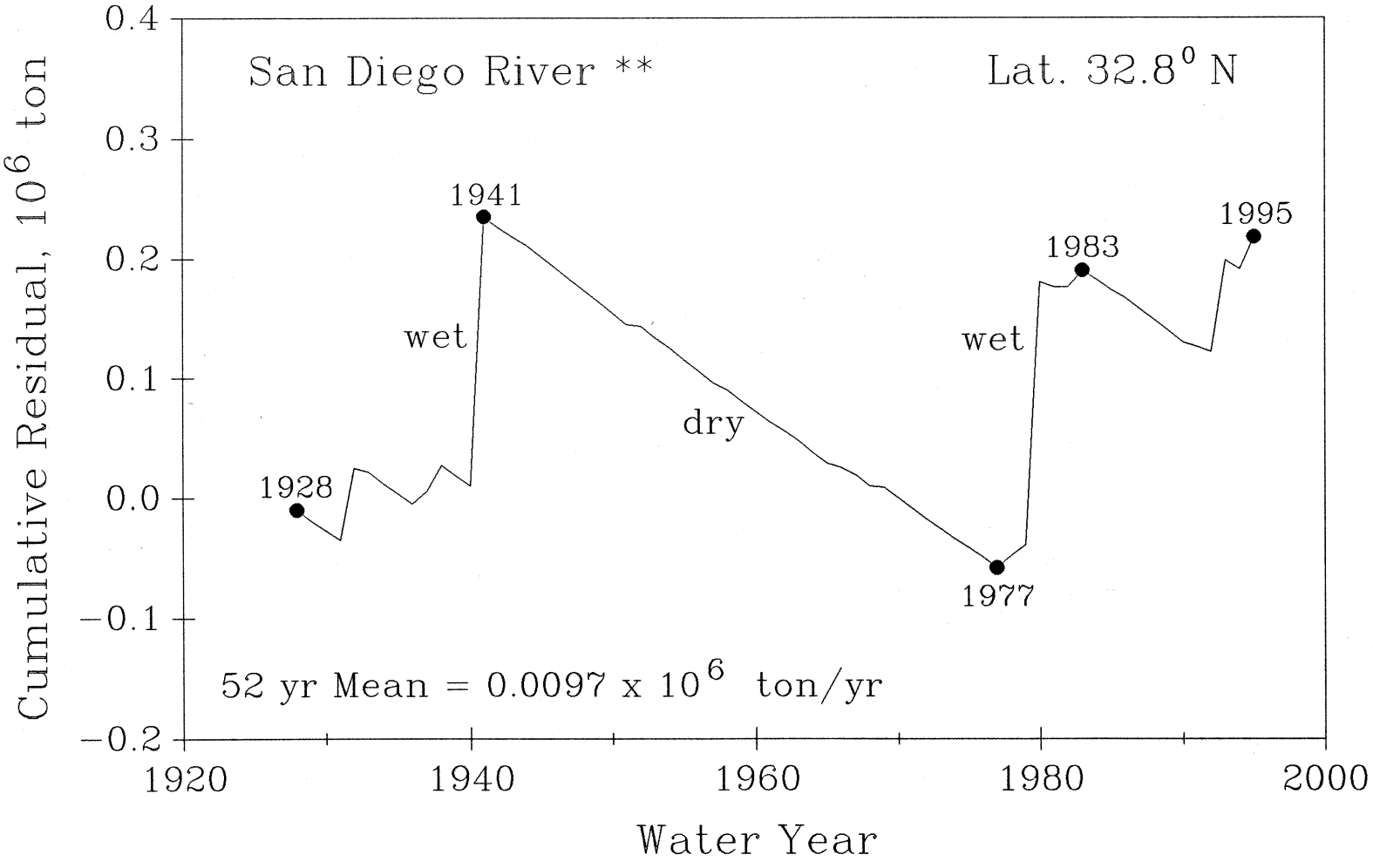

Figure 9 (18). Cumulative residual time series of sediment flux for San Diego River calculated using a 52-year mean (1944-1995) over the period of record of 1940-1995 (data from Appendix C).

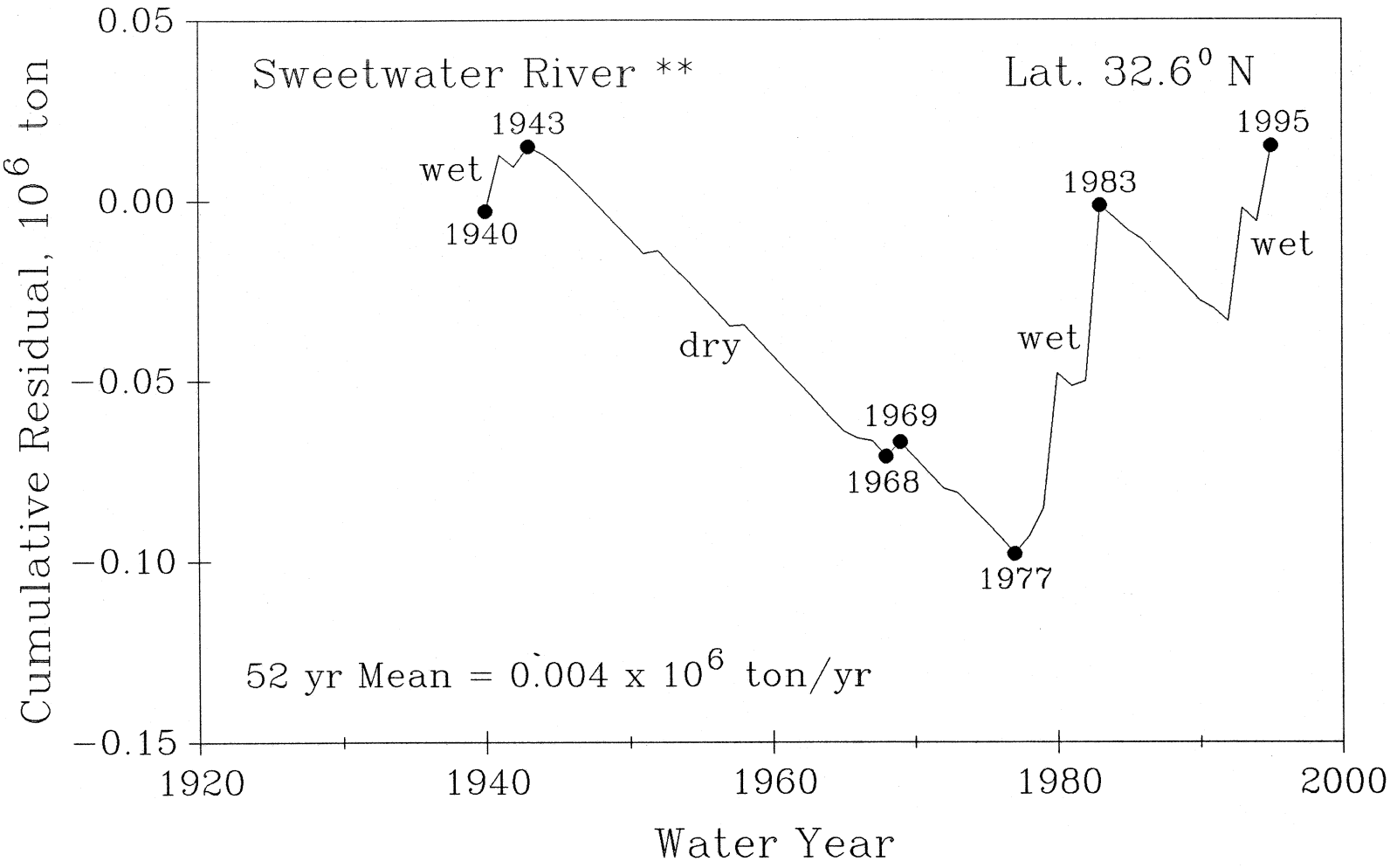

Figure 9 (19). Cumulative residual time series of sediment flux for Sweetwater River calculated using a 52-year mean (1944-1995) over the period of record of 1940-1995 (data from Appendix C).

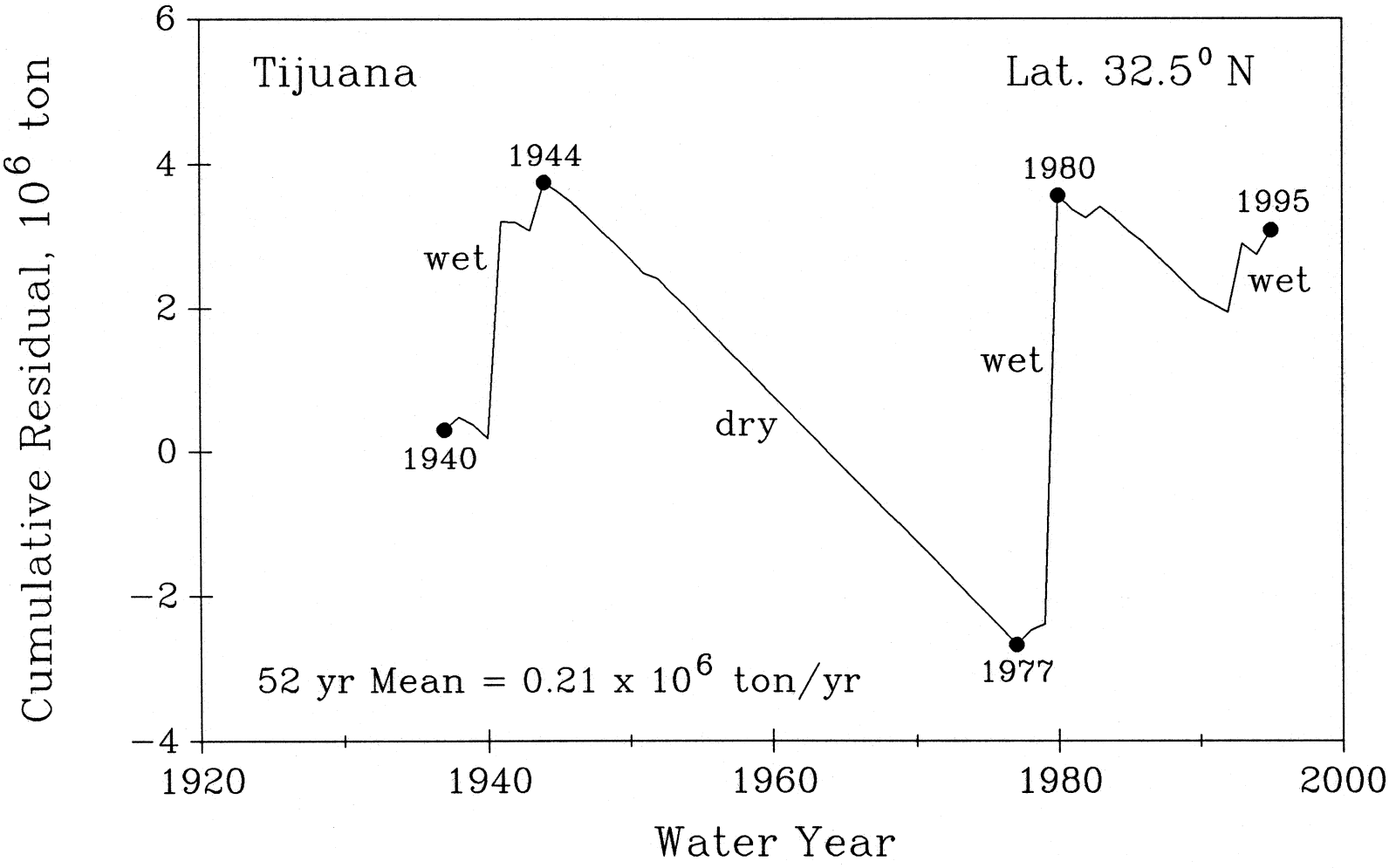

Figure 9 (20). Cumulative residual time series of sediment flux for Tijuana River calculated using a 52-year mean (1944-1995) over the period of record of 1940-1995 (data from Appendix C).

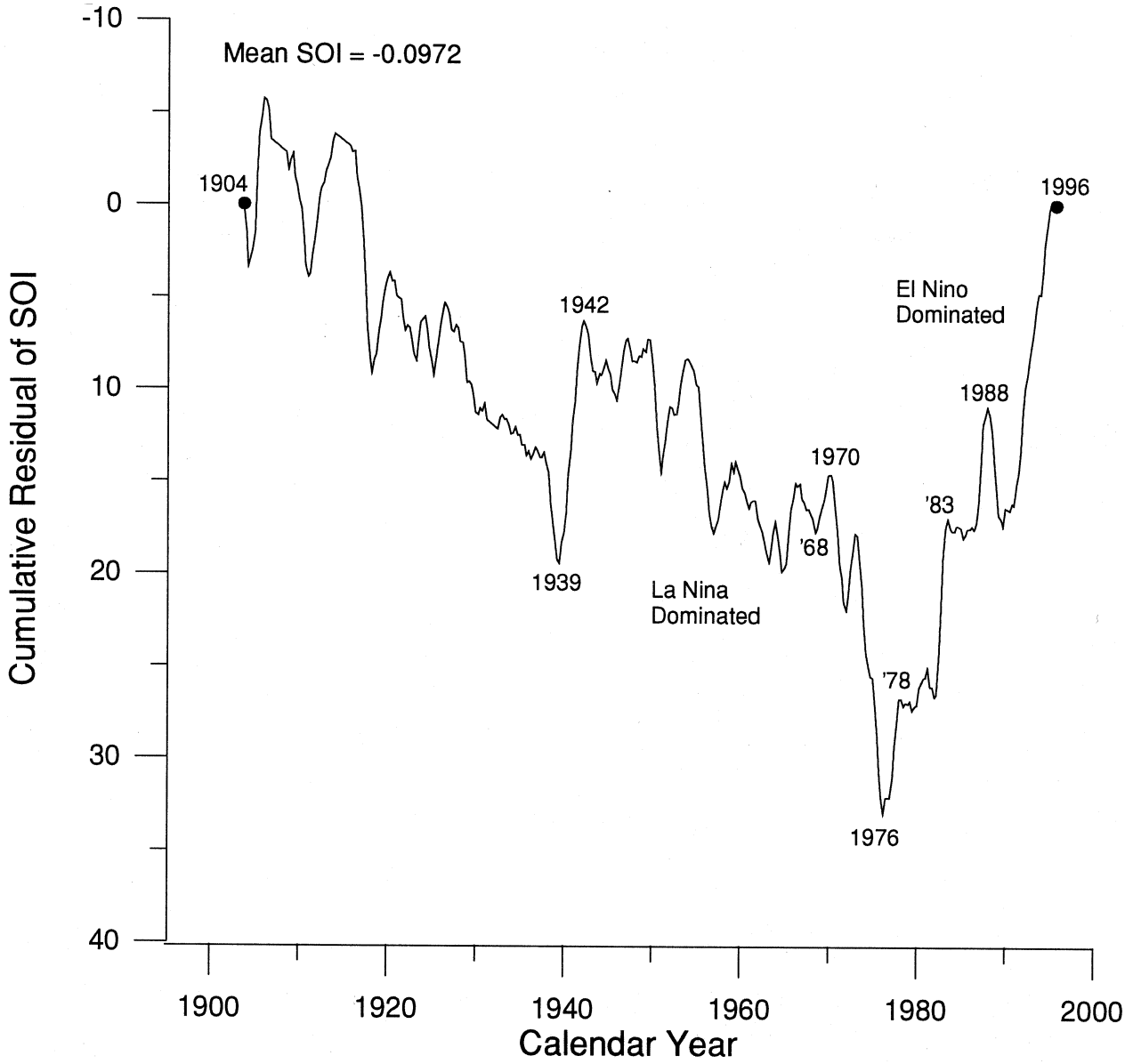

Figure 10. Cumulative residual time series of quarterly values of the Southern Oscillation Index for the period 1904-1995 (data from Appendix D).

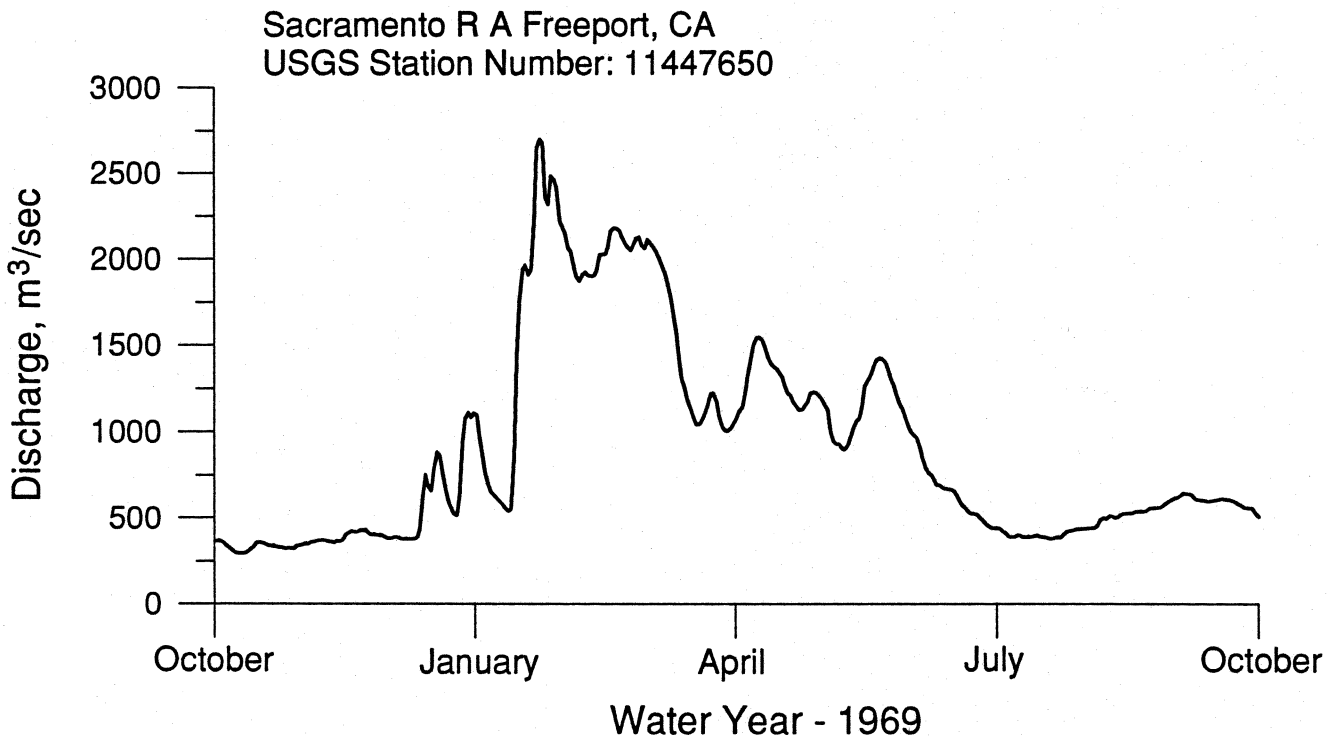

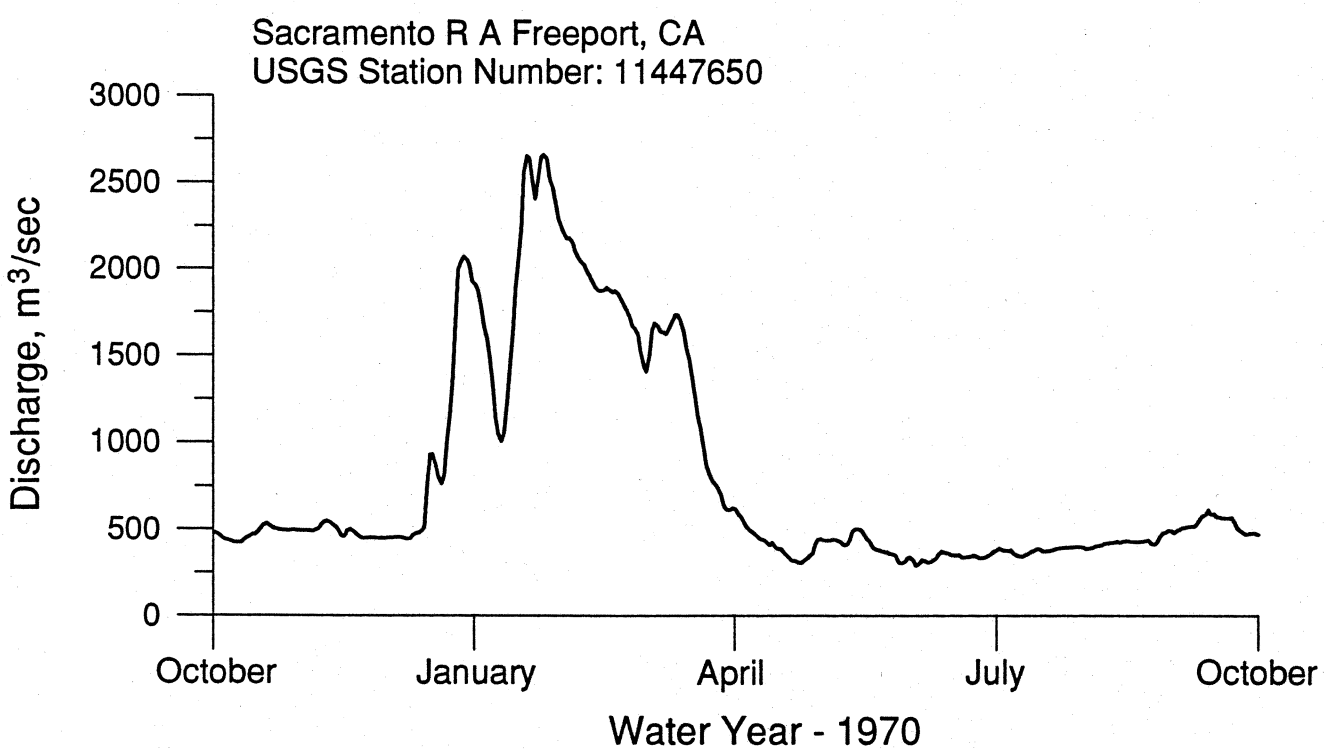

Figure 11. Hydrograph of daily mean streamflow (discharge) for the Sacramento River for water years 1969 and 1970 (data from USGS, 1997).

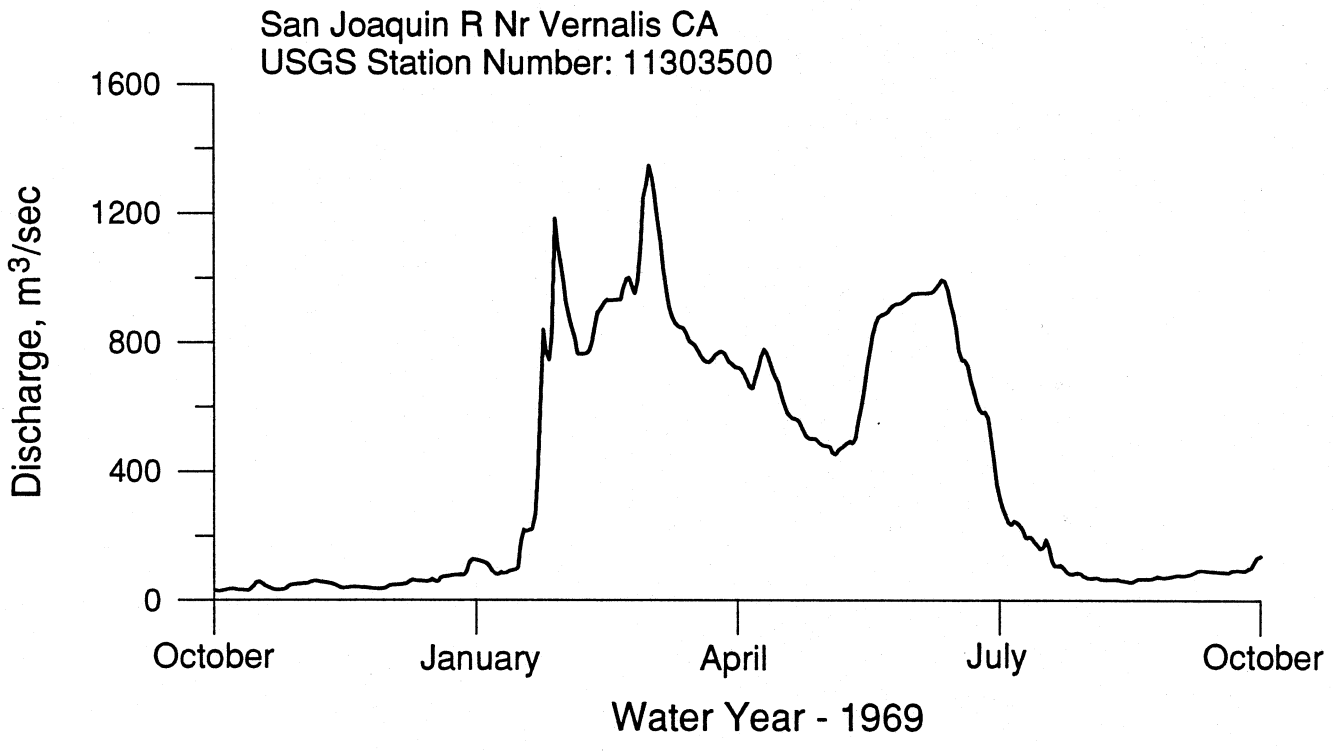

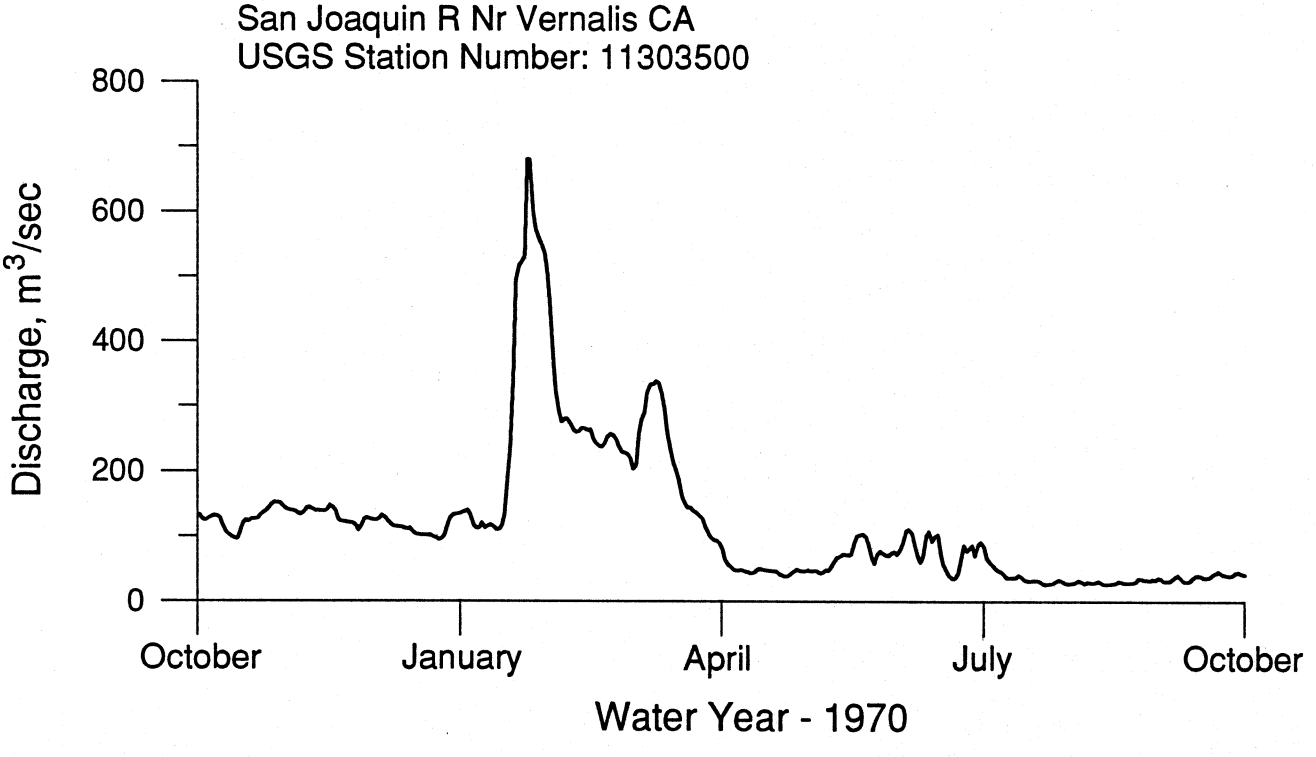

Figure 12. Hydrograph of daily mean streamflow (discharge) for the San Joaquin River for water years 1969 and 1970 (data from USGS, 1997).

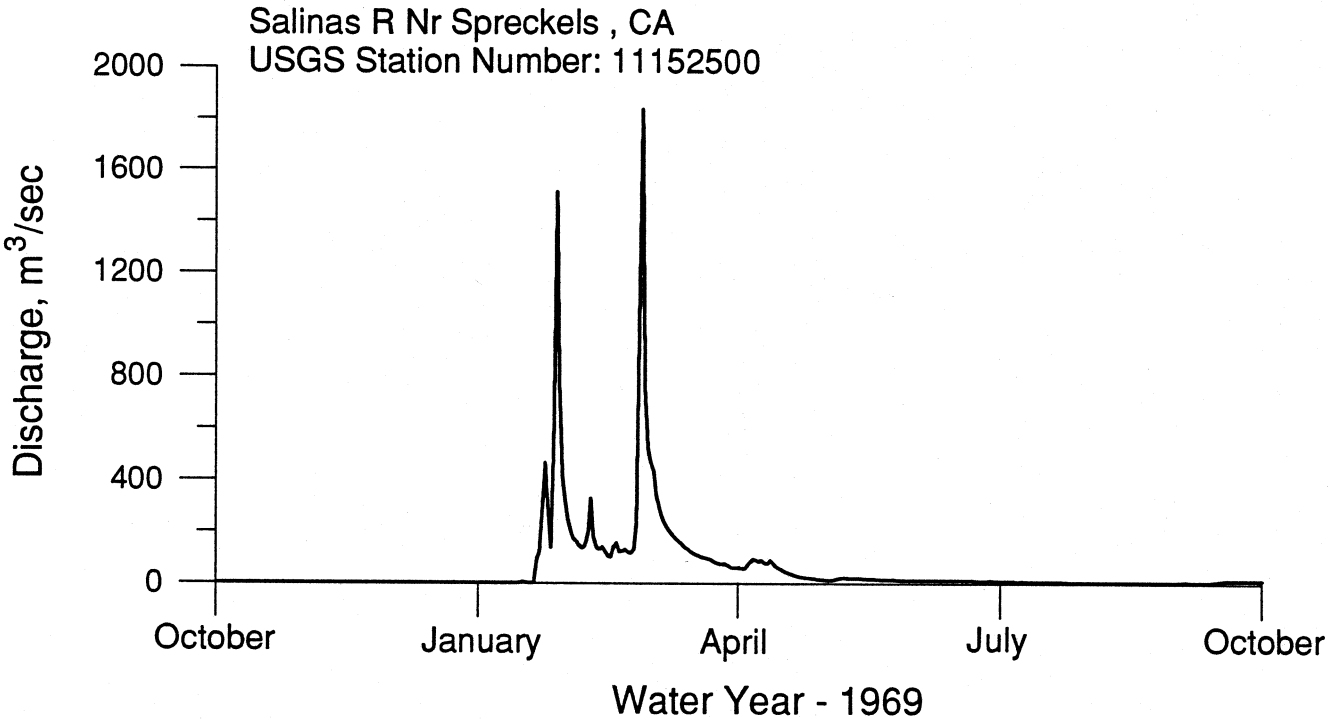

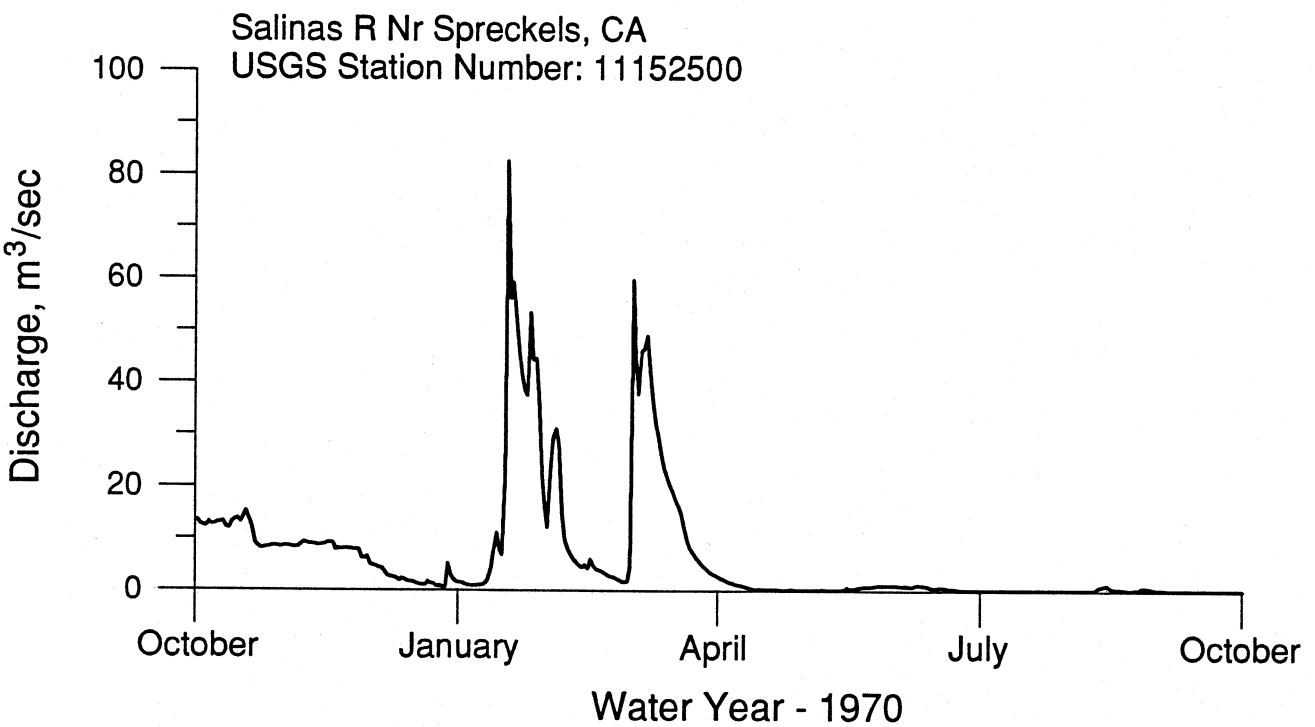

Figure 13. Hydrograph of daily mean streamflow (discharge) for the Salinas River for water years 1969 and 1970 (data from USGS, 1997).

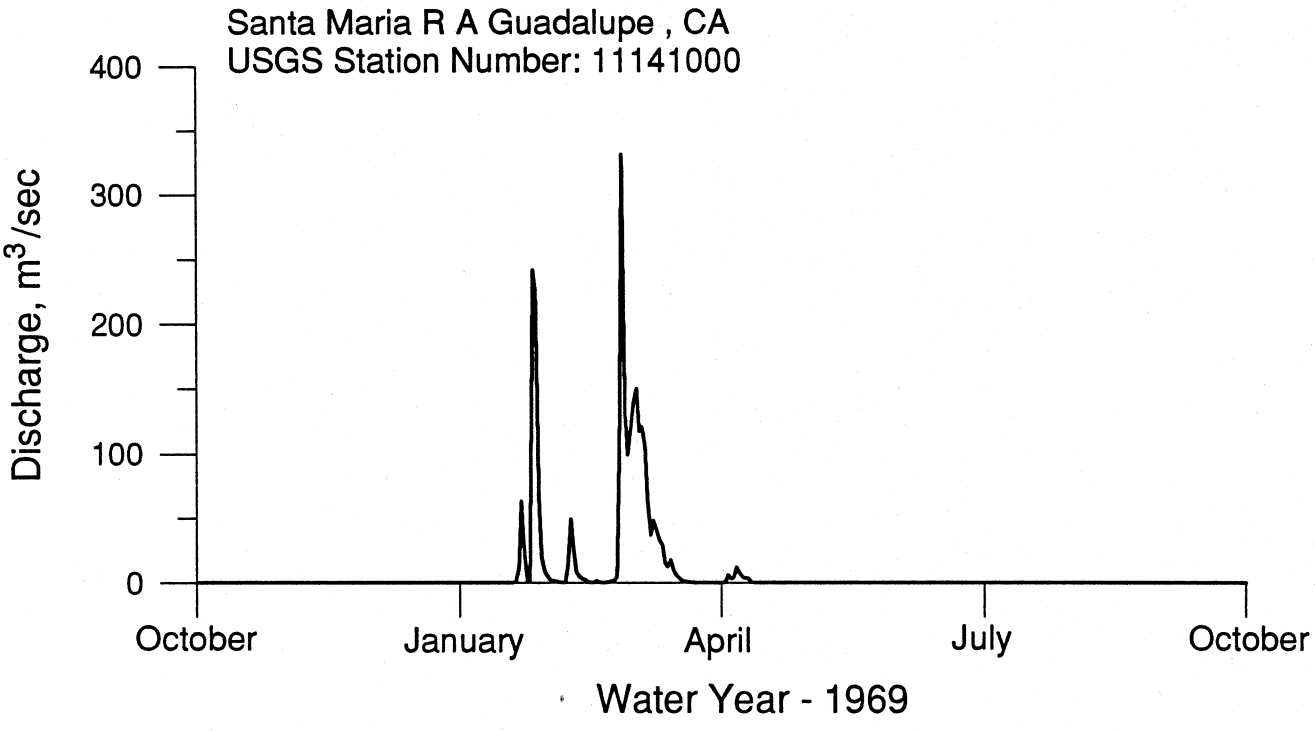

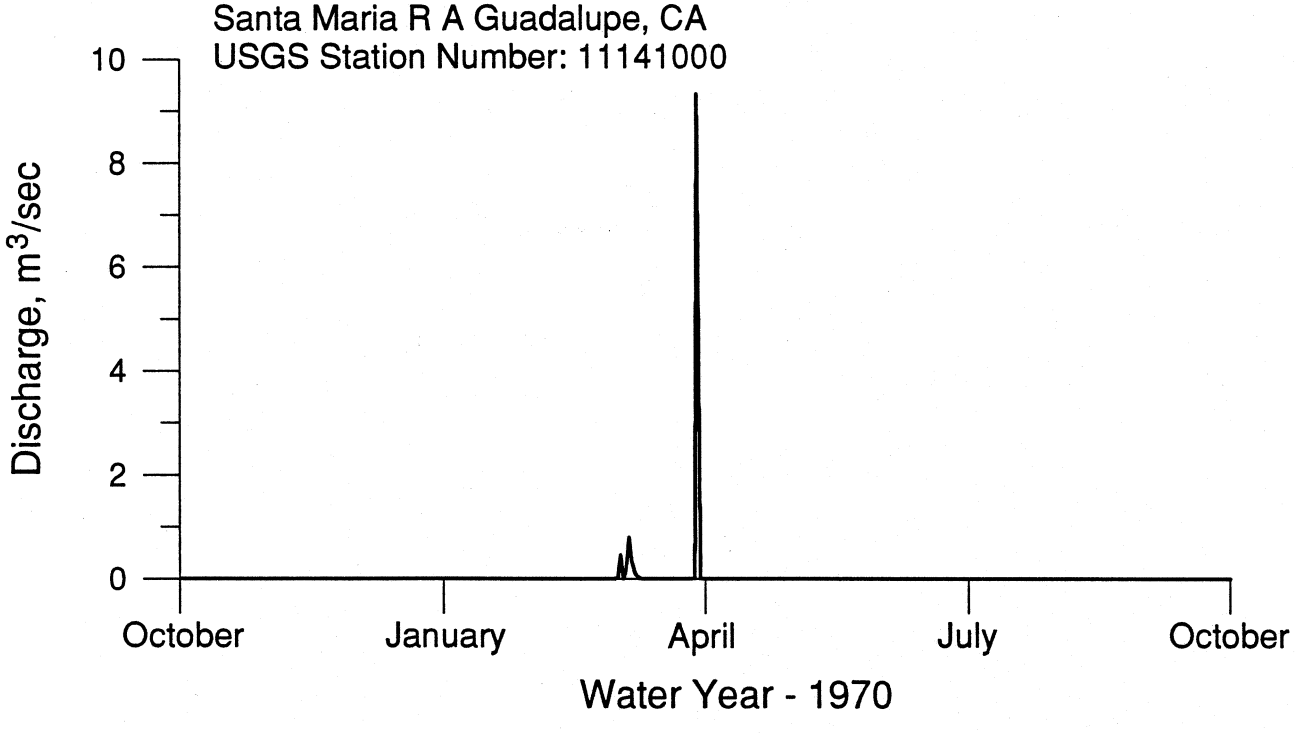

Figure 14. Hydrograph of daily mean streamflow (discharge) for the Santa Maria River for water years 1969 and 1970 (data from USGS, 1997).

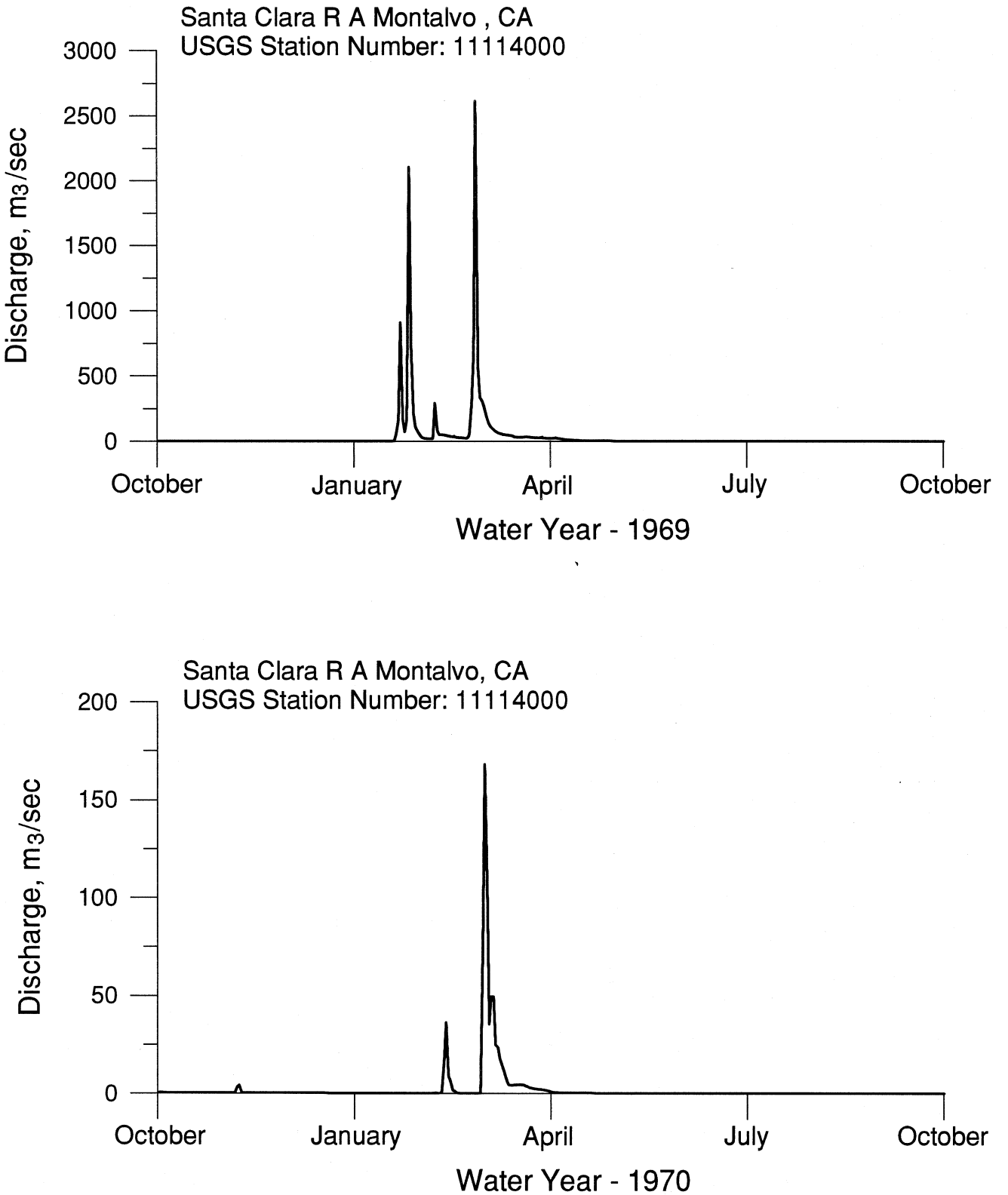

Figure 15. Hydrograph of daily mean streamflow (discharge) for the Santa Clara River for water years 1969 and 1970 (data from USGS, 1997).

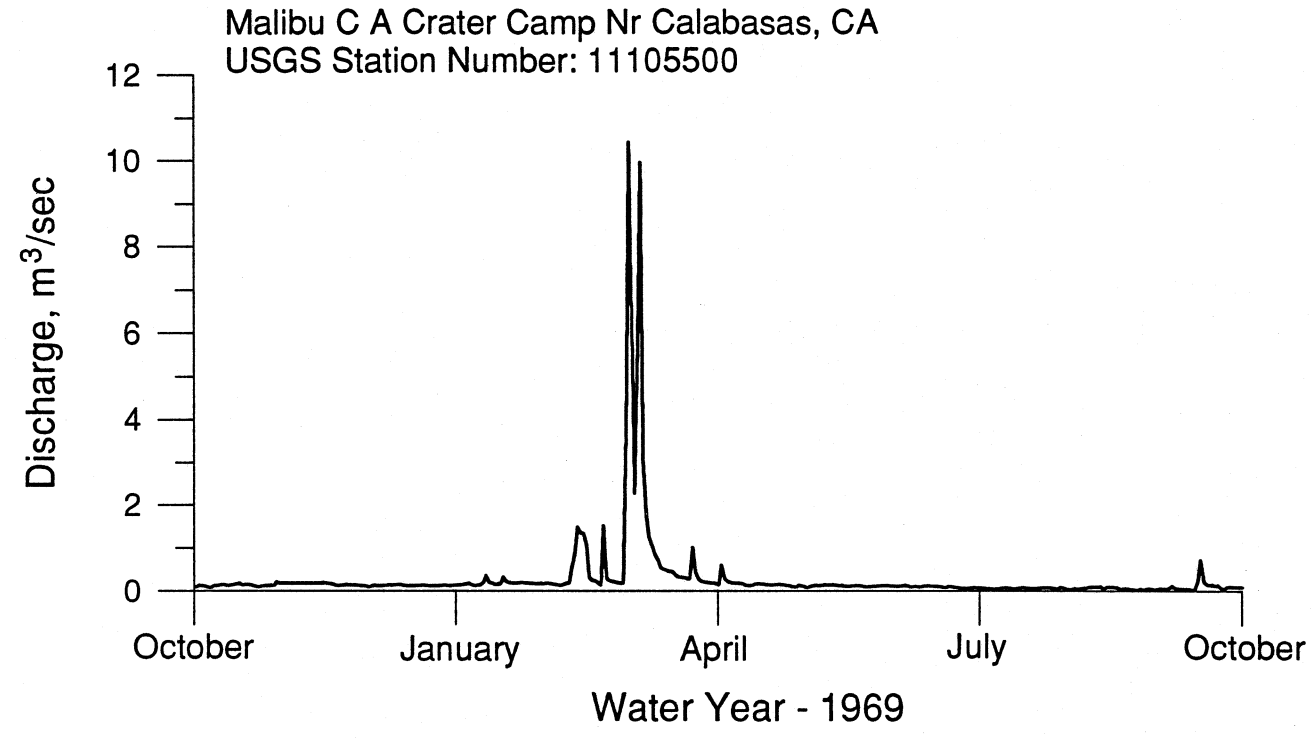

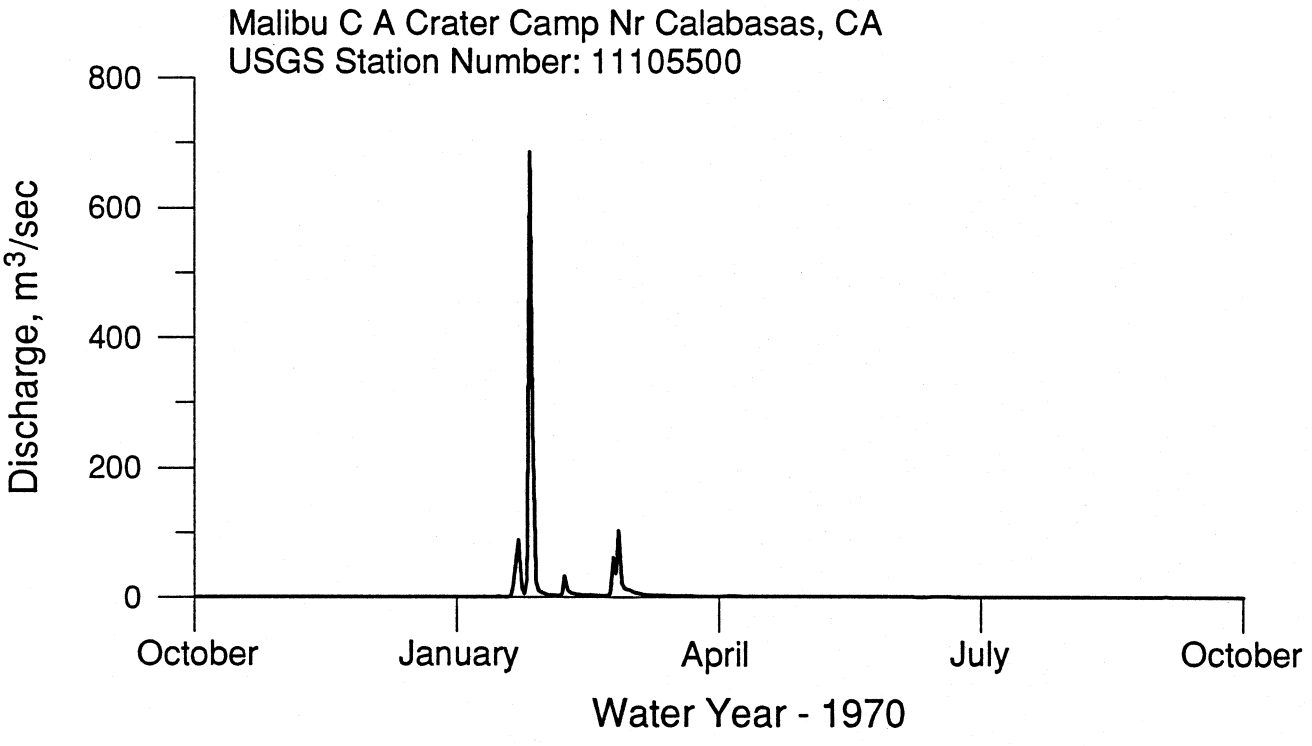

Figure 16. Hydrograph of daily mean streamflow (discharge) for the Malibu Creek for water years 1969 and 1970 (data from USGS, 1997).

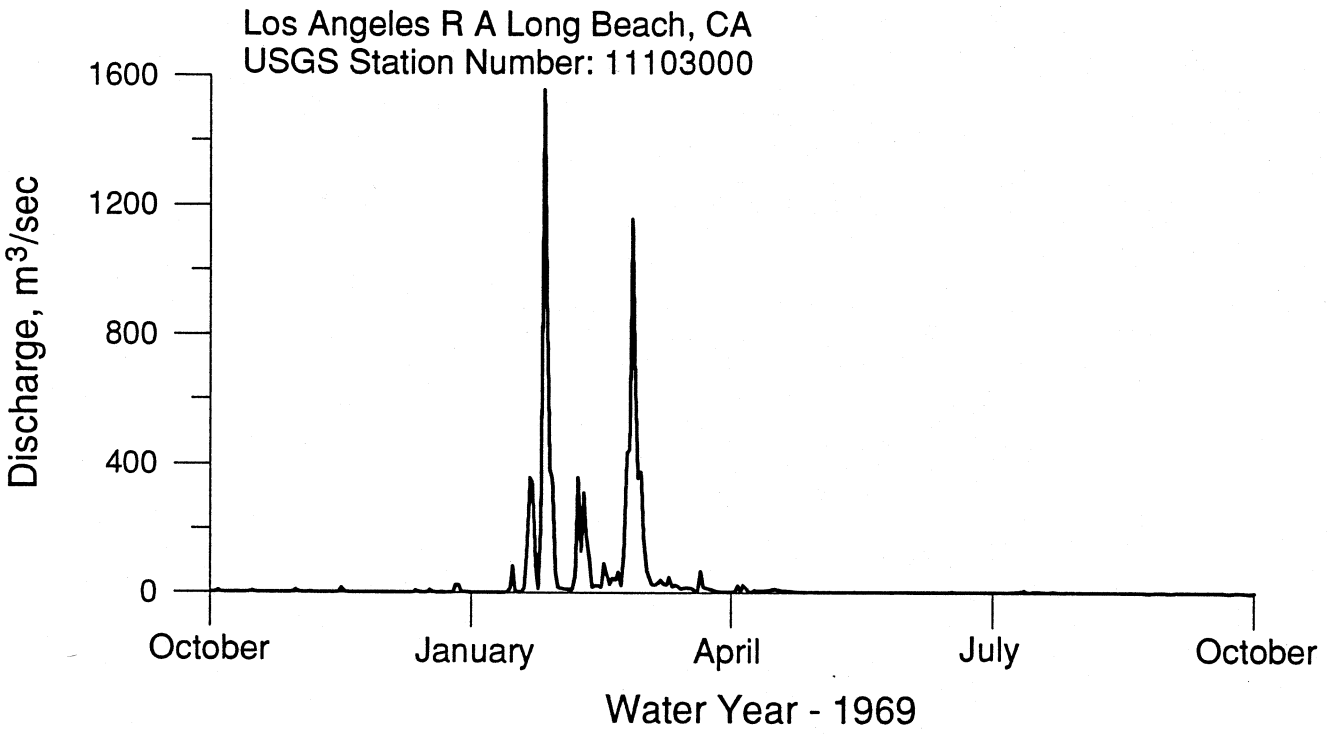

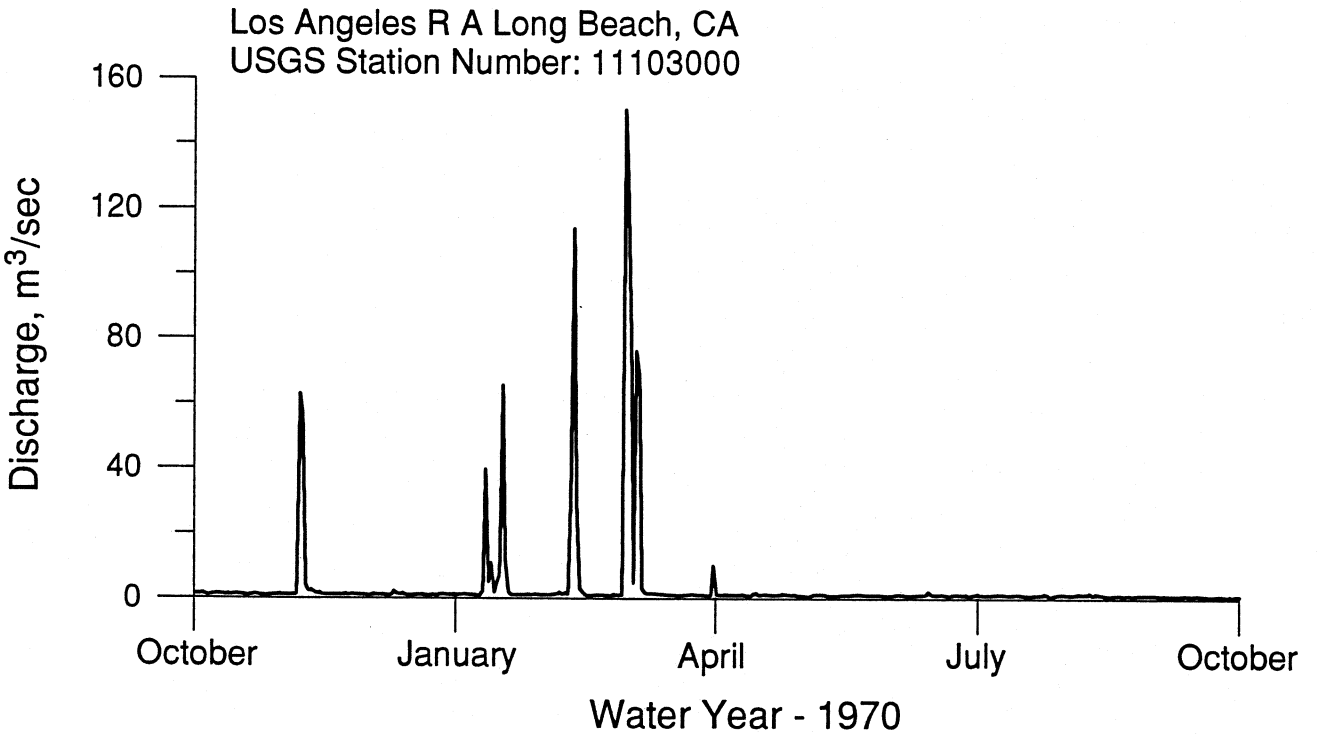

Figure 17. Hydrograph of daily mean streamflow (discharge) for the Los Angeles River for water years 1969 and 1970 (data from USGS, 1997).

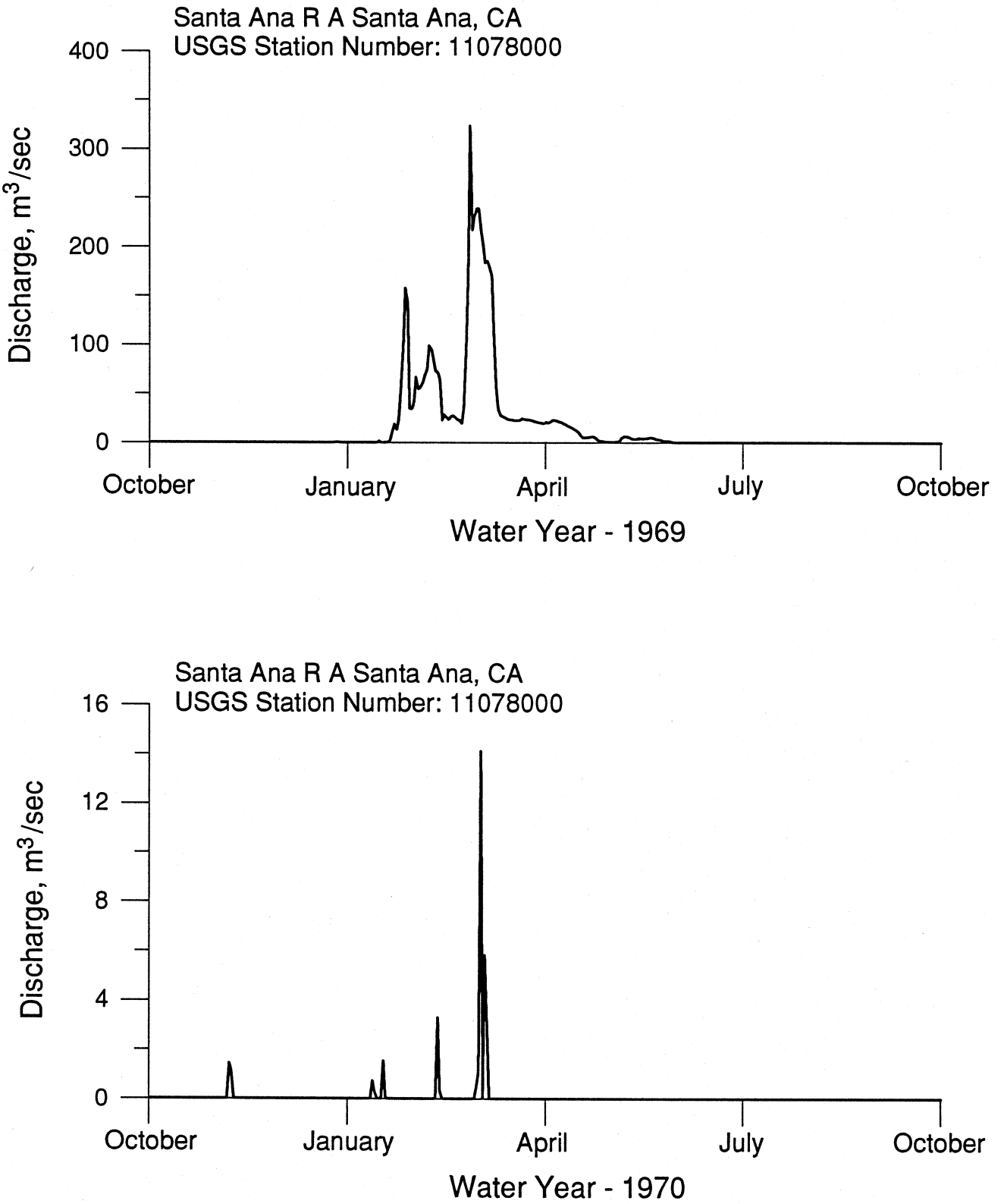

Figure 18. Hydrograph of daily mean streamflow (discharge) for the Santa Ana River for water years 1969 and 1970 (data from USGS, 1997).

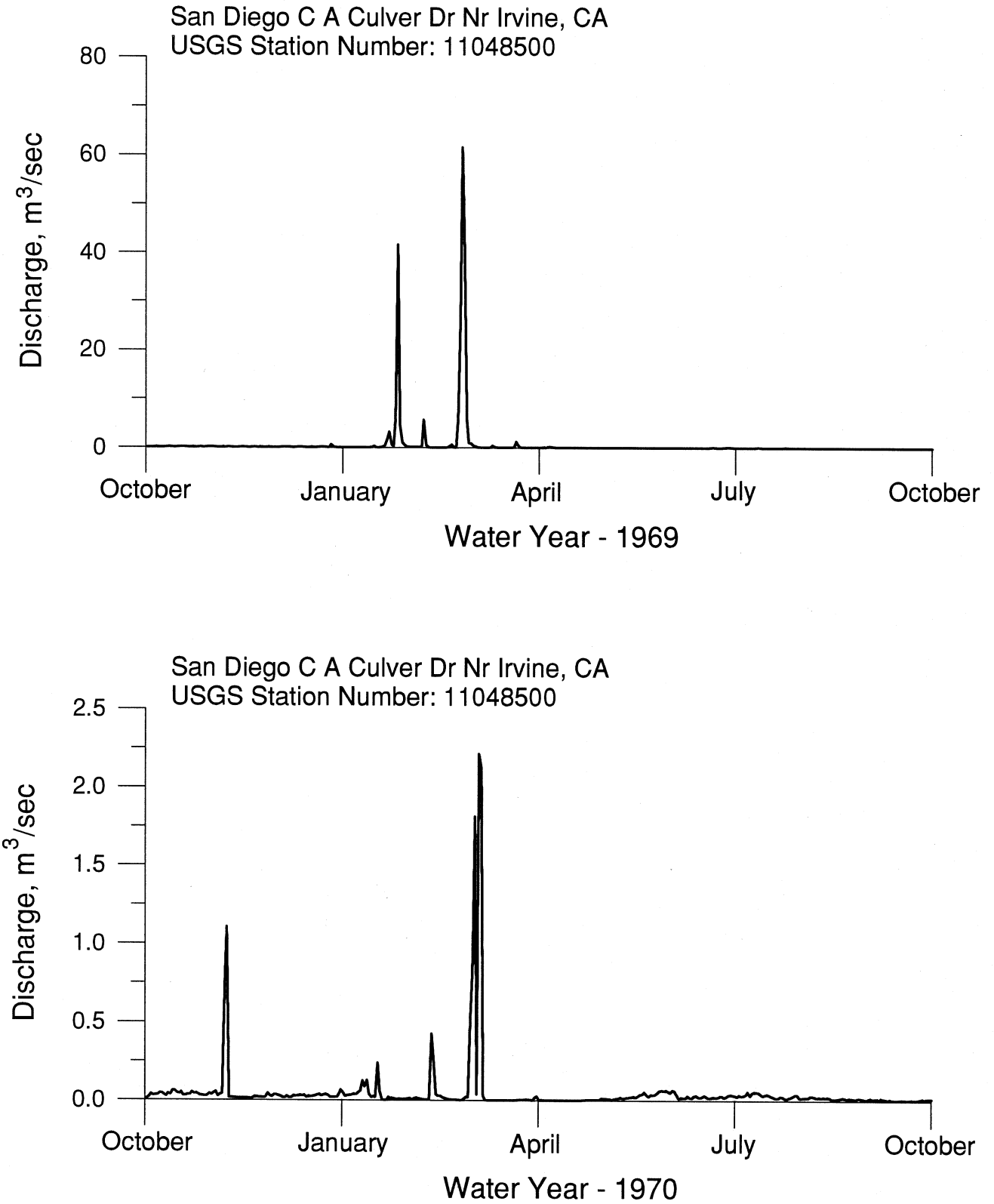

Figure 19. Hydrograph of daily mean streamflow (discharge) for the San Diego Creek for water years 1969 and 1970 (data from USGS, 1997).